20030227013

AD-A266 564

|||||||||||||||||||||

OXIDATION CHEMISTRY AND KINETICS OF MODEL COMPOUNDS
IN SUPERCRITICAL WATER:
GLUCOSE, ACETIC ACID, AND METHYLENE CHLORIDE

by

JERRY CHRISTOPHER MEYER

Captain, United States Army

B.S., United States Military Academy, West Point, 1983

Submitted to the Department of Chemical Engineering
in Partial Fulfillment of the Requirements for the Degree of

MASTER OF SCIENCE
in Chemical Engineering

at the

MASSACHUSETTS INSTITUTE OF TECHNOLOGY

June 1993

DTIC
ELECTE
JUL 12 1993
A

Signature of Author_____

Department of Chemical Engineering
May 7, 1993

Certified by_____

Professor Jefferson W. Tester
Thesis Supervisor

Accepted by_____

Professor Robert E. Cohen
Chairman, Committee for Graduate Students

93-15613

|||||||||||||||||||||

REPORT DOCUMENTATION PAGE

Public reporting burden for this collection of information is estimated to average 1 hour per response, including the time for reviewing instructions, searching existing data sources, gathering and maintaining the data needed, and completing and reviewing the collection of information. Send comments regarding this burden estimate or any other aspect of this collection of information, including suggestions for reducing this burden to Washington Headquarters Services, Directorate for Information Operations and Reports, 1215 Jefferson Davis Highway, Suite 1204, Arlington, VA 22202-4302, and to the Office of Management and Budget, Paperwork Reduction Project (0704-0188), Washington, DC 20503.

1. AGENCY USE ONLY (Leave blank)	2. REPORT DATE June 1993	3. REPORT TYPE AND DATES COVERED Final

4. TITLE AND SUBTITLE
Oxidation Chemistry and Kinetics of Model Compounds in Supercritical Water: Glucose, Acetic Acid, and Methylene Chloride

5. FUNDING NUMBERS

6. AUTHOR(S)
Jerry Christopher Meyer

7. PERFORMING ORGANIZATION NAME(S) AND ADDRESS(ES)
Massachusetts Institute of Technology
Dept. of Chemical Engineering
ATTN: Jefferson Tester
MIT Energy Lab, Rm E40-493
77 Massachusetts Ave; Cambridge, MA 02139

8. PERFORMING ORGANIZATION REPORT NUMBER

9. SPONSORING/MONITORING AGENCY NAME(S) AND ADDRESS(ES)
(Army Advanced Civil Schooling Program)
Commander
U.S. Army Student Detachment
ATTN: ATZI-TBD
Ft. Benjamin Harrison
IN 46216-5820

10. SPONSORING/MONITORING AGENCY REPORT NUMBER

11. SUPPLEMENTARY NOTES Portions submitted for publication to American Institute of Chemical Engineers Journal. This is a Masters Thesis with experimental and research work done by the author at M.I.T. under the Army's Advanced Civil Schooling Program.

12a. DISTRIBUTION/AVAILABILITY STATEMENT
Available to the Public

12b. DISTRIBUTION CODE

13. ABSTRACT (Maximum 200 words)

Supercritical water oxidation represents an innovative technology for complete and efficient destruction of hazardous wastes, without forming of harmful by-products. Organic compounds and oxygen are completely miscible in supercritical water at temperatures above 374°C and pressures above 221 bar, providing a single-phase medium for rapid oxidation of organic to CO_2, H_2O and N_2. The scale-up and reliable operation of commercial-sized process equipment require a thorough understanding of oxidation kinetics, reaction pathways and mechanisms.

Global rate expressions and product identification was performed under well-defined conditions of hydrolysis and oxidation of model compounds (glucose, acetic acid, and methylene chloride) in supercritical water.

The U.S. Army is investigating supercritical water oxidation as an alternative to incineration for the destruction of chemical weapons.

14. SUBJECT TERMS supercritical water, oxidation, hydrolysis, kinetics, glucose, acetic acid, methylene chloride

15. NUMBER OF PAGES 217

16. PRICE CODE

17. SECURITY CLASSIFICATION OF REPORT	18. SECURITY CLASSIFICATION OF THIS PAGE	19. SECURITY CLASSIFICATION OF ABSTRACT	20. LIMITATION OF ABSTRACT
Unclassified	Unclassified	Unclassified	UL

NSN 7540-01-280-5500

Standard Form 298 (Rev. 2-89)
Prescribed by ANSI Std. Z39-18

OXIDATION CHEMISTRY AND KINETICS OF MODEL COMPOUNDS IN SUPERCRITICAL WATER: GLUCOSE, ACETIC ACID, AND METHYLENE CHLORIDE

by

JERRY CHRISTOPHER MEYER

Submitted to the Department of Chemical Engineering
on May 7, 1993 in Partial Fulfillment of the Requirements for the
Degree of Master of Science in Chemical Engineering

ABSTRACT

Supercritical water oxidation represents an innovative technology for complete and efficient destruction of hazardous wastes, without forming of harmful by-products. Organic compounds and oxygen are completely soluble in supercritical water at temperatures above 374 °C and pressures above 221 bar, providing a single-phase medium for rapid oxidation of organic to CO_2, H_2O, and N_2. The scale-up and reliable operation of commercial-sized process equipment require a thorough understanding of oxidation kinetics, reaction pathways, and mechanisms.

Glucose ($C_6H_{12}O_6$) hydrolysis and oxidation were done in collaboration with Richard H. Holgate. Experiments were done in an isothermal, isobaric, tubular plug-flow reactor apparatus. Both hydrolysis and oxidation occurred rapidly in supercritical water at 246 bar. A diverse set of products, present in the liquid effluent and also subject to hydrolysis, was formed. At 600 °C and a 6-second reactor residence time, glucose is completely gasified, even in the absence of oxygen. In the presence of oxygen, destruction of liquid-phase products is enhanced, with none found above 550 °C at a 6-second reactor residence time. Major products formed were acetic acid, acetonylacetone, propenoic acid, acetaldehyde, carbon monoxide, methane, ethane, ethylene, and hydrogen. Methane and hydrogen were present at temperatures up to 600 °C for reactor residence times of 6 seconds.

Acetic Acid (CH_3COOH) hydrolysis and oxidation in supercritical water was examined from 425 - 600 °C and 246 bar at reactor residence times spanning 4.4 to 9.8 seconds. Over the range of conditions studied, acetic acid oxidation was globally 0.72 ± 0.15 order in acetic acid and 0.27 ± 0.15 order in oxygen, with an activation energy of 168 ± 21 kJ/mol and an induction time of about 1.5 seconds at 525 °C. Pressure (water density) effect studies in the range 160 - 263 bar and 550 °C indicated that pressure did not affect the rate of acetic acid oxidation as as much as previously observed with hydrogen or carbon monoxide. Major products of acetic acid oxidation in supercritical water are carbon dioxide, carbon monoxide, methane, hydrogen, and propenoic acid. Other minor products were observed, but not identified. In the absence of oxygen, approximately 35% conversion of acetic acid was obtained at 600 °C, 246

bar, and 8-second reactor residence time.

Methylene Chloride (CH_2Cl_2) hydrolysis and oxidation in supercritical water was examined from 450 - 575 °C and 246 bar at reactor residence times spanning 4.4 to 10.8 seconds. Regression of experimental data at 500 °C and 525 °C gave a global oxidation rate first order in methylene chloride and independent of oxygen, with an activation energy of 142±32 kJ/mol and possible induction time of about 1 second. Major gaseous products were carbon monoxide, carbon dioxide, and hydrogen, with no chlorinated gases detected. Liquid products included *cis*-1,2 dichloroethylene, *trans*-1,2 dichloroethylene, formic acid, oxalic acid, and propenal (acrolein), along with other unidentified products. Hydrolysis accounted for a significant portion of methylene chloride destruction and gave some results that need further verification.

Thesis Supervisor: Jefferson W. Tester

Title: Professor of Chemical Engineering
                  Director, Energy Laboratory

Many people made the completion of this thesis possible. At the risk of omitting someone, the following deserve particular recognition:

First, and foremost, credit and thanks goes to God, through whom all things are possible.

My wife, Robin, and my daughter, Jerin, for their unconditional love, support, understanding, and patience.

My parents, Dean and Addie Meyer, and my six brothers, who have always been a source of encouragement and given me a sense of perspective.

Professor Jeff Tester, for his understanding, patience, commitment, and true leadership. His optimism kept me going when the going was tough.

The U.S. Army, for giving me opportunities and experiences no other career could have given me.

Rick Holgate, my predecessor, who set high experimental standards and answered my numerous and less than astute questions.

Faculty at MIT who helped me understand the concepts of chemical engineering, but in particular, Adel Sarofim and Klavs Jensen, who gave extra effort in helping me attain the level of understanding expected of a graduate of this institute.

Fellow students in Lab 66-553, who helped in innumerable ways academically and experimentally, in addition to being just good friends. Particular acknowledgment goes to Gabe Worley for his computer prowess; Matt DiPippo, for his inexhaustible willingness to help in anyway at anytime; Brian Phenix, for his helpful and competent assistance with the experimental work; and especially Phil Marrone, whose questions kept me thinking, and without whose time this work would ot be completed;

Other students who helped me in the academic challenges encountered, to include Mike Szady, Fred Armellini and Brian Cumpston.

The personnel at MODAR, Inc., for their interest in our work and willingness to share experiences, thoughts and ideas.

Personnel of the Energy Lab and Departmental Headquarters, who handle the administrative and day-to-day activities competently and professionally.

DTIC QUALITY INSPECTED 8

This thesis is dedicated to my wife, Robin, and my daughter, Jerin.
I'm coming home.

"Trust in the Lord with all thine heart; and lean not unto thine own understanding. In all thy ways, acknowledge Him, and he shall direct thy path."

-Proverbs 3:5,6

Table of Contents

List of Figures

List of Tables

1.1 Introduction

Supercritical water oxidation (SCWO) is a resourceful method that can be used to destroy harmful wastes without producing unsafe byproducts. Supercritical water (SCW), above 374 °C and 221 bar, exhibits properties distinctly different than water at subcritical conditions. Specifically, its solvation characteristics change drastically. Significant decreases in water's dielectric constant, ionic dissociation constant, and hydrogen bonding at and above the critical point results in supercritical water acting as a single phase, non-polar, dense gas that has solvation properties similar to low polarity organics. Hence, hydrocarbons and gases (e.g., O_2, N_2, CO_2, etc.) are highly soluble while ionic species, namely inorganic salts, are practically insoluble in supercritical water. With no interphase mass transport limitations and sufficiently high temperatures, the kinetics of organic oxidation in SCW are fast and complete. Hydrocarbon oxidation products consist of CO_2 and H_2O, while heteroatoms (F, Cl, S, P) are usually converted to mineral acids, or insoluble salts in the presence of neutralizing caustic. Despite high enough temperatures for rapid kinetics, supercritical temperatures are low enough to preclude formation of NO_x or SO_2 (Killilea *et al.*, 1991).

Two types of SCWO processes exist. The above-ground method (MODAR process, Modell patent) uses high pressure pumps or compressors to achieve the desired pressures, while an underground method (Oxidyne process, Oxidyne patent) uses the natural hydraulic head of the fluid in a deep well to provide a significant source of

pressurization. In both, the organic is in the form of aqueous waste, while the oxidant could be obtained from a number of sources (e.g., air, oxygen, or hydrogen peroxide).

The above ground process can be generalized into seven major steps: feed preparation and pressurization; preheating; reaction; salt formation and separation; quenching, cooling and heat recovery; pressure letdown; effluent water polishing (Tester *et al.*, 1993)

An understanding of model compound reaction kinetics and mechanisms is essential in optimizing the SCWO process design. An isothermal, isobaric, plug-flow reactor has been constructed and used since 1983 to obtain global rate expressions from the correlated data (Helling and Tester, 1987, 1988; Webley *et al.*, 1991; Webley and Tester, 1991; Holgate, 1993). A diagram of the reactor apparatus is shown in Figure 1.1. Organic solutions (typically <1% by weight) and oxygen saturated water are pumped through the preheater system such that they attain the desired reaction conditions just prior to mixing. Upon mixing in the inlet of the coiled reactor, oxidation begins. Reactions occur under well-defined conditions of temperature, pressure, feed concentration, and residence time. Liquid-phase and gas-phase product flow rates are monitored and liquid and gaseous products are analyzed by gas chromatography, high performance liquid chromatography (with detection by UV absorption), and ion-electrode analysis.

1.2 Objectives

The objective of this investigation was to gather and analyze kinetic data on the oxidation of simple (model) compounds in supercritical water under well-defined experimental

Figure 1.1   Isothermal, Plug-Flow Reactor Apparatus.
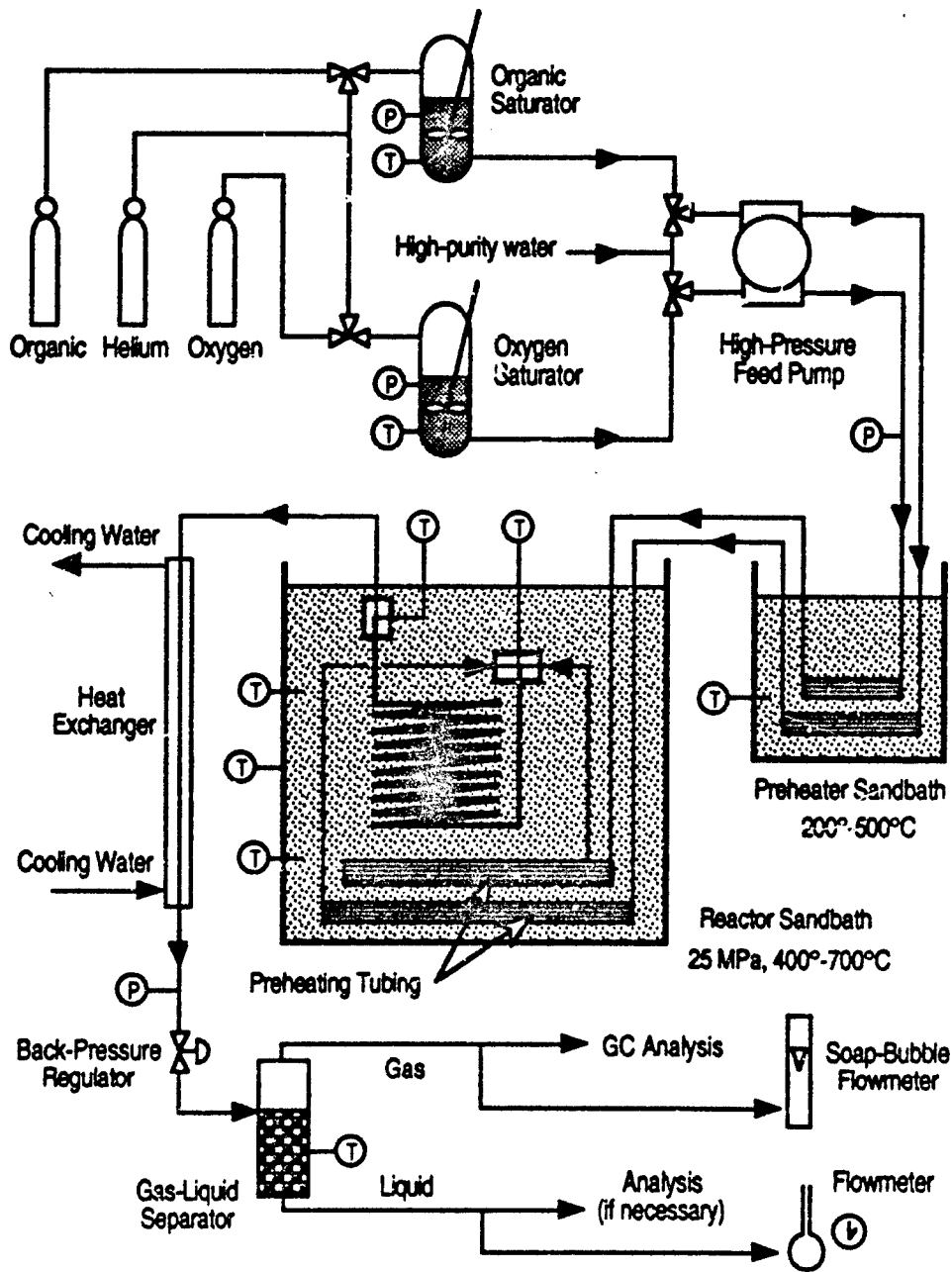
conditions. Specific objectives in augmenting the knowledge of supercritical water oxidation kinetics were as follows:

1. Investigate glucose oxidation in supercritical water.

2. Obtain kinetic data for acetic acid oxidation in supercritical water.

3. Obtain kinetic data for methylene chloride oxidation in supercritical water.

4. Identify the effects of pressure (density) on oxidation kinetics.

1.3 Glucose Hydrolysis and Oxidation in Supercritical Water

The hydrolysis and oxidation of glucose in supercritical water was undertaken collaboratively with Holgate (1993). Glucose, as a model compound of more complex cellulosic wastes, was fed to the reactor at an inlet concentration of 1×10^{-6} mol/cm^3 at reactor conditions of 246, 6 seconds residence time, and over a temperature range of 425 - 600 °C. Hydrolysis was performed by allowing pure water to flow through the oxygen side pump. To begin oxidation, the oxygen-side feed was switched to water with a stoichiometric feed concentration of 6×10^{-6} mol/cm^3 of oxygen. This allowed for direct comparison between hydrolysis and oxidation. Even in the absence of oxygen and at the lowest temperature investigated, glucose conversion was over 90%. This made kinetic measurements unattainable.

Significant amounts of gaseous product were produced in both hydrolysis and oxidation. For oxidation at 500 °C and above, 100% of the glucose carbon was in the form of a gaseous product. These products included CO, CO_2, CH_4, H_2, and smaller amounts of C_2H_4 and C_2H_6. A temperature of 600 °C was necessary to produce 100% gasification in the absence of oxygen (hydrolysis). Hydrolysis produced the same

aforementioned gases, but yielded almost entirely hydrogen and carbon dioxide. This is indicative of a fast, water-gas shift.

Hydrolysis also gave copious liquid products. Extensive testing via high performance liquid chromatography resulted in identification of some of the liquid products of hydrolysis. Liquid products identified included acetic acid, acetonylacetone, propenoic acid, and acetaldehyde. These products, along with carbon monoxide, methane, ethane, ethylene, and hydrogen, showed little change in product yield over a residence time variation of 5 to 10 seconds, indicating that they are the major, persistent intermediate products of glucose hydrolysis and oxidation.

1.4 Acetic Acid Hydrolysis and Oxidation in Supercritical Water

Acetic acid has been identified as a refractory intermediate in the oxidation of more complex organics (Ploos van Amstel and Rietema, 1970; Skaates *et al.*, 1981; Tongdhamachart, 1990; Shanableh, 1991; Holgate, 1993) at and near supercritical conditions. Because of its relative stability, acetic acid may be the destruction-limiting species in the path to total oxidation of an organic. Acetic acid's refractory nature has led many investigators to study its destruction via supercritical water oxidation (Wightman, 1981; Lee *et al.*, 1990; Wilmanns and Gloyna, 1990; Frisch, 1992), but most research has focused on measurements of destruction efficiency rather than product identification and reaction kinetics. In an effort to substantiate and improve on previous studies, characterization of the supercritical water oxidation of acetic acid was undertaken.

Ten hydrolysis and forty-five oxidation experiments were conducted in

supercritical water. Reactor temperatures spanned 425 - 600 °C, and residence times varied from 4.4 to 9.8 seconds. These experiments were conducted at 246 bar of pressure and the runs included both fuel-rich and fuel lean conditions. Multivariable, nonlinear regression of the oxidation data yielded the following rate expression:

$$R_{CH_3COOH} = 10^{9.9\pm1.7} \exp(\frac{168\pm21}{RT}) [CH_3COOH]^{0.72\pm0.15} [O_2]^{0.27\pm0.15}$$

This expression was in close agreement with Frisch (1992), but refined his assumption of zero-order oxygen dependence, and corroborated a similarly fractional order oxygen dependence seen by Lee (1990), who used hydrogen peroxide as the oxidant. As observed by Holgate (1993) with hydrogen and carbon monoxide oxidation in supercritical water, acetic acid oxidation possessed a distinct induction time, which is a strong indication of a free radical mechanism. This is portrayed in Figure 1.2.

Despite its reputation as refractory compound, a considerable (35%) amount of acetic acid was destroyed at temperature of 600 °C, pressure of 246 bar, and 8 seconds reactor residence time.

Two sets of experiments were conducted to determine the effect of pressure (water density) on acetic acid oxidation. Results indicate that acetic acid oxidation kinetics are less influenced by pressure than other previously studied compounds.

Product identification was such that almost all oxidation runs had a carbon balance closure >90%. Identification of hydrolysis liquid products, like glucose were less successful.

Figure 1.2 **Normalized Decay Profiles for Stoichiometric Oxidation of Acetic Acid in Supercritical Water, Showing Induction Times. Curves are exponential fits to data points.**
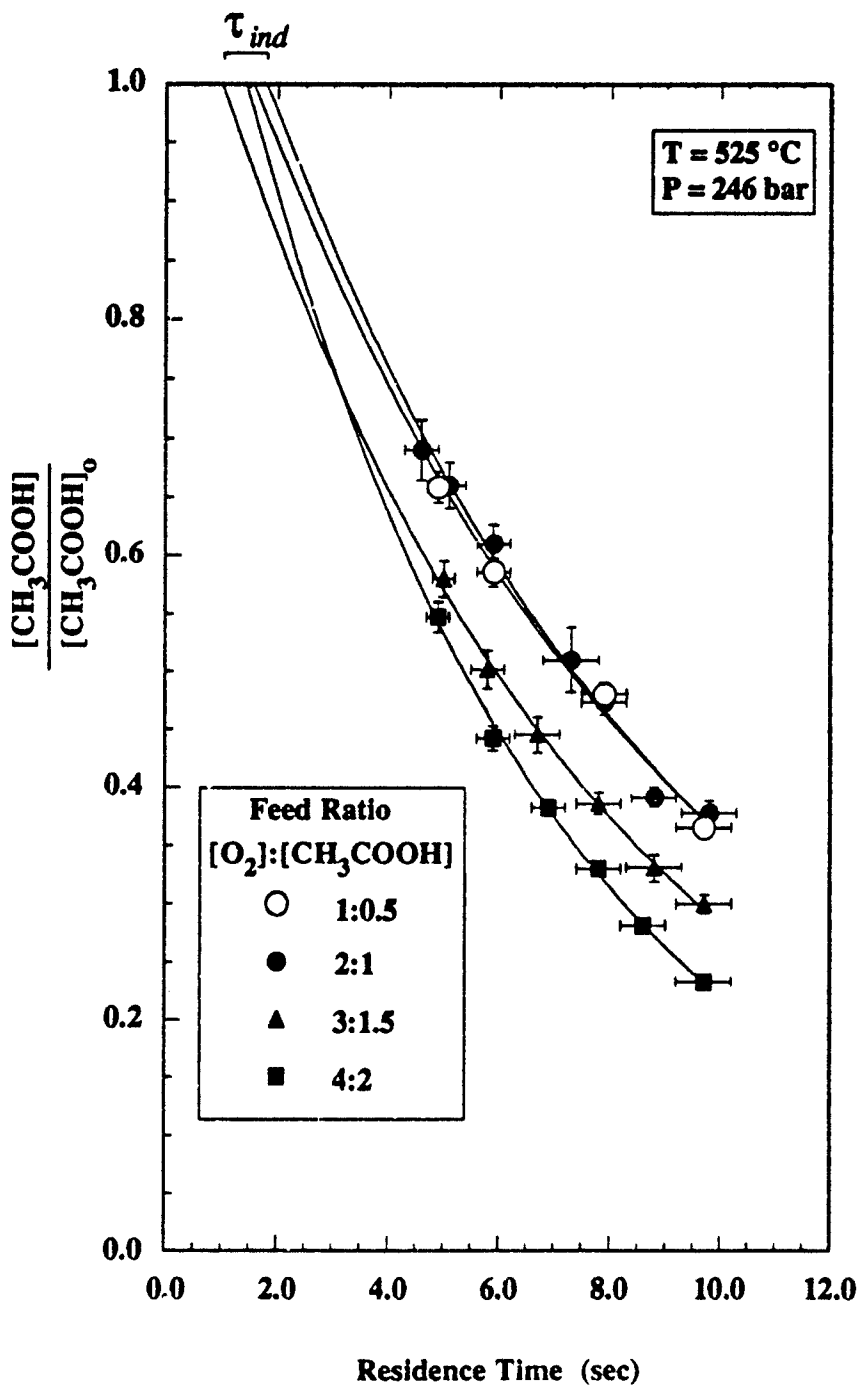
1.5 Methylene Chloride Hydrolysis and Oxidation in Supercritical Water

As a significant class of hazardous wastes, chlorinated hydrocarbons are excellent candidates for destruction via SCWO. In particular, methylene chloride (dichloromethane, methylene dichloride) is one of the more elementary chlorinated organics that is also a real-world contaminant. Its simple structure and chlorinated organic characteristics make it an excellent choice for study in a supercritical water environment.

Investigation of CH_2Cl_2 kinetics in supercritical water marked the first time a chlorinated compound had been studied in our reactor apparatus. It also was the first time we observed physical evidence of corrosion.

Thirty-four oxidation runs were conducted at a constant pressure of 246 bar. Temperatures ranged from 450 - 575 °C, although 23 of the oxidation experiments were carried out at 525 °C and seven at 500 °C to study concentration and density effects. Reactor residence times spanned 4.4 to 10.8 seconds. Initial concentrations of methylene chloride in the reactor were from 2.01×10^{-6} mol/cm^3 down to 7.22×10^{-7} mol/cm^3, while inlet oxygen concentrations varied between 2.02×10^{-8} (hydrolysis) and 2.08×10^{-6} mol/cm^3. These concentrations resulted in inlet molar oxygen-to-methylene chloride ratios from 0.019 (hydrolysis) to 2.21 (oxygen-rich), where the stoichiometric oxidation ratio is 1.00. Conversions ranged from $38.3 \pm 8.8\%$ to complete (100%) methylene chloride destruction (within analytical detection limits).

The global rate expression obtained for the oxidation of methylene chloride in

supercritical water was:

$$R_{CH_2Cl_2} = 10^{8.5\pm2.1} \exp(\frac{-142\pm32}{RT})\ [CH_2Cl_2]$$

Hydrolysis played a major role in CH_2Cl_2 destruction. In the absence of oxygen, CH_2Cl_2 conversion was approximately 45% at even the lowest temperature (450 °C), and rose to 80% at 600 °C and 6 seconds reactor residence time. Conversion under oxidizing conditions were little better than hydrolysis conversion in the temperature range 450 - 525 °C, indicating oxygen may preferential react with CH_2Cl_2 hydrolysis products rather than CH_2Cl_2 itself. Suspiciously, the methylene chloride conversion remained near 50% over nearly a 100 °C temperature range. Gaseous and liquid hydrolysis chromatograms are shown in Figure 1.3, and indicate that despite being a medium for destruction of wastes, constructive chemistry is also possible in supercritical water.

Figure 1.4 illustrates that extrapolation of data to time $t = 0$ suggests ignition delay. Reactor liquid effluent was highly acidic (pH of 1.0 - 2.0), with chloride ion concentrations doubling over the residence time range of 4.5 to 10 seconds.

No chlorinated products were detected in the gas-phase effluent and carbon monoxide selectivity was high, even in the presence of excess oxygen feed.

Although our method of detecting chlorinated products gave reproducible results, not all liquid products were identified, and carbon and chlorine material balance closures were generally poor (50 -70%).

Coloring of liquid effluent occurred any time pure water was fed to the reactor, following oxidation experiments. This effluent was the color of "creamed coffee" and

Figure 1.3   Gas and Liquid Chromatograms for CH_2Cl_2 Hydrolysis at 575 °C, 246 bar, and Residence Time of 6 Seconds. $[CH_2Cl_2]_o = 1 \times 10^{-6}$ mol/cm^3, $[O_2]_o = 1 \times 10^{-6}$ mol/cm^3.
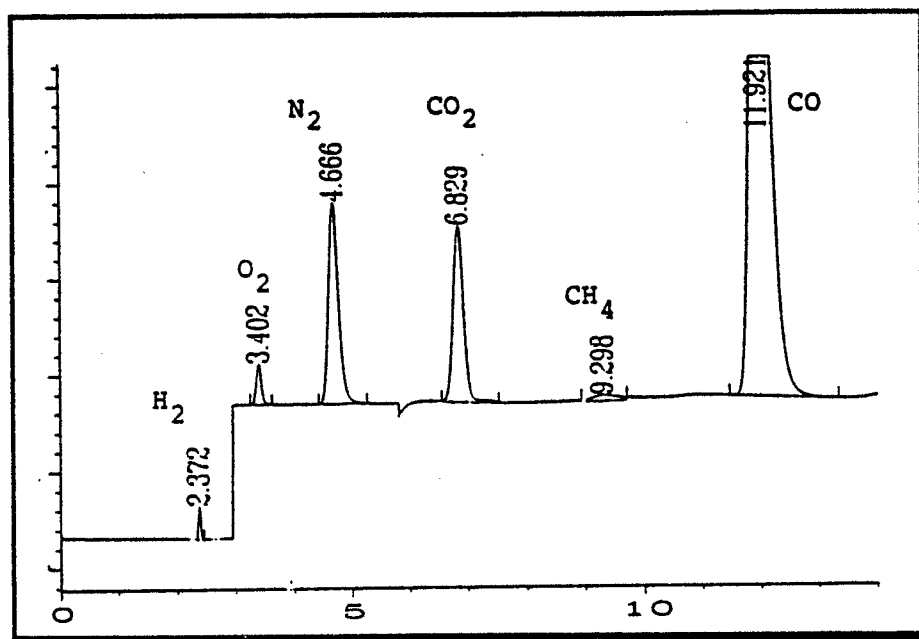
Hydrolysis Gas Chromatogram
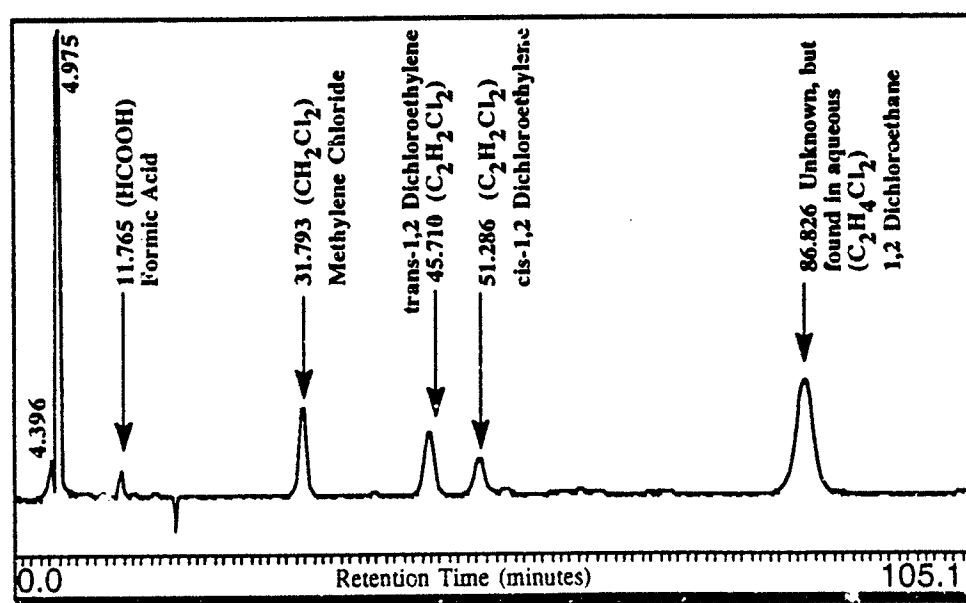
Hydrolysis Liquid Chromatogram

Figure 1.4   **Normalized Decay Profiles for Stoichiometric Oxidation of Methylene Chloride in Supercritical Water at 525 °C and 246 bar, Showing Induction Times.** Conditions as in Figure 7.6, but concentration ordinate is on alogarithmic scale. Lines are linear fits to data, indicating exponential decay.
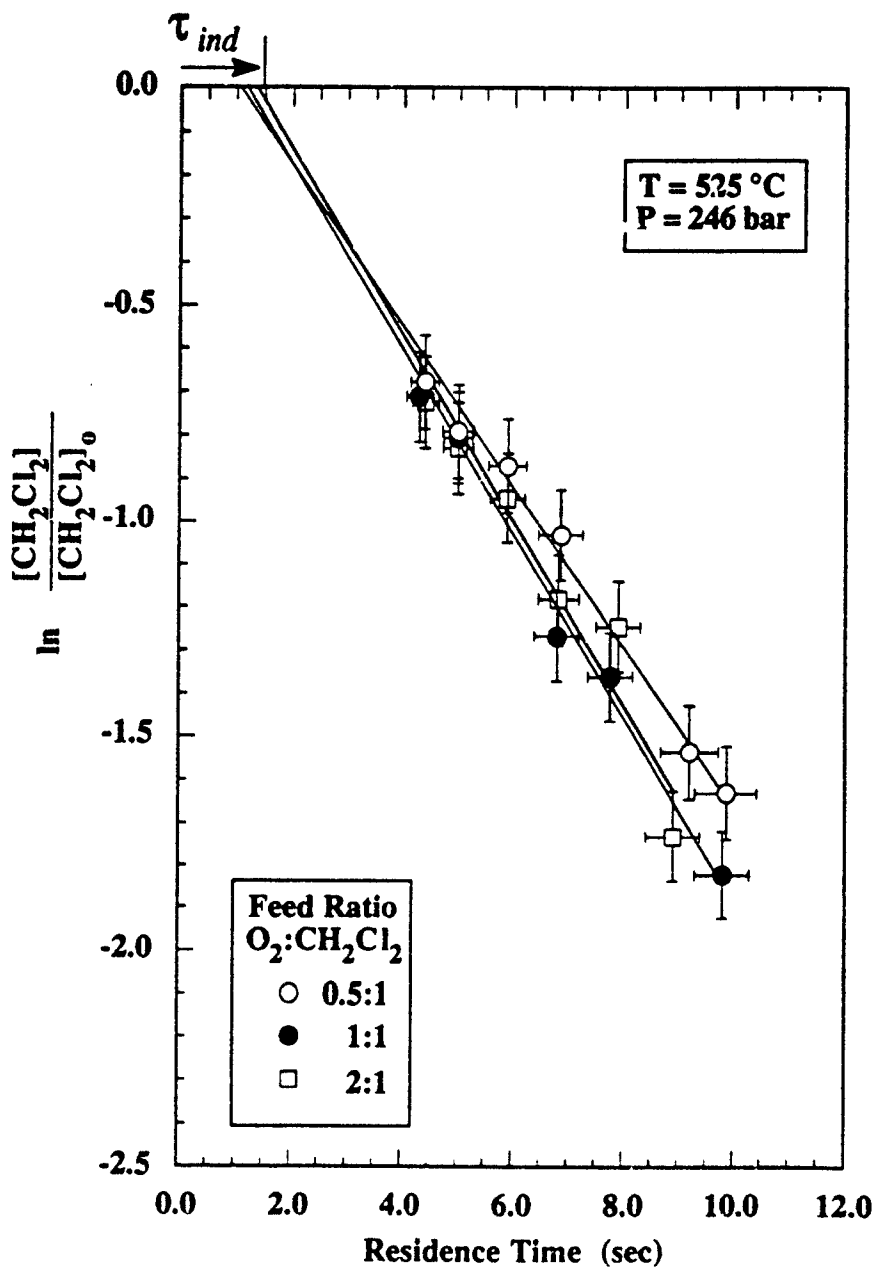
precipitate settled out of suspension. No discernable color change was evident in the liquid effluent during oxidation experiments. When initial methylene chloride concentration was doubled to 2×10^{-6} mol/cm³, the liquid effluent did acquire a distinct, but pale yellow taint. Analysis of the precipitate identified nickel, iron, and chromium among the components.

1.6 Conclusions

1. Glucose hydrolysis and oxidation. Glucose is quickly destroyed under hydrolysis and oxidative conditions in supercritical water. Both reactions produce significant gasification, although oxygen accelerates destruction of the intermediate products. Reaction kinetics were too fast under our operating conditions in our reactor apparatus to obtain a global rate expression. Major intermediate products in the liquid-phase of glucose hydrolysis and oxidation are acetic acid, acetonylacetone, propenoic acid, and acetaldehyde. Gas-phase intermediate products are carbon monoxide, methane, ethane, ethylene, and hydrogen.

2. Measurement of oxidation kinetics. The oxidation kinetics of acetic acid were examined at 246 bar and 425 - 600 °C and over an extended range of fuel equivalence ratios. Over the range studied, the reaction is nearly first-order (0.72 ± 0.15) in acetic acid and fractionally (0.27 ± 0.15) dependent on oxygen, with an activation energy of 168 ± 21 kJ/mol. Methylene chloride oxidation is first-order in CH_2Cl_2 with an activation energy of 142 ± 32 kJ/mole. Methylene chloride hydrolysis plays a significant role in the destruction of CH_2Cl_2 in supercritical water.

3. Identification of induction times. As found in previous studies of model compound

oxidation in supercritical water (Holgate, 1993), acetic acid and methylene chloride exhibit a delayed reaction ignition, or induction time. This is indicative of free-radical mechanisms and complicates global reaction modeling.

4. Effects of operating pressure. Acetic acid oxidation is less pressure (water density) dependent than carbon monoxide or hydrogen (Holgate, 1993).

5. Corrosion. Methylene chloride oxidation and hydrolysis in supercritical water can cause visible signs of corrosion.

1.7 Recommendations

1. Changes to the current apparatus system, or construction of a new system are necessary to widen the operating conditions (namely, concentrations and residence time). Larger diameter reactors would decrease surface effects observed by Holgate (1993). Use of higher capacity feed pumps would also require more heating capacity than currently available with the present fluidized sand bath, and more cooling capacity than the current shell-and-tube countercurrent heat exchanger.

2. Dedication of an analytical lab facility or analytical chemist is needed. Although SCWO of compounds rapidly destroys many compounds, identification of refractory products and intermediates is needed to fully characterize reaction mechanisms. Positive identification of intermediates and products will require more sophisticated analytical techniques, such as liquid chromatography with mass spectrometry.

3. A packed reactor currently available in our lab should be used to investigate what effects reactor inner walls may have played in determining oxidation kinetics of acetic acid and methylene chloride.

4. More studies are needed to verify pressure effects of acetic acid oxidation in supercritical water. Pressure effect experiments are also needed to determine methylene chloride reaction response to changes in water density (concentration).

5. Lower operating pressures and/or temperatures are needed to quantify the global oxidation kinetics for glucose. Experiments in the subcritical regime (wet-air oxidation) may be sufficient to destroy glucose and, hence, cellulosic wastes.

6. Verification of the importance of hydrolysis in conversion of CH_2Cl_2 is needed, particularly over varying temperatures in the 450-550 °C temperature regime. Residence time studies at lower ($\sim$450 °C) temperatures and/or pressures may be needed to characterize oxidation and hydrolysis over the full range of conversion. Recalculation of carbon and chlorine balances upon identification of the liquid chromatography peak with 86.7 minute elution time should be done to determine if product effluent has been well characterized.

7. With a general understanding of global reaction rates and products for a growing list of model compounds, co-oxidation should be studied to investigate what kinetic effects (if any) compounds have on each other. This is more representative of the SCWO process, where mixtures rather than pure components of hazardous wastes are more likely to be processed.

8. The database of kinetic studies and products of model compound oxidation in supercritical water should be continued. Identified persistent intermediates should be added to a priority list of compounds to investigate. Investigation of additional model compounds containing nitrogen, sulfur, and phosphorus heteroatoms still represent an

important class of wastes that have not been adequately studied.

9. The applicability of using other compounds as a hydroxyl radical sources should be explored. Specifically, hydrogen peroxide has already been used and shows some enhancement of the oxidation process. Understanding of fundamental oxidation mechanisms could be improved through a careful study of this enhancement.

Chapter 2
Introduction and Background

In the absence of comprehensive pollution prevention technologies and the ability to completely recycle process by-products, destruction of hazardous wastes is a necessity. Growing interests in effective and economically feasible methods to destroy toxic wastes has motivated numerous universities and companies to investigate the oxidation of such wastes in supercritical water following the invention of the concept at the Massachusetts Institute of Technology in the mid-1970's (Amin *et al.*, 1975). Supercritical water oxidation (SCWO) exhibits improvement over incineration and other traditional thermal destruction technologies by providing rapid and complete oxidation in a contained system without forming toxic byproducts (Swallow *et al.*, 1989; Modell, 1989; Thomason *et al.*, 1990). The application of SCWO technology to other waste treatment problems has also been investigated. These include processing human metabolic waste for use on long-term space missions (Timberlake *et al.*, 1982; Hong *et al.*, 1987, 1988); processing pulp mill sludges (Modell, *et al.*, 1992); and as an alternative to incineration in the destruction of military toxic wastes, including chemical agents, explosives, and propellants (Buelow *et al.*, 1990, 1992; Blank, 1992). A complete review of SCWO process technology and fundamental research by Tester *et al.* (1993) is contained in a recent American Chemical Society monograph .

2.1 Properties of Supercritical Water

Water in a supercritical condition behaves quite differently than at standard conditions,

in particular, its solvation characteristics change drastically. At the critical point (374 °C, 22.1 MPa) water has a density of approximately 0.39 g/cm^3, which is between that of ambient liquid water (1 g/cm^3) and low-pressure steam (< 0.001 g/cm^3). In the SCWO process, at pressures of 230 - 250 bar and temperatures between 400 and 600 °C, the density ranges from 0.13 to 0.07 g/cm^3. Water's static dielectric constant at 26 MPa decreases from a value of 80 at room temperature to approximately 5 or 10 near the critical point, and finally to about 2 or lower at temperatures above 450 °C (Tester, *et al.*, 1993). As seen in Figure 2.1, at 25 MPa the ionic dissociation constant (K_w = [H^+] [OH^-]) falls from an ambient value of 10^{-14} to 10^{-18} near the critical point, and to 10^{-23} above the supercritical region. Investigation reveals only a small amount of hydrogen bonding in the supercritical region. The overall result of these properties is that supercritical water acts as a non-polar dense gas that has solvation properties similar to low polarity organics. Hence, hydrocarbons and gases (e.g., O_2, N_2, CO_2, etc.) are highly soluble and usually completely miscible under typical SCWO operating conditions.

As would be predicted by a low dielectric constant and low ionic dissociation constant, ionic species, namely inorganic salts, are practically insoluble in supercritical water. Additionally, SCW has a high diffusivity (Tödheide, 1972; Lamb *et al.*, 1981) and low viscosity (Todheide, 1972; Dudziak and Franck, 1966).

With no interphase mass transport limitations and sufficiently high temperatures, the kinetics of organic oxidation in SCW are fast and complete. Hydrocarbon oxidation products consist of CO_2 and H_2O, while heteroatoms (F, Cl, S, P) are

Figure 2.1   Solvation Properties of Pure Water at 25 MPa. Properties shown are the dielectric constant ϵ (Uematsu and Frank, 1980) and the ionic dissociation constant K_w (Marshall and Franck, 1981).
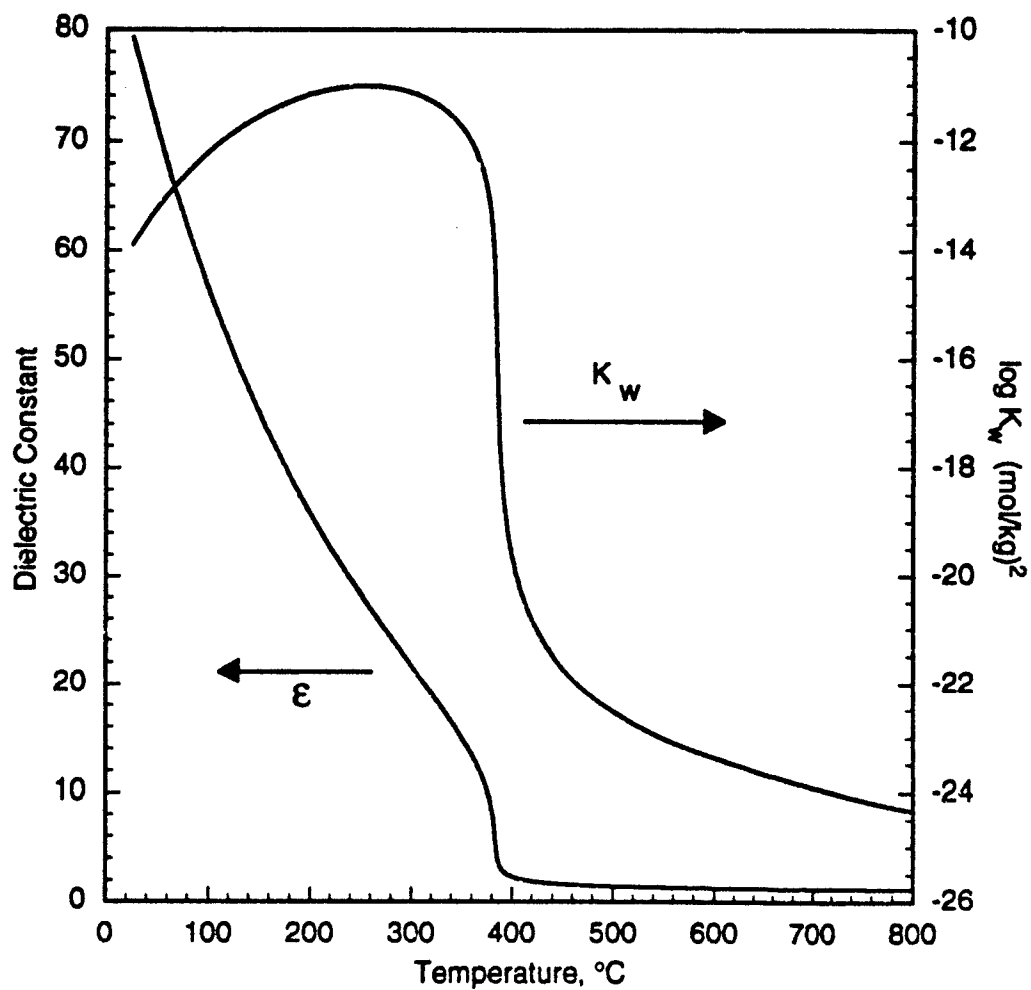
usually converted to mineral acids, or insoluble salts in the presence of neutralizing caustic. Despite high enough temperatures for rapid kinetics, supercritical temperatures are low enough to preclude formation of NO_x or SO_2 (Killilea *et al.*, 1991).

2.2 SCWO Process Description

A general description of the SCWO process is provided by Tester *et al.* (1993) and is paraphrased here.

Two types of SCWO processes exist. The above-ground method (MODAR process, Modell patent) uses high pressure pumps or compressors to achieve the desired pressures, while an underground method (Oxidyne process, Oxidyne patent) uses the natural hydraulic head of the fluid in a deep well to provide a significant source of pressurization. In both, the organic is in the form of aqueous waste, while the oxidant could be obtained from a number of sources (air, oxygen, or hydrogen peroxide).

The MODAR process is depicted in Figure 2.2 and can be generalized into seven major steps.

Feed preparation and pressurization consists of compressing the aqueous liquid waste and oxidant to reactor pressure. Due to process design considerations, the aqueous liquid waste has an upper heating value limit (4200 kJ/kg) that can be controlled by adding water to a high heating-value waste. When the aqueous waste has too low a heating value, higher heating-value wastes or fuels can be added to make the lower-valued waste economical for destruction. When the organic feed contains heteroatoms (e.g., Cl, F, P, or S), caustic is injected to neutralize the acids formed. Therefore, salts of these acids are a by-product. The oxidant can be in the form of compressed air,

**Figure 2.2   MODAR Process Flow Sheet with Heat Recuperation but No Recycle.
Adapted from Barner *et al.*, 1991.**
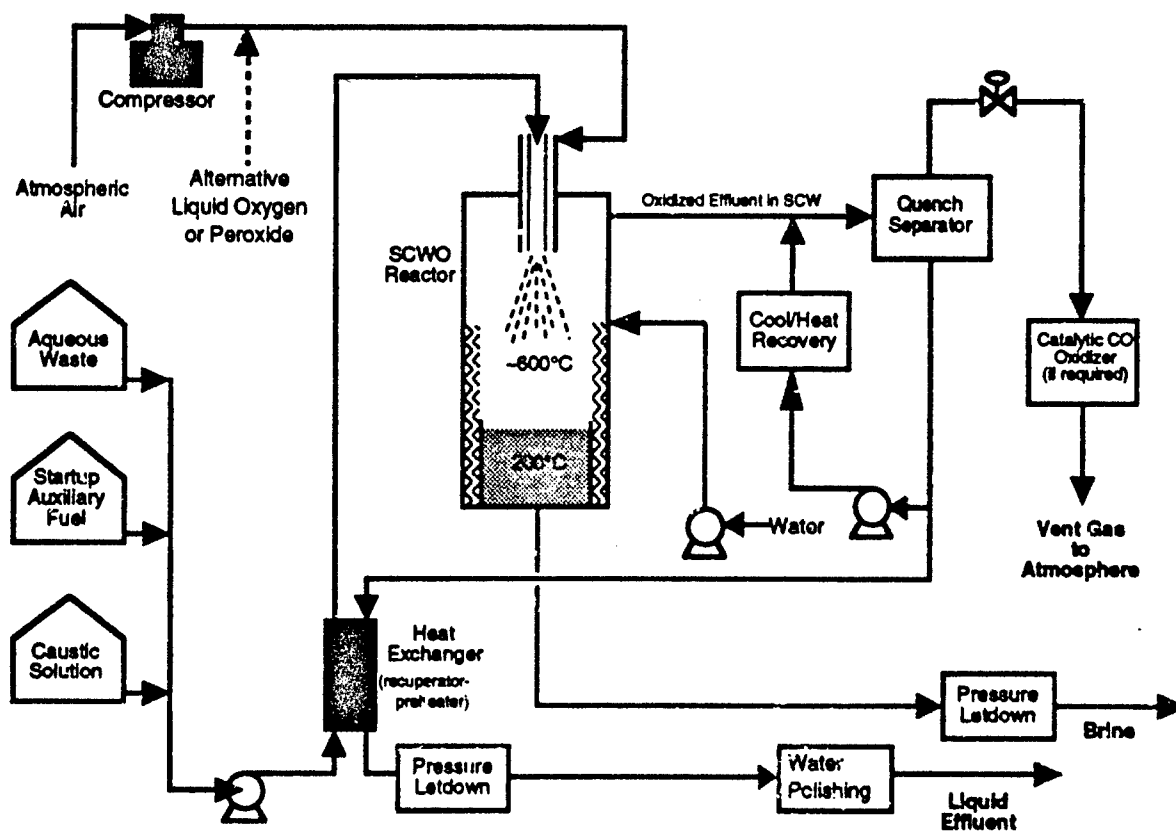
gaseous or liquid oxygen, or hydrogen peroxide. These are pressurized to reactor conditions prior to being fed to the reactor.

Preheating of the oxidant and organic can be accomplished by heat exchange with the hot reactor effluent. Preheating helps in rapid initiation of the oxidation reaction and optimizes plant efficiency through heat integration.

The *reaction* itself is initiated by the mixing of the pressurized, preheated organic and oxidant. This exothermic reaction heats the reactor temperature to about 550 - 600 °C, further accelerating the reaction and reducing the reactor residence time needed for complete destruction of the organic. Highly toxic or refractory compounds can be destroyed to even higher efficiencies via a second stage reactor or recycle.

Salt formation and separation is a critical step in the process. Salts are formed from the neutralization of acids resulting from the oxidation of heteroatoms. They precipitate rapidly due to their virtual insolubility (~ 100 ppm or less) in supercritical water. These salts can be separated by removing them as solids as they fall to the bottom of the reactor or by redissolving the salts and removing a liquid brine. A small fraction of salt is entrained in the overhead effluent.

In the *quenching, cooling and heat recovery stage,* gaseous effluent exits the top of the reactor. The remaining reactor effluent consists of supercritical water, carbon dioxide, a small amount of entrained salt, and possibly some nitrogen. This mixture is first mixed with cold water to redissolve the salt and then is further cooled and discharged at atmospheric conditions. Thermal energy recovery from the effluent can be achieved in numerous ways and used for heating needs or to produce electricity.

After *pressure letdown*, the cooled effluent separates into liquid and gaseous phases. The gas phase is comprised primarily of carbon dioxide and oxygen (when oxidant is used in excess of the amount required for complete oxidation). If air is used as the oxidant, nitrogen is also present. This phase disengagement is carried out in multiple stages in order to minimize corrosion and maximize separation.

Effluent water polishing may be necessary if heavy metals are entrained in the organic feed. Ion exchange or selective adsorption may be needed.

The underground SCWO process is not discussed in detail here. For a more in-depth discussion see Gloyna (1989). One noteworthy characteristic of the underground process is that the savings accrued from *in situ* pressurization in this process are unfortunately offset by other losses, such as heat loss to the surrounding rock formation and startup energy requirements.

The objective of this investigation was to gather and analyze kinetic data on the oxidation of simple (model) compounds in supercritical water under well-defined experimental conditions. Specific objectives in augmenting the knowledge of supercritical water oxidation kinetics were as follows:

1. Investigate glucose oxidation in supercritical water. Treating cellulosic wastes and sludges has many possible advantages over current techniques. Complete oxidation of CO_2, H_2O, and N_2 can be performed along with significant recovery of waste heating value, without the need to add auxiliary fuel or remove water from the sludge (Hossain and Blaney, 1991; Modell et al., 1992; Takahashi et al., 1989). Wet air oxidation of glucose has also been investigated (Ploos van Amstel and Rietema, 1970; Brett and Gurnham, 1973; Skaates, et al., 1981), but extrapolation of these subcritical results to the supercritical regime would be suspect.

Glucose ($C_6H_{12}O_6$) provides the important chemical structure characteristic of more complex sludges and cellulosic wastes, and thus can serve as a model compound for SCWO. Although the aforementioned studies have been conducted to determine destruction efficiency on these types of wastes, they do not characterize oxidation kinetics. Few glucose oxidation studies identify product compounds or yields of products. In general, the oxidation kinetics of glucose is not well characterized or

understood. Therefore, careful study of glucose oxidation in supercritical water was undertaken to provide better understanding of kinetics and reaction pathways as well as to identify intermediate products.

2. Obtain kinetic data for acetic acid oxidation in supercritical water. Acetic acid (CH_3COOH) represents a logical progression in molecular complexity in our group's continuing study of model compound oxidation in SCW (Tester *et al.*, 1993). In addition, acetic acid has been identified as a refractory intermediate in the oxidation of more complex organics such as glucose and cellulose (Ploos van Amstel and Rietema, 1970; Holgate, 1993). Other investigations into the SCWO of acetic acid (Wightman, 1981; Lee *et al.*, 1990; Wilmanns and Gloyna, 1990; Frisch, 1992) were done with less well-controlled experimental conditions and thus were more susceptible to experimental and systemic errors. Accurate characterization of the oxidation kinetics of acetic acid as a simple, refractory molecule is important in SCWO optimization.

3. Obtain kinetic data for methylene chloride oxidation in supercritical water. An important class of waste whose oxidation kinetics in SCW have not yet been fully investigated are compounds containing heteroatoms, such as chlorine, nitrogen, sulfur, and phosphorus. Selection of methylene chloride (dichloromethan , CH_2Cl_2) as a simple chlorinated compound is a logical step in the broadening of our kinetics database. It also represents a real world pollutant found in soils, sediments, and water. Thus, its individual oxidation kinetics need to be characterized prior to a study of its destruction

via SCWO in heterogeneous mixtures such as a soil slurry or in co-oxidation studies. Characterization of the kinetics of oxidizing the C-Cl bond of CH_2Cl_2 should provide important insight into the behavior of other more complex chlorinated compounds.

4. Identify the effects of pressure (density) on oxidation kinetics. Potential advantages of operating the SCWO process at lower, even subcritical pressures, but at temperatures above the critical temperature of pure water (374 °C), have been proposed by Hong (1992) (so-called "semicritical" water oxidation). Correlations between operating pressure and oxidation rates in SCWO are just beginning to be developed (Holgate, 1993). This objective addresses the effect of water density on the kinetics of oxidation. Kinetics will be studied by varying operating pressure at specified conditions of composition, temperature and residence time.

Chapter 4

Experimental Techniques

4.1 Apparatus

The experimental apparatus used in this research was the isobaric, isothermal plug-flow reactor used and described in similar supercritical water oxidation studies at MIT by previous investigators (Helling, 1986; Webley, 1989; Holgate, 1993) and is shown in Figure 4.1. Many improvements have been made to the apparatus throughout the years, but the current configuration shown in Figure 4.1 is exactly as that described by Holgate (1993). Reiteration of that description is provided here for documentation completeness.

Feed solutions are prepared in two, three-liter tanks (saturators) made of stainless steel (Hoke 8HD3000, maximum pressure 1800 psig). Approximately 2500 mL of high-purity water (Barnstead NANOpure water purification system) is placed into each saturator. Oxygen (Airco) pressure in the oxygen saturator is adjusted to achieve the desired concentration. A single-head, positive-displacement pump (LDC Analytical/Milton Roy minipump) circulates the water throughout the saturator. Overnight agitation circulates approximately twice the saturator volume, helping to achieve equilibrium. The relatively low solubility of oxygen in water, maximum oxygen pressure and maximum pump flow rate limit the concentration of oxygen in the reactor to about 4×10^{-3} mol/cm^3 at 246 bar. Hence, reaction kinetics can only be investigated over a limited range of concentrations. Low concentrations, however, aid in the maintenance of reactor isothermality, as larger concentrations could produce radial or

Figure 4.1   Isothermal, Plug-Flow Reactor Apparatus. From Holgate (1993).
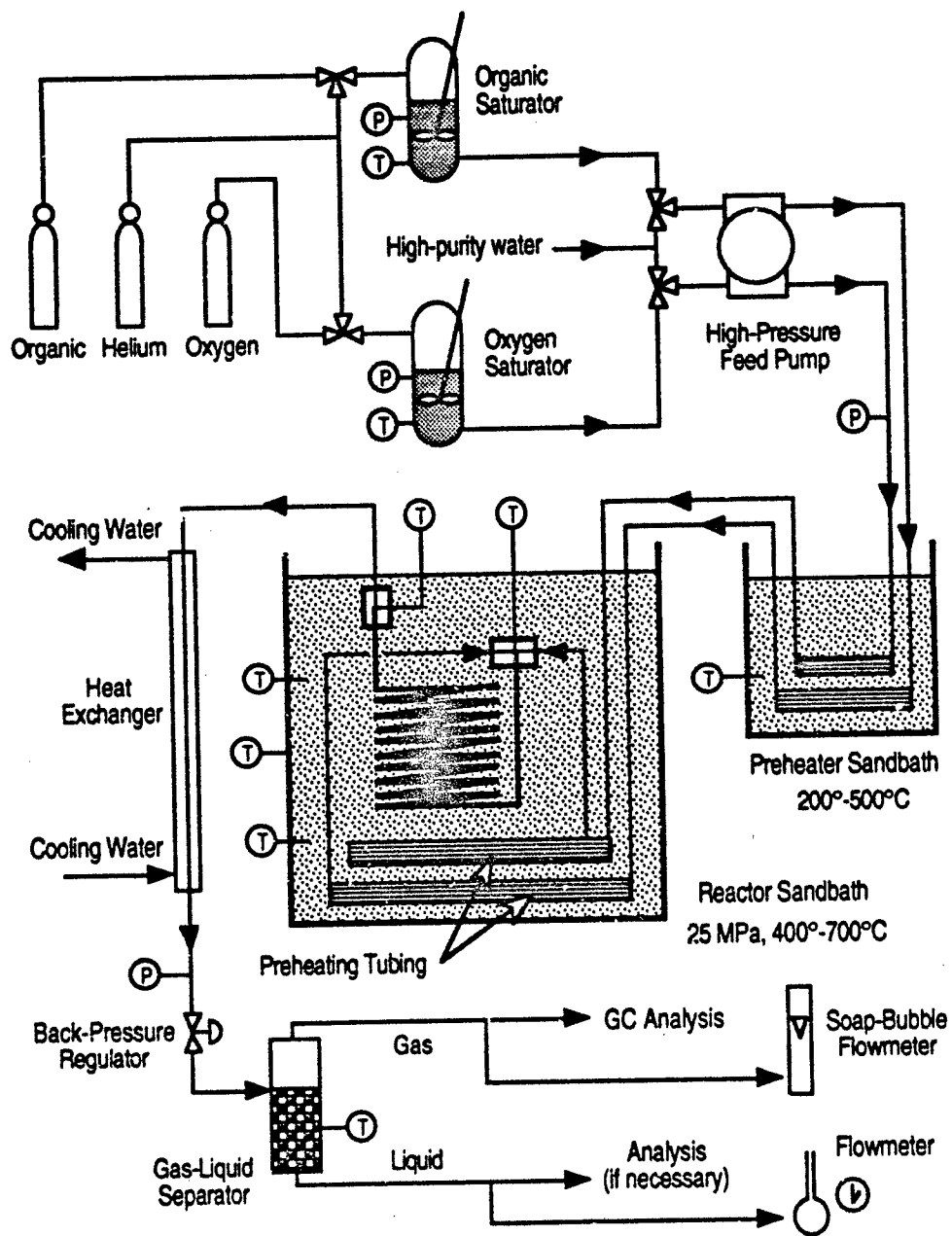
axial temperature gradients along the reactor due to the highly exothermic nature of the oxidation reactions. Organic feed preparation is similar to the oxygen feed preparation when the organic is gaseous at ambient conditions. But, in the case of glucose, acetic acid and methylene chloride, desired concentrations were prepared in aqueous solutions and loaded into the organic saturator. The relatively low solubility of methylene chloride in water (1.32 g/100 mL of water at 25 °C) constrained stoichiometric and organic-rich feed concentrations (rather than oxygen solubility) in the CH_2Cl_2 oxidation experiments. Rather than relying on gravity feed of organic solution to the high-pressure feed pump, the organic saturator is pressurized with low-pressure (10 psig) helium (Airco).

A high pressure, variable-speed, duplex feed pump (LDC Analytical/Milton Roy minipump) delivers feed solutions at operating pressure to the reactor. A back-pressure regulator (Tescom) at the end of the heat exchanger governs system pressure. Pressure is monitored by a pressure transducer (Dynisco μPR690, 0 - 10,000 psig) just upstream of the back-pressure regulator and by a pressure gauge (Omega Engineering, 0 - 7,500 psig range) just downstream of the feed pump. The readings of these two instruments assure that the pressure drop through the system is negligible relative to the operating pressures of 118 to 263 bar. Pure water (with headspace pressure of approximately 10 psig helium) is pumped through the reactor system during heatup. The flow is switched to oxygen and organic feeds once desired reactor conditions have been attained. The feeds pass separately through 1.5 m (5 ft.) of 1.59 mm (1/16 in.) 316 stainless steel tubing in the preheater fluidized sand bath (Techne). This sand bath normally operates at about 80% capacity (approximately 175 °C) and brings the separated feeds to

approximately 175 °C to lower the load on the final preheating step. The separated feeds are further preheated to reactor conditions in the reactor sand bath (Techne) using another 3.0 m (heated length 2.8 m) of 1.59 mm (1/16 in.) Hastelloy C276 tubing to ensure the desired reactor temperature is reached. Oxidation begins when the separated feeds are mixed via cross-injection in a Hastelloy C276 high-pressure cross fitting (High Pressure Equipment) at the entrance of the reactor. The cross fitting contains four ports - two horizontal, diametrically opposed feed injection ports; an upper vertical port that houses a 1.59 mm (1/16 in.), Inconel-sheathed, type K thermocouple (Omega Engineering); and a lower verticle port that attaches the reactor tubing. The thermocouple measures the mixing temperature. Another internal thermocouple (Inconel-sheathed, type K) is at the reactor exit. Externally, thermocouples (type K) are located at the top and bottom of the reactor. Typically, all thermocouple measurements are within 3 - 5 °C of each other and reactor entrance and exit temperatures are usually within 2 °C. A natural thermal gradient exists within the fluidized sand bath such that the top bath temperature is about 2 - 4 °C higher than the bottom. The average of the mixing temperature and the reactor exit fluid temperature is taken as the reactor temperature.

The reactor is a coiled tube, 4.71 m long, with an inner diameter of 1.71 mm (0.067 in.) and an outer diameter of 6.35 mm (1/4 in.). It is made of Inconel 625 and has a total internal volume (including fittings at the entrance and exit) of 11.11 cm^3. Flows in the reactor are maintained in the turbulent or transition region (Reynolds number > 2100) ensuring relatively flat concentration and velocity profiles. The

supercritical reactions are immediately quenched upon exiting the reactor via a shell-and-tube countercurrent heat exchanger that is water-cooled. The effluent then passes through the back pressure regulator and is reduced to ambient pressure. A gas-liquid separator divides the two phases. It is assumed the two streams are in equilibrium when they separate. Gas flow rate is measured with a soap-bubble flowmeter and the liquid flow rate is measured by noting the time required to fill a flask of specified volume.

4.2 Analytical Procedures

Liquid effluent analysis was done by isocratic high-performance liquid chromatography. A Rainin HPXL solvent delivery system with an Interaction ORH-801 analysis column and Interaction Ionguard guard column was used. A Rainin Dynamax UV-1 UV/visible detector was also used, at wavelengths of 210 and 290 nm. A Timberline column heater maintained column temperature at 65°C. The mobile phase was 0.002 M H_2SO_4 delivered at 0.5 mL/min. Sample injection volumes were 100 μL. This setup and method were developed by Swallow and Holgate (1993). The entire HPLC system was interfaced to a Macintosh IIsi for data acquisition and analysis. Peaks were identified by injecting standard solutions of pure compounds and comparing retention times. Following peak identification, the HPLC was calibrated using varying concentrations of each pure compound that matched the experimental retention time. Peak height and area gave equally good results, but peak height was used for quantification since occasional peak overlap occurred and distorted peak area. These procedures are discussed in detail in Section 5.2 HPLC analysis was typically done within a few hours of sample collection with acetic acid, but due to the long run times in glucose and (especially) methylene

chloride product analysis, some samples were not analyzed until the next day. All liquid product effluent samples were analyzed within 24 hours of collection.

Two gas chromatographs (GCs) were used to analyze the gaseous effluent. All gases except hydrogen and helium were analyzed with a Hewlett Packard 5890 Series II GC, equipped with thermal conductivity and flame ionization detectors. This was interfaced with a Hewlett Packard Vectra 386/25 computer for data acquisition and analysis. Thermal conductivity was used exclusively to detect O_2, N_2, CO_2, C_2H_4, C_2H_6, CH_4, C_2H_2, and CO (order of elution). The setup included two columns, a 12 ft. × 1/8 in. stainless steel column packed with 80/100 Poropak T (Column I) and an 8 ft. × 1/8 in. stainless steel column packed with 60/80 mesh molecular sieve 5A (Column II), connected through an air actuated switching valve. The carrier gas (helium) flow rate was 20 mL/min. The method used (developed by Helling, 1986 and Webley, 1989) was to hold the oven temperature at 60°C for 7 minutes, then increase the temperature at a rate of 40°C/min. to 100°C. Once the oven temperature reached 100°C, it was held for 6 minutes, making the total method time 14 minutes. The switching employed allowed samples to pass through Column I and Column II initially; immediately after the elution of N_2 and O_2, the valve (and order of columns) is switched so that CO and CH_4 pass through columns I, II, and I a second time, while CO_2 and the other gases pass through a single column (Column I). At very high CO_2 concentration, a small C_2H_4 peak can be lost; otherwise, this method provides excellent peak separation and resolution.

A second GC was employed to detect hydrogen and helium. Hydrogen's thermal

conductivity is similar to the helium carrier gas used in the aforementioned method and is therefore only detectable in large quantities. This Perkin Elmer Sigma 1B GC used nitrogen as the carrier gas and thereby was very sensitive to trace amounts of hydrogen and helium. Trace helium amounts were occasionally observed because the saturator liquids were pressurized with helium in loading the saturators; additionally, the pure water feed and organic solutions were pressurized with helium during the heatup and reaction times, respectively. The method employed used a constant oven temperature of 60°C with a carrier gas (nitrogen) flow rate of 40 mL/min. for a duration of 7 minutes.

Actual gases were used to volumetrically calibrate both GCs. During actual runs, a 200 μL sample of gaseous effluent was taken and injected into the Hewlett-Packard GC. Another 200 μL sample was immediately taken and injected into the Perkin Elmer GC. At the end of analytical method run times, this dual sampling procedure was repeated. During a typical run, 4 to 6 samples were injected into each GC. Gas composition (mole fractions) was calculated from the volume fractions (volume of an individual gas divided by the sum of the volumes of all gases). Final gas compositions for an experiment were typically averaged over four to six sets of dual sample analyses.

Glucose concentrations were determined using a standard enzymatic technique (Sigma Chemical Co.) and spectrophotometer. In the analytical technique, glucose is converted by hexokinase to glucose-6-phosphate, which is then consumed by glucose-6-phosphate dehydrogenase with concurrent conversion of NAD to NADH. The resulting NADH concentration is equivalent to the original glucose concentration. The NADH concentration was determined by its absorption at 340 nm using a UV/visible

spectrophotometer (Shimadzu UV160U). This method is glucose specific and not easily subject to interference by other compounds. Detectability with this method was as low as 5×10^{-5} moles of glucose per liter of effluent.

Measurement of chloride ion concentration in the liquid product of methylene chloride hydrolysis and oxidation was done by using an ORION Model 96-17B Combination Chloride Electrode in conjunction with an ORION Model 701A digital pH/mV meter. The electrode has a low-level calibration detectability limit of 1.0×10^{-5} mol/L chloride concentration and is accurate to an upper limit of approximately 1×10^{-2} mol/L. The pH/mV meter covers the range of ± 1999.9 mV with ± 0.1 mV precision. Since most of our product effluent was near the upper detectability limit, our samples were diluted to one-tenth their effluent concentration prior to analysis. This reduced variability in our voltage readings. Higher-level (linear) calibrations were made using five NaCl solutions of known concentration. Low-level (non-linear) serial calibration was accomplished as per the electrode's instruction manual. Calibration was periodically checked throughout the day. If the calibration drifted by more than .3 mV ($\sim 10^{-5}$ mol/L), the apparatus was recalibrated. Samples were allowed to collect 2 - 3 days before chloride analysis.

4.3 Data Reduction

Calculations used in data analysis have been expounded on by Helling (1986), Webley (1989), and Holgate (1993) and an in-depth presentation can be found in these authors' works. An overview of important assumptions and calculations is given here for document completeness.

Equilibrium between the gas and liquid phases is assumed once the effluents have exited the gas-liquid separator. The total gaseous molar flow rate must include gas dissolved in the liquid effluent as well as the gas flow measured via the bubble-flow meter. Liquid-phase composition is determined from the measured gas-phase composition by Henry's law:

$$y_i \, \phi_i \, P = H_i(T,P) \, x_i \qquad (4.1)$$

where y_i = gas-phase mole fraction of species i

ϕ_i = gas-phase fugacity coefficient

P = pressure

$H_i(T,P)$ = Henry's law constant

x_i = liquid-phase mole fraction of species i

and x_i is the desired quantity. The gas-phase mole fraction is determined by gas chromatography, and since the exit pressure is ambient, ϕ_i is set to unity. Henry's law constants are functions of temperature near ambient and were obtained for oxygen (Benson *et al.*, 1979), carbon monoxide (Rettich *et al.*, 1982), hydrogen, helium, nitrogen, carbon dioxide (with a correction for the dissociation of carbonic acid), ethylene, and acetylene (Wilhelm *et al.*, 1977), and methane and ethane (Rettich *et al.*, 1981). Liquid-phase contribution to the molar gaseous flow was usually small, although carbon dioxide's high solubility in water made its contribution significant.

Conversions and reaction rates are based on product formation and reaction stoichiometry. Reactor inlet O_2 concentrations were based on the liquid-phase mole

fraction in the oxygen saturator as calculated from Henry's law, and the flow rates of the two feed pumps. The gas-phase fugacity coefficient, Φ_i, accounts for the non-ideality of the high-pressure (8-110 bar) gas phase in the saturator. The Peng-Robinson equation of state with parameters found in Reid *et al.* (1987) was used to calculate the fugacity coefficient for oxygen. Pressure dependence of the Henry's law constants was taken into account through a Poynting-type correction

$$H_i(T,P) = H_i(T,P_o) \, \exp[\bar{V}_{i,\infty}(P-P_o)/RT] \qquad (4.2)$$

The infinite-dilution partial molar volume ($V_{i,\infty}$) for oxygen was obtained from Brelvi and O'Connell (1972). Atmospheric pressure was used as the reference pressure (P_o). Tests of this method were conducted with the reactor operating at ambient temperature. Complete recovery (within 2%) of the calculated gas feed was attained, adding credence to the technique.

4.4 Experimental Uncertainty

Experimental errors are estimates based on uncertainties in measured values. All measured quantities are given as approximate, normal, 95% confidence intervals (2 standard deviations). Measurement uncertainties are propagated to uncertainties in calculated quantities using standard propagation-of-error formulas (Aikens *et al.*, 1984).

Typically, five to fifteen liquid flow rates were measured during each run. These measurements were averaged, with two standard deviations of the data taken as the 95% confidence interval. Similar calculations were done for the gaseous effluent flow rates (normally five to fifteen measurements). The six pairs of gas samples were analyzed and

the average composition was determined. In some cases, the first gas sample(s) taken indicated the reactor had not reached steady state, and these samples were not included in the average. Two standard deviations were taken as the confidence interval for the amount of each species present. Analytical results of three liquid samples of each run were averaged to obtain the concentration of liquid products in the liquid effluent, again with two standard deviations as the confidence interval. Error in the measurement of the organic concentrations was estimated by multiple injections of the same feed into the HPLC, which had been calibrated with known concentrations (the Experimental Results Sections of Chapters 6 and 7 describe the error associated with acetic acid and methylene chloride, respectively). These averaged values with their respective 95% confidence intervals were used to make calculations necessary to interpret the results. Propagated error for simple sum and difference calculations was calculated as the square root of the sum of the squares of the absolute errors of the values being added or subtracted. For calculations involving products and quotients, the propagated relative error is equal to the square root of the sum of the squares of the relative errors used in the calculations (where relative error - also called fractional error - is defined as the absolute error divided by the average value of the quantity). Error in slopes of linear fits to data employed a modified computer program (Press *et al.*, 1986) that required input of data points with their respective 95% confidence intervals, and then used a Monte Carlo technique that assumed normal distribution of error about each data point and drew 10,000 randomly generated lines through the data, resulting in 95% confidence intervals for the slope and intercepts.

Rigorously, Student's t distribution should be used to obtain confidence intervals, rather than the normal distribution. However, enough experimental measurements were typically made so that the difference between the two distributions was negligible.

Chapter 5

Glucose Hydrolysis and Oxidation in Supercritical Water

Introduction 5.1

Glucose supercritical water oxidation was done collaboratively with Rick Holgate with this researcher carrying out the actual experimental runs and Holgate doing the analytical work and presentation of results. Product resolution has continued beyond what was done collaboratively, but with little new insight. A forthcoming paper will cover these experiments and interpretation of the results. More detailed information can be found in Holgate's (1993) doctoral thesis.

Supercritical water oxidation of wastes containing solids can be carried out without addition of supplementary fuel. In addition to complete oxidation to CO_2, N_2, and H_2O, a meaningful amount of heat can be recovered from the oxidative process. SCWO becomes increasingly attractive considering conventional incineration of these types of wastes requires the removal of water from the sludge and/or additional fuel to increase the waste heating value. SCWO of sludges may even be more economical than landfilling (Modell *et al.*, 1992) in some instances. Sludges that contain dioxins and furans can also be efficiently destroyed (Hossain and Blaney, 1991; Modell *et al.*, 1992). The supercritical environment can also be controlled to the extent that wastes containing nitrogen compounds can be partially oxidized to ammonia; this is particularly useful in converting human waste to clean fertilizer (Takahashi *et al.*, 1989).

Sludges and human waste typically have high fiber (cellulose) content, some with weighty amounts of lignin as well. Characteristically acidic, heating causes hydrolysis and depolymerization of cellulose to its monomer, glucose (Skaates et al., 1981) and other products (Bobleter and Bonn, 1983; Mok et al., 1992). As a significant hydrolysis product, glucose is therefore a germane model compound for the study of human waste and sludges.

Most studies in the SCWO of these types of wastes has concentrated on destruction efficiency (Takahashi et al., 1989; Hossain and Blaney, 1991; Modell et al., 1992) rather than kinetics. However, many kinetic studies have been performed under wet-air oxidation environments (Ploos van Amstel and Rietema, 1970; Brett and Gurnham, 1973; Skaates et al., 1981). Extrapolation of these kinetic findings to the supercritical regime is speculative, since wet-air oxidation occurs at much lower temperatures and pressures than supercritical water oxidation. Additionally, little attempt has been made in the wet-air oxidation studies to determine product yields or identification (Skaates et al., 1981, did identify several oxidation products and Ploos van Amstel and Rietema, 1970, did determine, in general, that products of hydrolysis were more refractory than glucose).

Since oxidation of glucose in supercritical water remains relatively uncharacterized, an investigation into its oxidation kinetics as a model compound for cellulosic waste was initiated.

5.2 Literature Review

Literature pertaining to earlier glucose hydrolysis and pyrolysis experiments was used as a starting point in identifying possible supercritical water oxidation products. The availability of this material is attributable to the interest in converting biomass to liquid fuels and chemical feedstocks.

Cellulosic carbohydrate pyrolysis generates many smaller products to include char, liquid organics, and light gases (Antal, 1982; Evans and Milne, 1987). Whereas cellulose hydrolysis produces glucose as an intermediate, cellulose pyrolysis forms levoglucosan (1,6-anhydro-B-D-glucopyranose) as a transitional compound. More than 80 products have been identified in the pyrolysis of wood (Evans and Milne, 1987), many of which (phenols) are attributed to the presence of lignin.

Many aqueous glucose hydrolysis experiments have been conducted in the temperature range 100 to 250 °C. A major product identified is 5-hydroxymethylfurfural, which itself hydrolyzes to levulinic acid and formic acid or polymerizes to color the sugar solution (Wolfrom *et al.*, 1948; Singh *et al.*, 1948; Newth, 1951; Mednick, 1962). Workers at the University of Hawaii have researched the hydrolysis of fructose, sucrose and xylose, with and without acid catalyst, at 250 °C and 345 bar. Fructose and sucrose produced notable amounts of 5-hydroxymethylfurfural. Smaller amounts of furfural were also detected. Xylose hydrolysis produced furfural. Other products identified included formic acid, lactic acid, levulinic acid, pyruvaldehyde, and glyceraldehyde (Antal *et al.*, 1990a, 1991; Antal and Mok, 1988).

The first studies in glucose hydrolysis under supercritical and near supercritical conditions were carried out at MIT in the early to mid-1970's (Amin *et al.*, 1975). Among the important results, it was discovered that below the critical temperature of water, glucose hydrolysis produced char and liquid organics. Conversely, significant gasification of the glucose (20%) occurred above the critical temperature and at 221 bar. This gas was composed mostly of carbon monoxide, carbon dioxide, and hydrogen, with trace amounts of methane and two-carbon gases also present. Additionally, little char was noted, and the liquid products consisted namely of furans and furfurals (Amin *et al.*, 1975; Modell, 1985b). Woerner (1976) corroborates the results.

Recently, Antal *et al.* (1992) have studied supercritical water oxidation of glucose at conditions most directly relevant to this work. Complete gasification of glucose occurred at 600 °C, 345 bar, and 20 seconds residence time. This gas was comprised mainly of CO_2 and H_2. With temperature constant, residence time had little effect on gas yield. But, increasing temperature significantly increased gasification. Reactor material also affected gasification and gaseous composition. Reactors made of Inconel 625 and Hastelloy C276 were compared. Inconel 625 seemed to catalyze gasification as well as the water-gas shift in that CO yields decreased while hydrogen and carbon dioxide yields increased.

Most all of the above studies fail to address the environmental conditions directly applicable to the supercritical water oxidation process. Still, the pyrolysis and hydrolysis studies (most hydrolysis experiments were acid-catalyzed and skewed kinetics toward ionic chemistry not likely in SCWO) do provide a starting point from which glucose

SCWO products and kinetics may be developed.

5.3 Product Identification

Analyses of reactor effluent composition was done by gas chromatography (GC) for the gaseous phase and high-performance liquid chromatography (HPLC) for the liquid phase. These methods were discussed in the Analytical Procedures section of Chapter 4.

Gas phase product identification and quantification were relatively straightforward due to the limited number of products. Hydrogen, carbon monoxide, carbon dioxide, methane, ethane, and ethylene were identified in the gaseous effluent. Acetylene was specifically tested for but not detected. Three-carbon and higher gases were not specifically tested for, but the absence of spurious peaks in and between chromatographs indicated no other unidentified gases were present. Also, when glucose conversion resulted in almost exclusively gaseous products, the carbon balance closures were excellent (95 - 97% closure). The absence of spurious peaks and carbon closures led us to conclude that C_3 (or higher) gases were not present or were only formed in negligible amounts under all of our experimental conditions.

Liquid effluent products were considerably more of a challenge to identify. The aforementioned glucose studies gave us an initial list of would-be products. The abundance of these products in those studies as well as commercial availability reduced the list of potential compounds. Table 5.1 shows suspected compounds specifically tested. These compounds were diluted to known molarities and injected into the HPLC. The observed retention times were then compared to product peak retention times.

Table 5.1   Summary of Compounds Tested as Possible Liquid-Phase Products. From Holgate (1993).

Compound	RT[a], min	λ[b], nm	Present in Effluent from Hydrolysis	Present in Effluent from Oxidation
Acetaldehyde	15.9	290	✓	✓
Acetic Acid	13.1	210	✓	✓
Acetol (Hydroxyacetone)	10.4,14.8	210	?	
Acetone	18.3	290		
Acetonylacetone (2,5-Hexanedione)	19.75	210	✓	✓
2-Acetylfuran	42.9	290	✓	
Crotonaldehyde	28.9	210		
Crotonic Acid	21.7	210	?	
2-Cyclopenten-1-one	29.7	210	?	?
3,4-Dihydro-2H-pyran	ND[c]	—		
Dihydroxyacetone	11.9	210		
2,5-Dimethylfuran	M[d]	—		
Formaldehyde	ND	—		
Formic Acid	11.8	210	✓	
Furfuryl Alcohol	36.1	290		
2-Furaldehyde (Furfural)	35.8	290	✓	✓
Furan	31.9	210		
2,5-Furandimethanol	M	—		
2-(5H)-Furanone	23.1	210		
2-Furoic Acid	22.9	210		
Glucaric (Saccharic) Acid	6.8	210		
Gluconic Acid	8.0	210		
Gluconic Acid Lactone	8.0	210		
Glucose	ND	—	✓	✓
Glyceraldehyde	10.1	210	?	
Hydroxyacetic (Glycolic) Acid	10.7	210	?	
5-Hydroxymethylfurfural	25.1	290	✓	✓
Lactic Acid	11.1	210	✓	
Levulinic Acid	13.7	210		
5-Methyl-2(3H)-furanone	M	210		
2-Methyl-2-cyclopenten-1-one	41.7	210		
2-Methylfuran	ND	—		
5-Methylfurfural	51.9	290	✓	
Oxalic Acid	5.2	210		
Propenal (Acrolein)	21.0	210		
Propenoic (Acrylic) Acid	15.6	210	✓	✓
Propionaldehyde	19.6	290		
Propionic Acid	15.3	210		
Succinic Acid	10.1	210	?	

[a]Retention time.
[b]Wavelength for detection/maximum absorbance.
[c]Not detectable at either 210 or 290 nm.
[d]Gives multiple unidentified peaks.

Peak detection was accomplished by UV adsorption at two different wavelengths, 210 and 290 nm (2100 and 2900 Å). Analysis at dual wavelengths enabled discrimination between peaks by functional group, and allowed identification of additional species not detectable at a single wavelength. For example, UV absorption by a compound requires the presence of a double bond, either $C=C$ or $C=O$. Carboxylic acids have their maximum UV absorbance at approximately 210 nm, as do unsaturated or conjugated ketone and aldehydes. On the other hand, saturated aldehydes and ketone have their maximum absorbance at about 290 nm. Extended conjugation of aldehydes and ketone shifts the maximum absorbance at about 210 nm (Silverstein *et al.*, 1991). consequently, detection at a single wavelength (e.g., 210 nm) limits the ability to identify all species: at 210 nm, simple aldehydes have virtually no absorbance, while carboxylic acids have no absorbance at 290 nm. Furthermore, for compounds which adsorb at both 210 nm and 290 nm, the wavelength that maximizes sensitivity (with maximum adsorption) can be chosen. For example, furaldehydes may be detected in the liquid effluent at concentration as low as 10^{-7} mol/L by absorbance at 290 nm. The ability to discriminate on the basis of functional group is illustrated by acetaldehyde and propenoic (acrylic) acid in Table 5.1. Both compounds have almost the same retention time, but propenoic acid adsorbs exclusively at 210 nm while acetaldehyde adsorbs only at 290 nm. Thus these two compounds may be identified and their amounts quantitatively determined by the dual-wavelength analysis, even though their peaks overlap. Table 5.1 lists the better of the two wavelengths for the detection of each test compound.

A disadvantage in using UV adsorption in analysis is its inability to detect most

compounds without a double bond. Potential products lacking a double bond were therefore excluded as possibilities. A few compounds, despite having the needed double bonds for detection, were still not appreciatively detectable. This is attributable to the compound's ability to exist in a solution form that does not contain a C=O or C=C bond. For example, glucose itself does not exist with its detectable aldehyde group in solution, but rearranges into its cyclic, hemiacetal (glucopyranose) form, undetectable by UV adsorption. Similarly, formaldehyde in solution rearranges to formalin, or methanediol, that no longer contains the C=O bond that would be detectable in its non-aqueous form. Fortunately, unambiguous glucose detection was possible using the enzymatic technique described in Section 4.2.

Another characteristic in using UV adsorption was the tendency of some seemingly pure compounds to give multiple peaks in aqueous solution. Evidently these compounds partially react in water, making identification of the parent and auxilary peaks quite challenging.

Phenolics and other six-membered aromatics were not tested as possible products. Although phenolics have been identified in biomass pyrolysis, these have been attributable to decomposition of lignin, not cellulose (Evans and Milne, 1987). Likewise, sugar hydrolysis done at the University of Hawaii indicates that furans, furaldehydes and their derivatives are the dominant products (Antal *et al.*, 1990a,b, 1991). Antal (1990b) has noted, however, that 1,4-butanediol may form and West and Gray (1987) report the formation of dioxanes from 1,4-butanediol in supercritical water. Theander and Nelson (1978) show that aromatics (hydroxybenzenes) may form. Hence, since phenols or larger

compounds cannot form without some type of combination of glucose molecules, their presence is suspect. Still, they cannot be entirely ruled out. HPLC chromatograms were run for as long as 90 minutes with no peaks detectable after 60 minutes. Since UV adsorption should be sensitive to highly conjugated species, the absence of peaks would indicate that larger condensation products (phenolics, oligimers, etc.) are not appreciably present. The reproducibility of chromatograms also supports the absence of any spurious peaks which may elute after the 90 minute run times. These observations indicate that there were no high molecular weight products present in the liquid reactor effluent.

Two typical HPLC chromatograms for glucose hydrolysis and oxidation are shown in Figure 5.1. Detection was at 210 nm and reactor conditions were 246 bar, 500 °C, and a residence time of 6 seconds. Reactor inlet concentrations for oxidation were 1×10^{-6} mol/cm^3 for glucose and 6×10^{-3} mol/cm^3 for oxygen. Known or suspected peak identities have been shown. Note the considerably fewer products of oxidation compared to hydrolysis.

Glucose hydrolysis gives many unidentifiable products, in accordance with many of the aforementioned difficulties in using UV adsorption. Still, identification has been made on some compounds. These compounds include acetic acid, acetaldehyde (detectable only at 290 nm), acetonylacetone (2,5-hexanedione), 2-acetylfuran (trace amounts and not quantified), formic acid, furfural (2-furaldehyde), 5-hydroxymethylfurfural, lactic acid, 5-methylfurfural, and propenoic (acrylic) acid. These compounds are shown structurally in Figure 5.2. The basis for these identifications is described by co-worker Holgate (1993) and follows.

Figure 5.1   **Comparison of HPLC Chromatograms of Liquid Effluent from Glucose Hydrolysis and Oxidation in Supercritical Water.** Nominal initial conditions: 500 °C, 1×10^{-6} mol/cm^3 glucose, 6×10^{-6} mol/cm^3 oxygen (for oxidation), 6 seconds reactor residence time. UV detection at 210 nm. From Holate (1993).
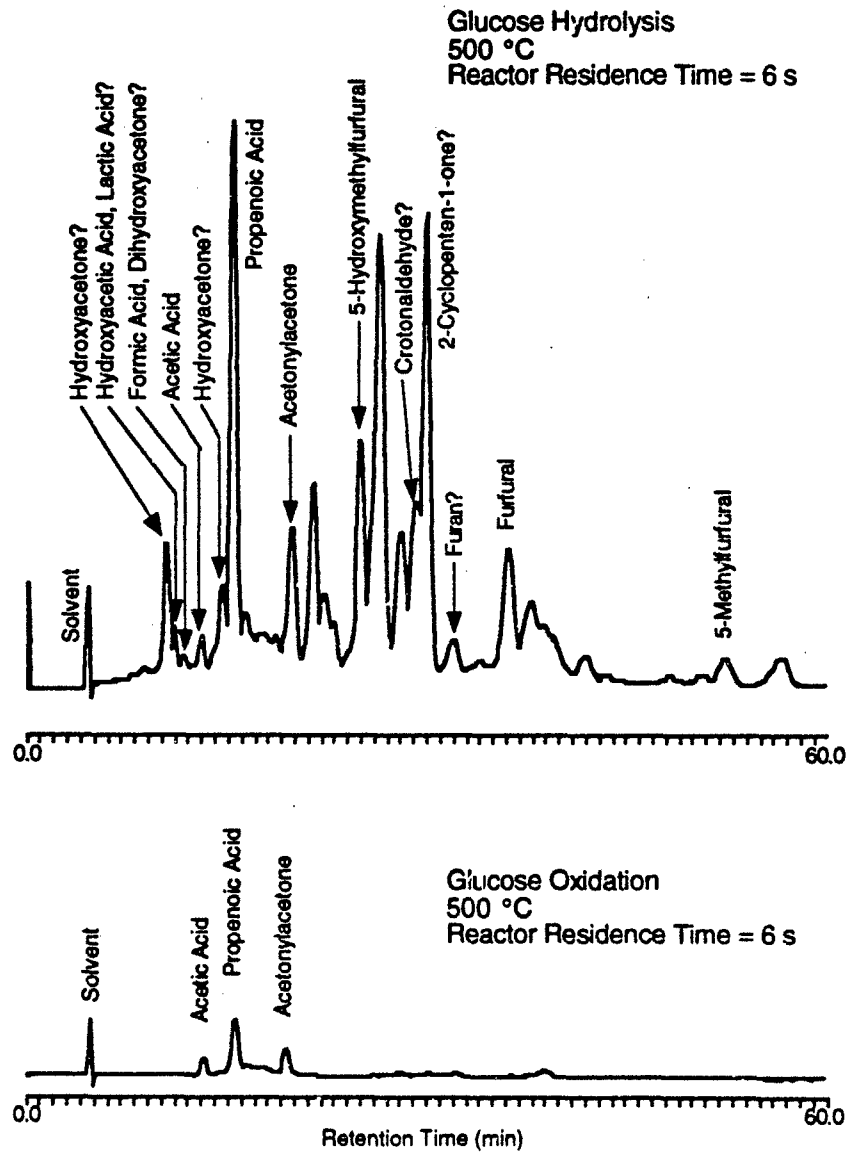
Figure 5.2 Compounds Identified in Liquid Effluent of Glucose Hydrolysis and/or Oxidation.
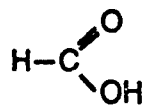
Formic Acid
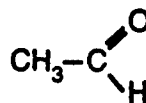
Acetaldehyde
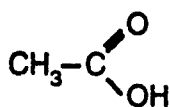
Acetic Acid
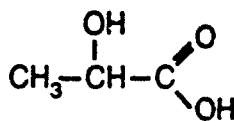
Lactic Acid
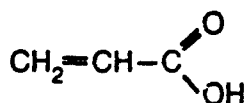
Propenoic (Acrylic) Acid
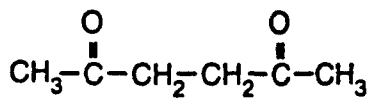
Acetonylacetone (2,5-Hexanedione)
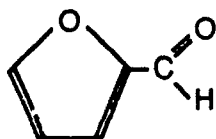
Furfural (2-Furaldehyde)
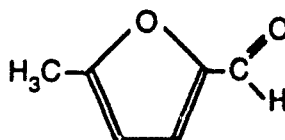
5-Methylfurfural
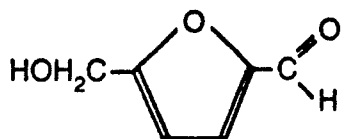
5-Hydroxymethylfurfural
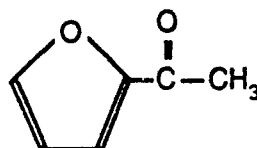
2-Acetylfuran

Formic acid and dihydroxyacetone have virtually identical retention times (11.8 vs. 11.9 min.; see Table 5.1). However, dihydroxyacetone has a much lower absorbance than formic acid, and the peak at this retention time should be considered to be formic acid, in accordance with Antal *et al.* (1990a, 1991). No matter what the peak identity, it appears to be fairly unstable and disappears from the hydrolysis effluent for temperatures above 500 °C.

Acetol (hydroxyacetone) gives two peaks (at 10.4 and 14.8 min.), indicating that it undergoes rearrangement in solution, most likely forming 2-hydroxypropanal. The HPLC method in this work was based on the method of Antal *et al.* (1991) for detection and quantification of the products of xylose hydrolysis; comparison of relative retention corresponds to acetol; the peak at 10.4 min. is probably 2-hydroxypropanal.

A cluster of peaks with similar retention times exists near the 10-min. mark. Compounds eluting in this narrow retention-time range include glyceraldehyde, succinic acid, hydroxyacetic acid, and (tentatively) 2-hydroxypropanal. With the natural drift in retention times between samples, these peaks are not adequately resolved and no positive identifications are possible. At higher temperatures, these peaks are unimportant. Under oxidizing conditions, the peaks disappear at 450 °C and above. For hydrolysis conditions, the peaks persist to higher temperatures, but disappear at 525 °C and above. The identification of lactic acid at a retention time of 11.1 min. may not be positive, since Antal *et al.* (1991) indicate that glycolaldehyde (which was not tested here) elutes at the same time as lactic acid; however, Antal *et al.* (1990a) did not detect glycoaldehyde during fructose hydrolysis at 250 °C and 345 bar. Like the peaks at

approximately 10 min., the lactic acid peak disappears at higher temperatures.

Propenoic (acrylic) acid and propionic (propanoic) acid have very similar retention times; the very tall peak at about 15.5 min. present in effluent samples could belong to either compound. However, the height of the peak suggests that it is probably propenoic acid, because of its much higher adsorption due to conjugation. To create such large peaks, propionic acid would have to be present at concentrations so large that carbon-balance closures on the reactor would be adversely affected. The tall peak is therefore attributed to propenoic acid.

Crotonaldehyde, crotonic acid, and 2-cyclopeten-1one all exhibit retention times near those of peaks observed in effluent samples. Unfortunately, retention times are not sufficiently close to warrant a positive assignment of identity to the peaks. furthermore, a peak at about 30 min. exists in the effluent samples for detection at both 210 nm and 290 nm. If the peak at 210 nm is 2-cyclopeten-1one, then the peak at 290 nm must correspond to another unknown species, since 2-cyclopenten-1-one does not adsorb at 290 nm.

The peak in the effluent samples at about 36 min. was quantified as furfural rather than furfuryl alcohol, since furfuryl alcohol did not absorb at 210 nm and gave a small peak at 290 nm; the peak in the effluent sample, on the other hand, occurred at both 210 and 290 nm and was large at 290 nm, consistent with the behavior of the furfural peak.

Acetonylacetone was identified since it appears to be a hydrolysis product of 2,5-dimethylfuran, which has been detected among the products of cellulose pyrolysis (Antal, 1982) and glucose caramelization (Shallenberger and Birch, 1975). A path to

acetonylacetone from glucose through 2,5-dimethylfuran therefore apparently exists. Acetonylacetone was also listed as a suspected product by Woerner (1976) for hydrolysis of glucose in near-critical water. However, oxidation experiments in the present study at 450 and 475 °C gave in excess of 100% carbon recovery (118% and 111%, respectively), and indicated that the acetonylacetone peak may have been improperly assigned. Had the peak been a C_3 compound instead of a C_6, carbon-balance closures would have been much improved. The assignment of the acetonylacetone peak must therefore be regarded with high uncertainty.

5.4   Product Distribution

Glucose hydrolysis and oxidation experiments were conducted at 246 bar, from 425 to 600 °C, at a residence time of 6 seconds (these temperatures and pressure are pertinent to a commercialized SCWO process). At reactor conditions, the inlet glucose concentration was 1×10^{-6} mol/cm^3 for both hydrolysis and oxidation. Such conditions allowed separation between products and rates of the hydrolysis and oxidation pathways. In oxidation experiments, stoichiometric oxygen (6×10^{-6} mol/cm^3) was supplied as detailed in Section 4.1. Oxygen solubility at ambient temperature and pressures less than 2000 psig constrained oxygen concentration and hence glucose concentration, since it was desirable to have glucose concentration the same during both oxidation and hydrolysis. The concentrations used were the highest achievable oxygen concentrations over the range of range of temperatures studied.

Oxidation experiments were performed immediately after their corresponding hydrolysis experiment. After pressurization and heatup to the desired reactor conditions,

the glucose feed was switched on and hydrolysis begun. Pure water pressurized with low pressure helium flcwed through the oxygen-side pump. Upon completion of the hydrolysis experiment, the oxygen feed was turned on (oxygenated water flowed through the oxygen-side pump) and oxidation was begun. The high pressure oxygen saturator solution diluted the glucose feed somewhat more than the water under low-pressure helium, but this perturbation was minor and the conditions of the hydrolysis and oxidation experiments were essentially identical except for the presence or absence of oxygen.

Complete hydrolysis of glucose yields considerable hydrogen:

$$C_6H_{12}O_6 + 6H_2O \rightarrow 6CO_2 + 12H_2 \qquad (5.1)$$
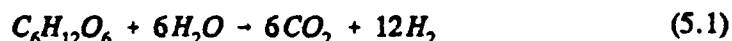
Approximately 97% of glucose was converted at even the lowest temperature investigated (425 °C). Despite the absence of oxygen, glucose reactivity was high. Determination of glucose consumption was therefore not attainable with our apparatus under supercritical temperatures and pressure. The extent of gasification during hydrolysis, defined as the moles of carbon present in the gaseous effluent divided by the moles of carbon fed to the reactor, is shown in Figure 5.3. All error bars and confidence intervals are at 95% confidence unless otherwise stated. Gasification under hydrolysis conditions spanned a range of 12% at 450 °C, to essentially 100% at 575 and 600 °C. In the current system, extremely high (around 40 ml/min) gas flow rates are difficult to measure precisely (up to 18 moles of gas can be produced from 1 mole of glucose via hydrolysis); the measured rates fluctuated more widely, and therefore more error is associated with

Figure 5.3   Variation of Extent of Glucose Gasification with Temperature During Hydrolysis and Oxidation. Nominal initial conditions: 1×10^{-3} mol/L glucose, 6×10^{-3} mol/L oxygen; 6 seconds reactor residence time. Error bars represent a 95% confidence interval. From Holgate (1993).
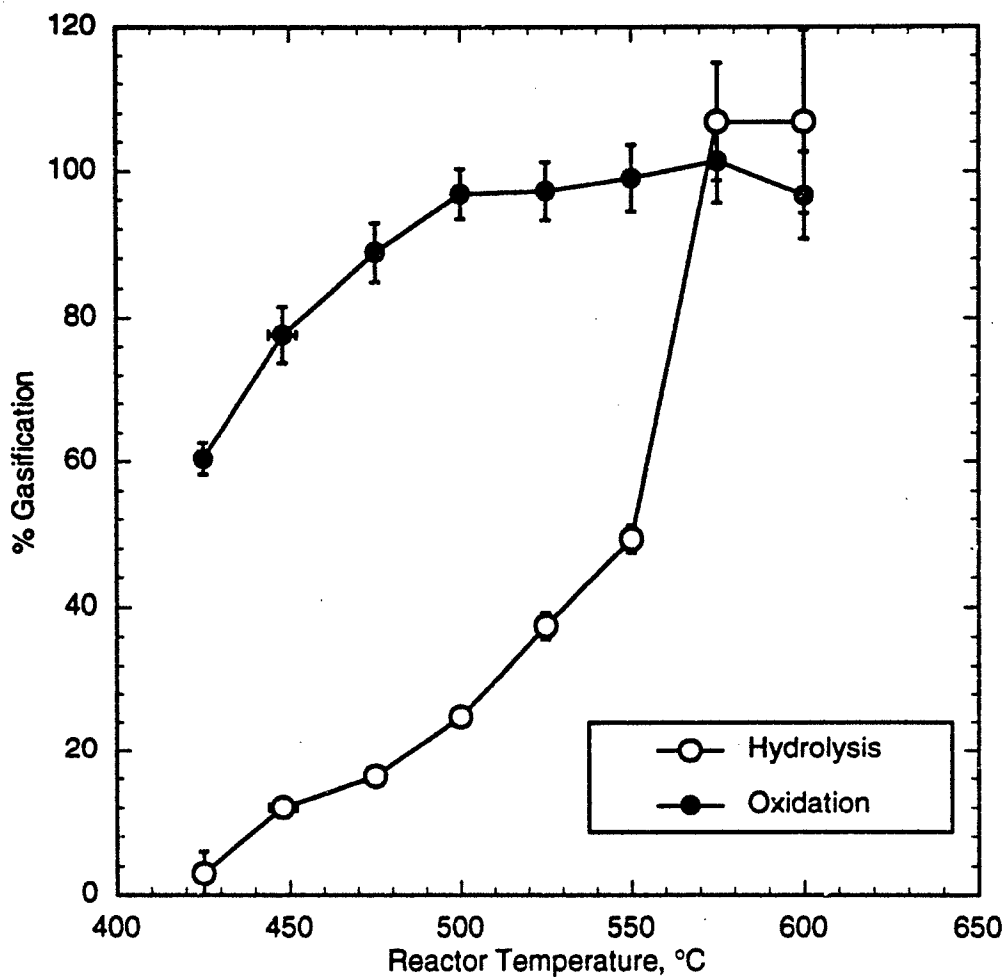
the gasification at the higher temperatures.

Figures 5.4 - 5.6 show the major products identified in glucose hydrolysis. The product yield is defined as the moles of product divided by the moles of reacted glucose. By this definition, the maximum yield of hydrogen is 12 and of carbon dioxide is 6 (see Equation 5.1). The product yield on a per-mole-*reacted* basis is basically equal to the yield on a per-mole-*fed* basis, since conversion was at least 97% in all experiments. Carbon dioxide, carbon monoxide, hydrogen, and methane, with smaller amounts of ethylene and ethane make up the gaseous products of glucose hydrolysis, as depicted in Figure 5.4. As mentioned in Section 4.2, due to inadequate peak separation, the ethylene peak may be lost when large amounts of carbon dioxide are present. The disappearance of ethylene at 575 and 600 °C may be a result of this analytical error. As CO would be expected to be an intermediate in the conversion of glucose to CO_2, the absence of CO at higher temperatures (575 and 600 °C) indicates that the water-gas shift $(CO+H_2O \rightarrow CO_2+H_2O)$ must also be present and appreciably fast. This is consistent with the findings of Antal *et al.*(1992).

The hydrolytic liquid effluent contained many products, especially at lower temperatures. Inability to identify these species as discussed earlier gave correspondingly low carbon balance closures (approximately 50%). As higher temperatures increased gasification (where products were more exactly defined), carbon balance improved, with complete closure at 100% gasification (575 to 600 °C). Acetic acid, acetaldehyde, acetonylacetone, 5-hydroxymethylfurfural (5HMF), furfural, propenoic acid, and 5-methylfurfural (5MF) were identified as liquid products. An unknown peak obscured

Figure 5.4 **Variation of Product Yields with Temperature for Glucose Hydrolysis at 246 bar.** Experimental conditions: $(1.02\pm0.02)\times10^{-3}$ mol/L glucose, 6.1 ± 0.3 seconds reactor residence time. Error bars represent a 95% confidence interval. From Holgate (1993).

Figure 5.5   Variation of Product Yields with Temperature for Glucose Oxidation at 246 bar. Experimental conditions: $(0.99 \pm 0.02) \times 10^{-3}$ mol/L glucose, $(6.2 \pm 0.2) \times 10^{-3}$ mol/L oxygen, 5.9 ± 0.3 seconds reactor residence time. Error bars represent a 95% confidence interval. From Holgate (1993).

Figure 5.6   Variation of Product Yields with Residence Time for Glucose Oxidation at 500±2 °C at 246 bar. Experimental conditions: $(1.01\pm0.02)\times10^{-3}$ mol/L glucose, $(6.1\pm0.2)\times10^{-3}$ mol/L oxygen. Error bars represent a 95% confidence interval. From Holgate (1993).
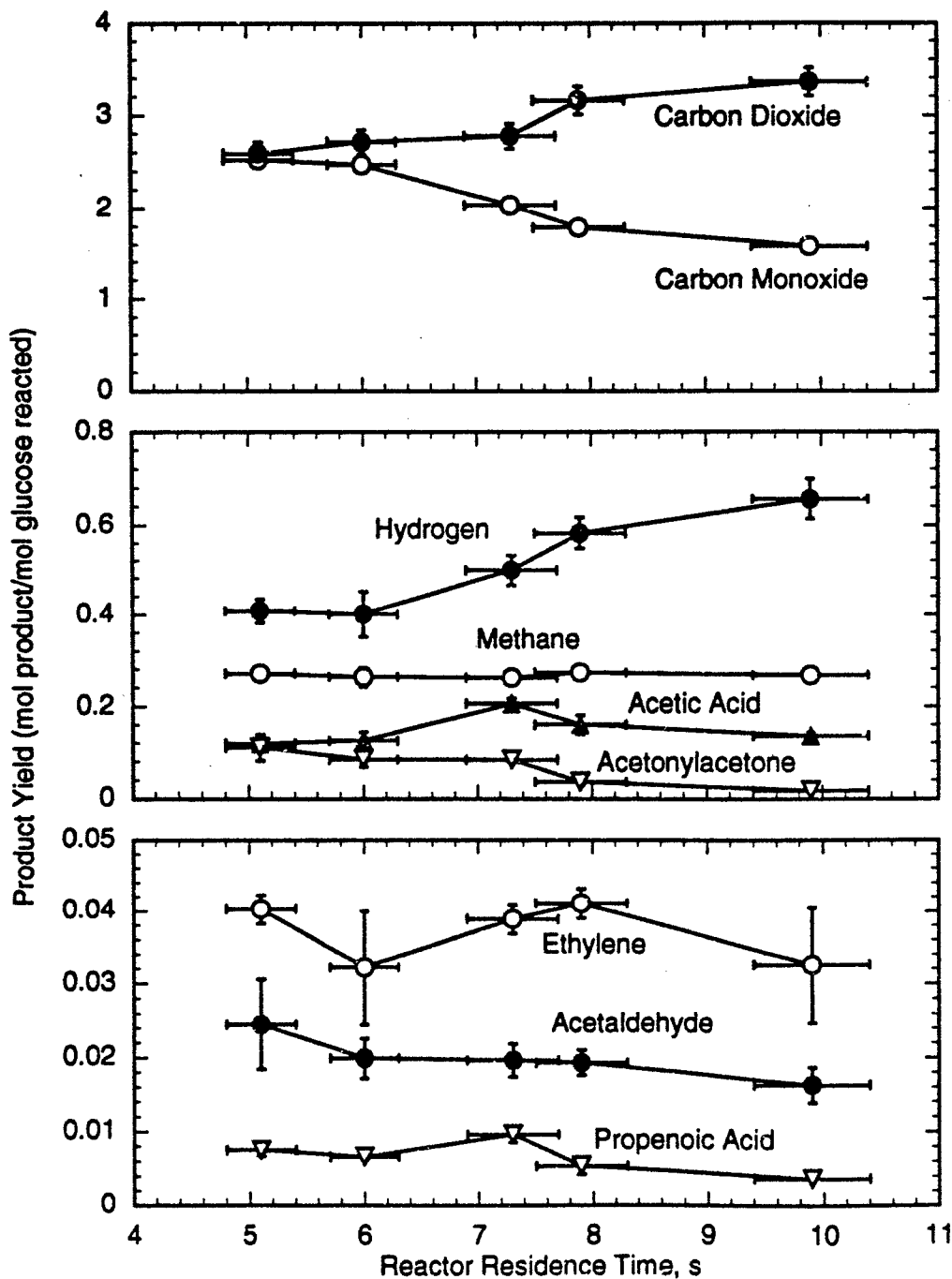
acetaldehyde below 475 °C, rendering it undetectable. Acetaldehyde and 5MF formation is seemingly favored at 475 to 550 °C, but the yields of all other liquid-phase products decrease with temperature, indicating deteriorating stability. Ethane, methane, and ethylene yields increase with temperature, suggesting these gases are products of the liquid-phase intermediates. Liquid effluent pH ranged from 3.5 at 425 °C to about 4.75 at the highest temperature investigated (600 °C). The more acidic values at higher temperatures may be attributable to an increased concentration of CO_2 in solution (carbonic acid).

The complete oxidation of glucose proceeds stoichiometrically as:

$$C_6H_{12}O_6 + 6O_2 \rightarrow 6CO_2 + 6H_2O \qquad (5.2)$$
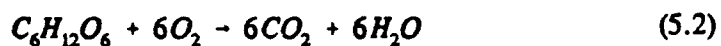
As evidenced by the fast reaction rate of hydrolysis, oxidation will occur in parallel with hydrolysis. Since reaction in the absence of oxygen was fast and complete ($\geq 97\%$ conversion), independent measurement of glucose oxidation kinetics was also not possible at temperatures above 425 °C in this apparatus. In fact, hydrolysis may have occurred prior to the mixing of the oxygen and glucose feeds. Residence time in the preheater tubing has been calculated to be from 14.7 seconds at 600 °C to 11.7 seconds at 425 °C (Holgate, 1993). Approximately 4 seconds of this residence time is spent near the reactor temperature. It is possible that a significant amount of glucose no longer existed in the inlet of the reactor where oxidation was initiated. Oxidation results suggest that even if this is the case, most hydrolysis products are also easily destroyed.

Gasification of glucose was even more pronounced in the presence of oxygen. As seen in Figure 5.3, Supercritical water oxidation produced 5 times more gas than hydrolysis at 425 °C, and essentially all carbon was converted to gas at 500 °C and above.

Product yields of glucose oxidation in supercritical water are presented in Figure 5.5. Liquid-phase products are reduced in quantity and distribution with oxygen present, with no detectable liquid products at all present above 550 °C, including the more refractory acetic acid and furan derivatives. At 600 °C, nearly complete oxidation of glucose to CO_2 and H_2O is observed with only minute amounts of hydrogen and methane present. Again, the huge carbon dioxide peak in the gas chromatograms may obscure any ethylene that was present, but with an average carbon-balance closure of 103.4 $\pm$ 7.1%, significant levels of products other than CO_2 and CH_4 are unlikely. The presence of methane is in agreement with the relatively high stability of methane observed earlier in our laboratory as reported by Webley and Tester (1991).

The pH level of oxidation liquid effluent was also most likely influenced by the level of CO_2 dissolved, ranging from 4.25 to 4.75 over the temperature range investigated.

To investigate the effect of residence time on product distribution, a sequence of experiments was conducted for stoichiometric oxidation at 500 °C and 246 bar over residence times varying from approximately 5 to 10 seconds. These results, shown in Figure 5.6, exhibit that for the conditions described, little change in product yield occurs. Combined with the effects of changing reactor residence time by changing pump flow

rates is the concurrent changing of time the reactant spends in the preheater tubing. According to Holgate's (1993) calculations, at the 9.9 second reactor residence time investigated at 500 °C, glucose also spends 16 seconds in preheater tubing, with about 3 seconds of that time near 500 °C. Similarly, at the flow rate necessary to obtain a 5.1 second residence time, it takes 9 additional seconds to pass through preheater tubing. Of this additional time, only about 1 second is spent near 500 °C in the preheater tubing. The final result is a residence time at reaction temperature of 6.1 to 12.9 seconds. Little change in yield over this time range is somewhat extraordinary and is in consonance with observations by Antal *et al.* (1992). This small change in yield suggests that the disappearance of glucose and all other intermediates (other than those listed in Figure 5.6) must occur in the preheater and/or first 5 to 6 seconds of the reactor. The identified products are the most resilient species derived from glucose oxidation in a supercritical water environment.

Product yield performance in Figures 5.4 and 5.5, combined with little variability in product yield demonstrated in Figure 5.6 implies that glucose hydrolysis and oxidation is fast, forming acetic acid, acetaldehyde, acetonylacetone, and propenoic acid as predominant liquid intermediates. These products are further broken down much more slowly into light gases, to include methane and ethylene. These gases are ultimately converted to carbon dioxide and water.

Although this study of the supercritical water hydrolysis and oxidation of glucose was unable to obtain global kinetic data for glucose, the most destruction-resistant intermediates were (perhaps fortuitously) identified - an important and formidable result.

Additional investigation at lower temperatures (T < 425 °C) and shorter residence times

(τ < 4.5 seconds) would permit a quantitative kinetic determination for glucose.

Chapter 6

Experimental Studies of Acetic Acid
Hydrolysis and Oxidation
in Supercritical Water

6.1 Motivation

Acetic acid has been identified as a refractory intermediate in the oxidation of more complex organics (Ploos van Amstel and Rietema, 1970; Skaates *et al.*, 1981; Tongdhamachart, 1990; Shanableh, 1991; Holgate, 1993) at and near supercritical conditions. Because of its relative stability, acetic acid may be the destruction-limiting species in the path to total oxidation of an organic. Acetic acid's refractory nature has led many investigators to study its destruction via supercritical water oxidation (Wightman, 1981; Lee and Gloyna, 1990; Wilmanns and Gloyna, 1990; Frisch, 1992). As with previous studies on the effect of SCWO on compounds (e.g., glucose, Section 5.2), most research has focused on measurements of destruction efficiency rather than product identification and reaction kinetics. Those investigations that have focused on kinetics have been susceptible to less well controlled environmental conditions than those achievable in our current tubular, isothermal, isobaric reactor system. In an effort to substantiate and improve on previous studies, characterization of the SCWO of acetic acid was undertaken.

6.2 Literature Review

Acetic acid, CH_3COOH, has a formula weight of 60.05 and is a colorless, pungent liquid at ambient conditions with a boiling point of 118 °C and melting point of 16.7 °C. A

moderately strong carboxylic acid, it has an ionization constant of $K_a = 1.8 \times 10^{-5}$ at 25 °C (Wagner, 1987). Its critical temperature and pressure are 321 °C and 57.8 bar respectively, and it is completely miscible with water. In a pure vapor phase, it exists as both a monomer and hydrogen-bonded dimer. In the dimer, each OH group forms a hydrogen bond with the carbonyl oxygen of its partner.

Gas-phase studies of acetic acid are scarce, but some thermal decomposition studies of gaseous acetic acid do exist. In the temperature range 770 - 900 °C, Bamford and Dewar (1949) contend that pure acetic acid can undergo first order decomposition to either ketene ($CH_2=C=O$) and water, or, carbon dioxide and methane. In their flow system, decomposition to CO_2 and CH_4 had a first order rate constant $k = 10^{11.00} \exp(-62,000/RT)$ sec^{-1} (E_a in calories).

Similar results were obtained for the decarboxylation of acetic acid in a static system by Blake and Jackson (1968), with $k = 10^{11.12} \exp(-58,500/RT)$ sec^{-1} over the range 460 - 585 °C. Blake and Jackson (1969) also investigated decarboxylation in a flow system over the temperature range 531 - 762 °C and found $k = 10^{13.59\pm0.15} \exp(-69,800\pm700/RT)$ sec^{-1}. All the aforementioned vapor-phase reactions were under vacuum conditions and in a virtual absence of water and oxygen, making extrapolation to pyrolysis in supercritical water speculative, but of value for comparison, nonetheless.

Acetic acid has been specifically addressed in kinetic studies of oxidative pathways of acids. Rate constants in the temperature range 24 - 172 °C for the reaction of OH radicals with monomer and dimer acetic acid have been reported (Singleton *et al.*,

1989). The dimer was much less reactive than the monomer, indicating the OH interacts mainly with the carboxylic hydrogen of the monomer. This supported similar findings found by Jolly *et al.* (1986).

Results from other investigations of acetic acid oxidation in supercritical water are listed in Table 6.1. The wide range of activation energies, pre-exponential factors, and reaction orders among reported values prompted additional study. Even the agreement between first-order reactions ($a = 1$) seen in Table 6.1 is deceptive, because these researchers *assumed* first order kinetics. These results seem additionally precarious considering two of the investigators (Lee and Gloyna, 1990; Frisch, 1992) did their studies with the same apparatus, yet attained markedly different results. Although experimental conditions were not completely replicated among investigators, global rate law results should be in closer agreement. None of the studies reported product distributions, or mass balance closures which may have provided more mechanistic information and certainly would have added credibility to their findings.

A closer analysis of the experimental conditions used by each investigator reveals experimental variables that could account for some of this disparity. For example, Wightman (1981), who pioneered the study of acetic acid oxidation in supercritical water, experienced "considerable pressure fluctuations." The pulsed flow of his single cylinder piston pump against the back pressure controller (a capillary tube) caused reactor pressure to be determined by flow rate. He found this pressure gradient acceptable, since, according to him, "the reaction was independent of pressure." However, under supercritical conditions, a modest change in pressure can cause significant changes in

Table 6.1   **Global Kinetic Expressions for Supercritical Water Oxidation of Acetic Acid.** Confidence intervals are 95% where shown.

$$d\,[CH_3COOH]/dt = -A\,\exp(-E_a\,/\,RT)\,[CH_3COOH]^a\,[O_2]^b$$

Units: kJ, mol, L, s

Source	log A	E_a	a	b	Conditions
Lee and Gloyna (1990)	11.5 ±11.5	180 ±15	1.01 ±.09	*0.16 ±.08	225-310 atm, 415-525°C *H$_2$O$_2$ oxidant flow reactor
Lee et al. (1990)	4.91	106	1	0	400-500°C batch reactor
Frisch (1992)	9.73 ±???	165 ±37	1	0	ρ = 0.3 gm/cm^3 380-470°C same batch reactor as Lee et al.
Wilmanns & Gloyna (1990)	5.95 ±5.72	314 ±62	2.36 ±0.48	*1.04 ±0.35	272 bar, 400-510°C *H$_2$O$_2$ oxidant
Wightman (1981)	18.0	231	1	1	400-445 bar 338-445°C
Present Study	9.9 ±1.7	168 ±21	0.72 ±0.15	0.27 ±0.15	246 bar, 425-600°C isothermal, plug-flow reactor

water density and subsequently, concentrations (Webley and Tester, 1989, 1990; Holgate, 1993), that do influence extent of reaction. Gas samples were not collected in Wightman's experiments, and standardized sodium hydroxide and nitrogen stripping were used to determine acetic acid concentration in the liquid effluent. His methods are potentially less accurate than current technology using high performance liquid chromatography (HPLC). Wightman used excess oxygen, *assumed* oxidation was first order in both organic and oxygen, and fitted data by linear regression to an Arrhenius rate equation. Only seven data points were used in his regression.

Wilmanns and Gloyna (1990) developed four possible models to explain acetic acid oxidation in SCW using hydrogen peroxide as the oxidant; the best fit model is shown in Table 6.1. In their flow reactor study, H_2O_2 was mixed with the acid before the solution was pumped in to the reactor; up to 70% of the acetic acid was destroyed during preheating. Accurate inlet concentrations during oxidation runs could not be measured due to hydrogen peroxide back-flow in the reactor. Total organic carbon analyses were conducted on a few of the runs, but none of these results were presented.

Lee and Gloyna (1990) used hydrogen peroxide to attain excess oxygen conditions in a plug flow (assumed) reactor. Unfortunately, their results are clouded by their use of ammonium acetate rather than acetic acid as the feed. No conversion of acetic acid was observed in limited pyrolysis studies (contrary to our findings). A gaseous effluent product was not collected nor analyzed and hence no material balances were presented. Gaseous flow was reported to be negligible (0.1 ml/min.), yet 150 - 300% of the stoichiometric demand of hydrogen peroxide was used to oxidize 0.018 to 0.044 molar

concentrations of ammonium acetate. Even in the absence of reaction, oxygen flow should have been measurable.

Lee again investigated SCWO of acetic acid, this time with a batch reactor (Lee *et al.*, 1990), subsequently used by Frisch (1992). In Frisch's experimental data, temperatures varied widely, ±10 °C and greater. Because the reaction rate is exponentially temperature dependent and no attempt was made to correct for gradients, large errors were introduced. Additionally, the heatup time is a significant fraction of the total reaction time (17 - 83%) and oxygen and organic are mixed prior to heatup. Four stainless steel balls placed in the reactor and shaken in an effort to enhance mixing may well have influenced reaction rate. Again, only liquid effluent was analyzed, after release of gases and filtering. No measured or calculated reactor pressures are given, only that "the reaction density remained constant at 0.3 g/cm^3 and the pressure fluctuated proportionally with temperature." In making comparisons of this type, one must keep in mind the possibility that the reactor material, itself, may have catalyzed reactions to some extent, while different inner surface area to volume ratios may have also biased results.

Graphical comparison of previous investigator results with this study are shown in Figure 6.1. Data of each investigator was plotted *assuming a reaction rate first-order in acetic acid and zero-order with respect to oxygen and water* over the respective ranges of temperatures investigated. Data from Rice (1993) are preliminary, non-published results from experiments recently conducted at Sandia National Laboratory. The stacking of data points at 525 °C for this study was omitted for clarity, but discussed in detail later in this chapter.

Figure 6.1 Comparison of First-Order Arrehnius Plots for Oxidation of Acetic Acid in Supercritical Water. Data points shown are from this present study. Error bars represent 95% confidence intervals.
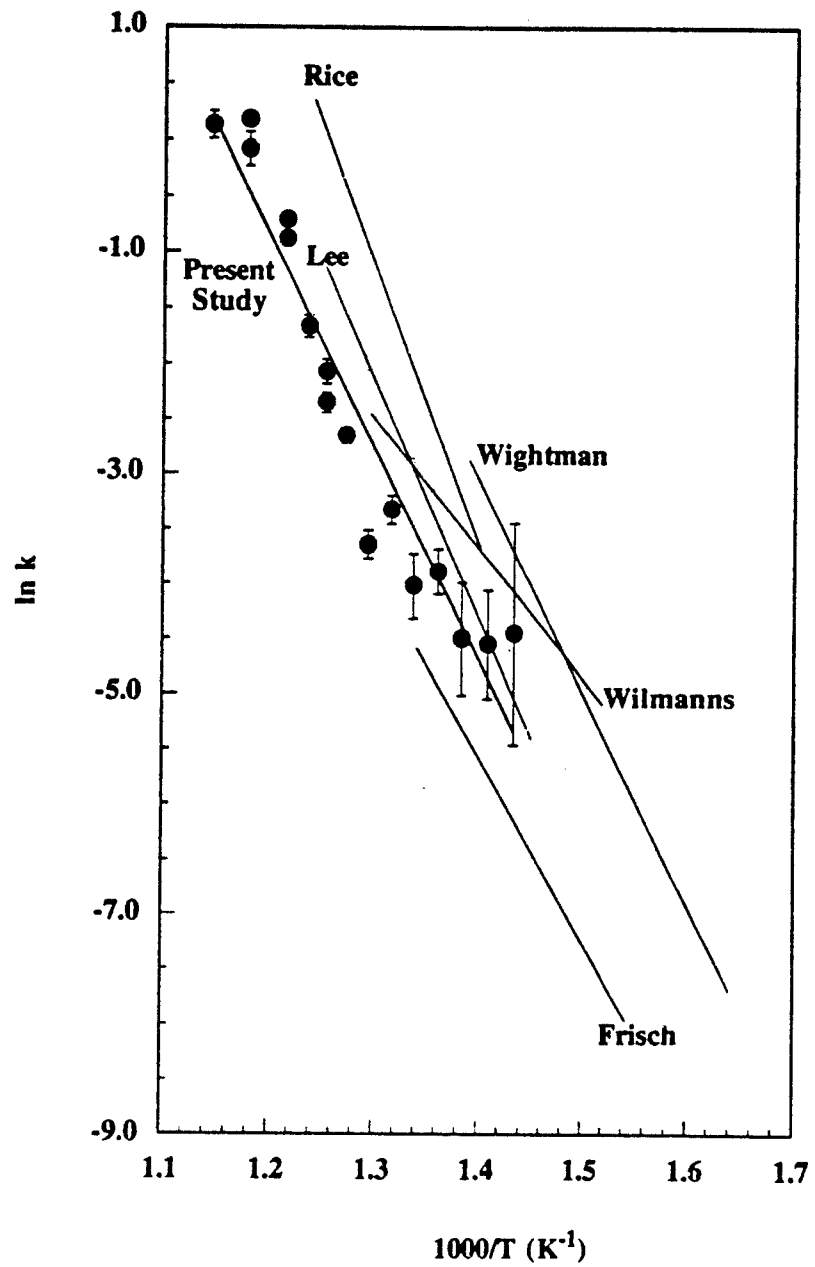
6.3 Experimental Results

Forty-five oxidation and ten hydrolysis experiments were conducted in supercritical water. Eleven additional oxidation experiments were performed to examine pressure/density effects on the rate of reaction and product distribution. The forty-five oxidation runs were conducted at a constant pressure of 246 bar to provide a comparable database to previous kinetic experiments in our laboratory (Helling and Tester, 1987, 1988; Webley and Tester, 1991; Webley et al., 1990, 1991; Holgate, 1993) The specified pressure is typical of proposed operating pressures in the SCWO process (Tester et al., 1993). Temperatures ranged from 425 - 600 °C, although 23 of the experiments were carried out at 525 °C to study concentration and residence time effects. Reactor residence times spanned 4.4 to 9.8 seconds. Initial concentrations of acetic acid in the reactor were from 9.8×10^{-8} mol/cm^3 to 2.02×10^{-6} mol/cm^3, while inlet oxygen concentrations varied between 1.91×10^{-8} (hydrolysis) and 3.95×10^{-6} mol/cm^3. These concentrations resulted in inlet molar oxygen-to-acetic acid ratios from 0.020 to 11.02 (stoichiometric oxidation is 2.00); the experiments included both fuel-lean and fuel-rich conditions. Conversions ranged from $7.89 \pm 3.71\%$ to 100% complete (within analytical detection limits) acetic acid destruction.

Treatment of experimental error was as discussed in Section 4.4. All intervals and error bars presented are at a 95% level of confidence.

As a test of calibration drift over the course of experiments, two different samples of liquid effluent were reinjected into the HPLC approximately one and three months after their initial analysis, respectively. Re-analysis of the three-month-old sample gave

an acetic acid concentration about 1.6% (0.15 millimole) lower than the first analysis. The one-month-old sample was 2.2% lower than its initial evaluation. These samples had been sitting in amber glass bottles in a refrigerator held at ~6 °C. Although decomposition of the stored acetic acid seemed unlikely, the possibility could not be ruled out and the measured decrease was taken as the combined effects of decomposition during storage and instrument calibration drift. As a result, it was assumed the acetic acid concentration measurements were ±1% of the true concentration. As a further test of calculation sensitivity to acetic acid concentration, recalculation of random experiments was done using an acetic acid concentration confidence of ±5%. In all recomputed analysis, calculated results (i.e., ln k, conversion, carbon balances) were still within the window of propagated error of the initial calculations that used an acetic acid concentration accuracy of ±1%. Hence, all experimental results were used in the regressions.

In some experiments, the measured liquid effluent flow rate deviated from the expected (calibrated) flow. This may have been caused by the oxygen pressure supplying the oxygen-side feed pump, gradual wear of pump seals and check valves, or imprecise back pressure. In most cases, this deviation was ±2% of the expected flow, and never greater than 10%. Still, this change in flow rate (and feed concentrations) was corrected for by assuming both oxygen and organic pump flow rates deviated equally from their expected values. With the deviation proportioned between the organic and oxygen pump flow rates, inlet concentrations were recalculated based on these "corrected" feed rates. This effect, as well as our ability to mix the organic (acetic acid) feed solution to about

±5% of the desired concentration, caused the reactor inlet concentrations (and O_2:CH_3COOH feed ratios) to vary from the target values. For example, experiments #287 - 292 resulted in an average O_2:CH_3COOH feed ratio of 3.90±.05 to 2.02±.02 rather than the targeted 4 to 2 stoichiometric ratio sought.

No spurious peaks were seen in the gas analysis chromatograms, so it was assumed that the gas phase was well-characterized by the identified products. Typically, twelve gas samples were analyzed during each experiment - six using a nitrogen carrier gas and six using a helium carrier (see Section 4.2).

Identifiable liquid effluent analyzed via liquid chromatography (see Sections 4.2, 5.3) with UV detection at 210 nm (2100Å) consisted of acetic acid and occasional propenoic acid (in concentrations of order 10^{-7} molar). Other reproducible oxidation peaks eluted at retention times of approximately 5.0 and 17.7 minutes. Since these species could not be identified among the compounds listed in Table 5.1, additional suspected compounds were tested. These are shown in Table 6.2. Unfortunately, none of these eluted at retention times of 5.0 or 17.7 minutes. No absorbance peaks were observed at 290 nm in initial oxidation experiments, so evaluation at this wavelength was not continued. Even without identification of unresolved peaks, carbon balance closures for oxidation were reasonably good, particularly at the higher temperatures (90+% carbon accounted for in all but 3 runs above 500 °C) where greater gasification, a disappearance in the 5.0 minute peak, and a reduction in the 17.7 minute peak occurred.

Experimental conditions and results are tabulated in the Appendix (Tables 10.1 through 10.4). Table 10.3 is a regrouping of all the runs in Table 10.2 conducted at

Table 6.2 Compounds Tested as Possible Liquid-Phase Products. Absorbance at 210 nm.

Compound	Formula	Retention Time (minutes)
Adipic Acid	$HOOC(CH_2)_4COOH$	13.3
N-Butanol	$CH_3(CH_2)_3OH$	29.3
Butyric Acid	$CH_3(CH_2)_2COOH$	18.5
3,3 Dimethylacrylic Acid	$(CH_3)_2CCHCOOH$	27.4
Ethanol	CH_3CH_2OH	18.2
Ethylacetate	$CH_3COOCH_2CH_3$	13.6, 15.8
Ethylene Glycol	$HOCH_2CH_2OH$	15.1, 15.6
Ethylmethacrylate	$H_2C_2(CH_3)CO_2C_2H_5$	47.8
Fumaric Acid	*trans*-$HOOC(CH)_2COOH$	10.1, 11.0
Glutaric Acid	$HOOC(CH_2)_3COOH$	10.6, 11.5
Isopropyl Alcohol	$(CH_3)_2CHOH$	19.9
Maleic Acid	*cis*-$HOOC(CH)_2COOH$	4.8, 5.8
Methanol	CH_3OH	16.1
N-Propyl Alcohol	$CH_3(CH_2)_2OH$	21.7

525 °C and stoichiometric feed ratios. It contains more detailed information for certain experiments listed in Table 10.2, but does not contain any new or different experiments.

A limited number of hydrolysis experiments were conducted at a reactor residence time of 8 seconds, a pressure of 246 bar, with reactor inlet concentrations of approximately 0.001 molar acetic over a temperature range of 475 - 600 °C. Conversions ranged from $5.86 \pm 3.45\%$ to $35.15 \pm 2.69\%$ with 95% confidence intervals as shown. UV absorbance of the liquid effluent at 210 nm gave propenoic acid as a consistent product and another unidentified peak with a retention time of about 18.4 minutes (less consistently).

Conversion of acetic acid in the preheater was considered negligible and not included in our calculations. Since a hydrolysis run at 525 °C and 8 seconds residence time yielded only 13% conversion, it was assumed that the shorter residence times in the preheater and lower temperatures produced little conversion.

6.4 Derivation of Global Rate Expression

Justification in assuming this apparatus acts as an isothermal plug-flow reactor has been provided by Webley (1989) and Holgate (1993). Based on their analysis, we estimate that plug-flow like conditions existed over our entire operating regime. Thus, the kinetics should obey the isothermal plug-flow design equation:

$$\frac{\tau}{C_{i_o}} = \int_0^{X_i} \frac{dX_i}{-R_i} \qquad (6.1)$$

where: X_i = conversion of reactant

R_i = rate of reaction for reactant i

C_{io} = initial concentration of reactant

τ = reactor residence time

Because water is in vast excess (mole fraction > 0.999) any change in volume due to reaction stoichiometry will have little effect on overall density. Since negligible pressure drop was measured through the reactor (typically ±70 psig with a system pressure of 3550 psig, or 246±6 bar) as well as negligible temperature variation, the constant water density assumption appears valid. We thereby assume that the volumetric flow through the reactor is also constant, such that the reactor residence time only depends on reactor volume, supercritical water density, and the water mass flow rate.

The reaction rate in Equation 6.1 is assumed to be in the form of a global rate expression,

$$R_{CH_3COOH} = k \, [CH_3COOH]^a \, [O_2]^b \qquad (6.2)$$

with the rate constant k in the Arrhenius form

$$k = A \, \exp(E_a / RT) \qquad (6.3)$$

Because water is present in such excess, its concentration was assumed virtually constant and thus not included in the rate form. Water's density (concentration) is strongly temperature dependent, but variations in temperature are likely to effect oxidation rate by changing k through the Arrhenius equation much more than changing water concentration.

Substituting Equation 6.2 and 6.3 into 6.1, and applying stoichiometry for total oxidation of acetic acid:

$$CH_3COOH + 2O_2 \rightarrow 2CO_2 + 2H_2O$$
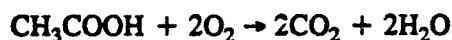
the following isothermal, plug-flow equation is derived:

$$[CH_3COOH]_o^{a+b-1} \, k\tau = \int_0^X \frac{dX}{(1-X)^a \, (F-2X)^b} \tag{6.4}$$

with: $[CH_3COOH]_o =$ initial concentration at reactor inlet

$F = [O_2]_o / [CH_3COOH]_o$

$X =$ acetic acid conversion

while τ and k are as previously defined.

A nonlinear multivariable regression program employing a modified Marquardt method (Press *et al.*, 1986) was used to obtain best-fit values of the rate parameters A, E_a, a, and b. With temperature as the predicted variable (see Chapter 10), the best fit expression is

$$R_{CH_3COOH} = 10^{9.9\pm1.7} \, \exp(\frac{168\pm21}{RT}) \, [CH_3COOH]^{0.72\pm0.15} \, [O_2]^{0.27\pm0.15} \tag{6.5}$$

Units for the rate is mole/cm^3 s^{-1}, concentration is in mol/cm^3, and activation energy is in kJ/mol. All parameter uncertainties are at the 95% confidence interval and were determined by an ANOVA routine (Press *et al.*, 1986). This nonlinear regression gives a significance level of 100%, with an F-statistic of 110 and a 0.85 R-squared value (adjusted for degrees

of freedom).

Previous investigators have assumed reaction orders of 1.0 with respect to acetic acid and zero with respect to oxygen. With such an overall first-order assumption, Equation 6.1 reduces to:

$$k = -\ln (1-X)/\tau \qquad (6.6)$$

and the *first-order* rate expression regressed from our data is:

$$R_{[CH_3COOH]} = 10^{11.1 \pm 1.6} \exp(\frac{183 \pm 24}{RT}) [CH_3COOH] \qquad (6.7)$$

with parameter 95% confidence intervals shown. Although there is significant error associated with the exact value of the order with respect to oxygen, Equation 6.5 implies *it is* still *non-zero* at a confidence level exceeding 99%. This fractional order dependence on O_2 is similar to the fractional order H_2O_2 dependence reported by Lee and Gloyna (1990) for acetic acid oxidation in supercritical water.

Figure 6.2 shows the Arrhenius plot obtained from the entire data reported in Tables 10.2 and 10.3 of the Appendix (Section 10). Again, error bars represent a 95% confidence interval. The straight line shown represents a *linear* regression - the behavior expected *if* the rate were strictly first-order in acetic acid and zero-order in O_2. The fact that previous investigators have assumed first-order reaction with respect to acetic acid and attained

relatively good fit is not entirely surprising. The data closely approximate first-order behavior consistent with previous studies in our own laboratory of other model compounds such as CH_4, CH_3OH, and H_2 (Helling and Tester, 1987; Webley and Tester, 1989; Holgate, 1993), where we have observed global kinetics independent of oxygen and first-order in the organic. Still, the experimental data presented deviate from first-order behavior (0.72 in acetic acid, 0.27 in oxygen), in accordance with the rate expression obtained from *nonlinear* regression (Equation 6.5).

The two data points in Figure 6.2 at both 550 °C and 575 °C give some indication of our ability to reproduce experimental conditions and results. Data points at each temperature were obtained about 2½ months apart, with the lower ln k values attained in the most recent experimental runs.

Two other characteristics of the Arrhenius plot are particularly noteworthy. The three data points at reactor temperatures of 450 °C and below show a leveling off, as well as a general increase in the size of the error bars. This is a result of the relatively low conversion (<10%) of acetic acid under the stated experimental conditions. As discussed in Section 10.1, a small error in conversion at low conversions (<20%) can lead to much larger propagated error than an equal experimental error at higher conversions (>70%). For example, an error of ±2% at a conversion of 80% gives an error of about 6% in the observed rate constant k. However, a ±2% error in conversion at 5% conversion propagates into an error of over 40% in k!

The other noteworthy observance occurs in the "stacking" of data points at 525 °C. This data set represents an isothermal study of the effect of residence time on

Figure 6.2 Assumed First-Order Arrhenius Plot for Acetic Acid Oxidation in Supercritical Water at 246 bar. *Linear* least squares fit is shown, corresponding to Equation 6.7.
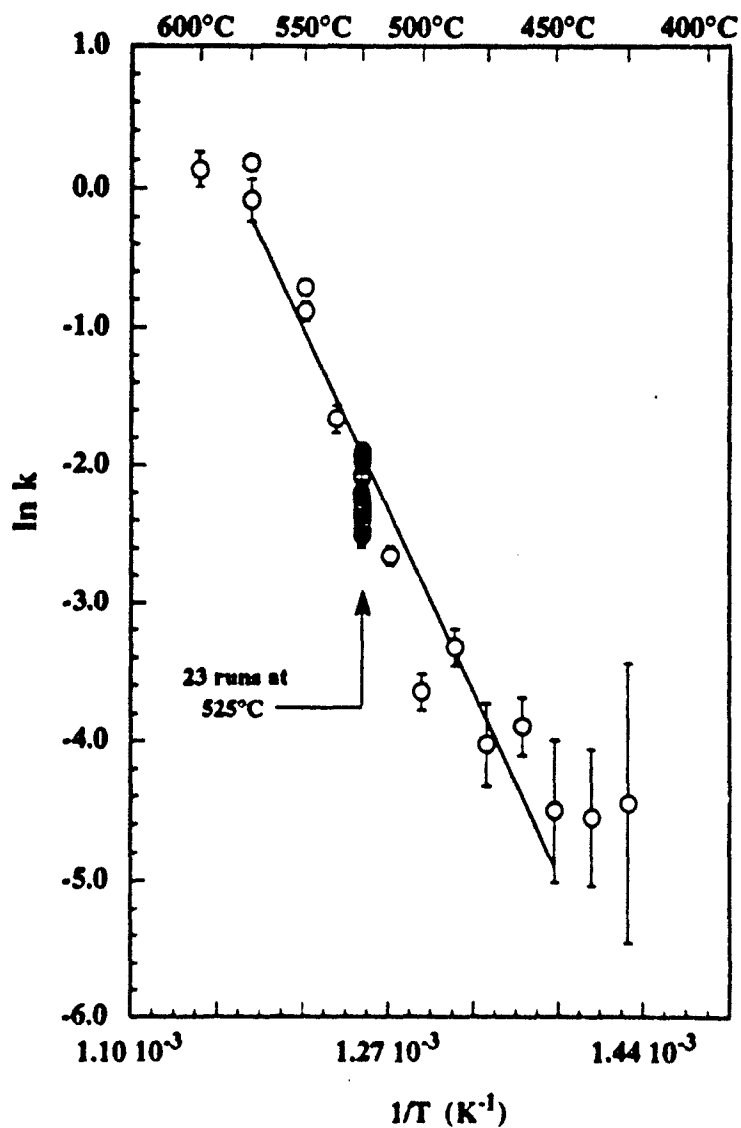
oxidation kinetics. Since approximately 50% conversion was attained at stoichiometric feed reactor conditions of 525 °C, 246 bar and residence time of 8 seconds, we decided to study concentration, residence time and pressure effects about this region, because it would allow for maximum changes in conversion both above and below the stoichiometric condition. Twenty-three experimental runs were conducted at stoichiometric ratio of organic feed to oxygen, but with varying concentrations. Six experiments were conducted at an initial feed ratio of 4 millimolar of oxygen to 2 millimolar acetic acid (4:2); six experiments at 3:1.5; seven runs at 2:1; and four runs at 1:0.5. If the data followed a first-order rate expression exactly, all data at one temperature would be represented by a single point. The scatter of these points is clearly not due to experimental error alone, but is likely due to an identified induction time and other possible non-first-order concentration effects (described in more detail later in Section 6.5).

As shown in Table 6.1 and Figure 6.1, our results are comparable with other investigators who performed similar experiments over somewhat different experimental conditions. Results from this study are in closest agreement to results achieved by Lee and Gloyna (1990) in a flow reactor using hydrogen peroxide as the oxidant .

The regressed global rate expression given in Equation 6.5 replicates the experimental data well. It indicates that acetic acid oxidation does show a fractional-order dependence on oxygen. The expression should be regarded as a simplified representation for correlating the experimental data.

6.5 Apparent Induction Times and Acetic Acid Decay Profiles

Four sets of experiments were conducted at a stoichiometric feed ratio at 525 °C and 246 bar. Two other sets of experiments were conducted to help verify global reaction order with respect to oxygen. These sets of runs were conducted at oxygen to acetic acid feed ratios of 4:1 (oxygen-rich) and 1:1 (oxygen-lean). All six sets of experiments were conducted at a pressure of 246 ± 7 bar and 525 ± 2 °C. These conditions were chosen to give a wide range of both residence time and conversion, as constrained by our apparatus.

Figure 6.3 displays acetic acid decay profiles as a function of residence time for the four stoichiometric feed mixtures. Acetic acid concentration has been normalized by the initial acetic acid concentration ($[CH_3COOH]_o$). The curves shown are exponential fits to each data set *with the initial concentration* ($[CH_3COOH]/[CH_3COOH]_o = 1$) *omitted*. Acetic acid appears to follow an exponential decay characteristic of a *first-order* reaction. This seems to hold for all four oxidation runs at stoichiometric feed conditions. This observed exponential decay suggests that the reaction *is indeed first-order* with respect to acetic acid and that the linear regressed global rate expression (Equation 6.7) may be preferred over the non-linearly regressed rate expression (Equation 6.5). However, as expounded by Holgate (1993), exponential decay is not unique to first-order reactions.

The exponentially regressed decay curves should extrapolate back to the initial acetic acid concentration (or $[CH_3COOH]/[CH_3COOH]_o = 1$) at time $t = 0$. This does not occur in the curve fits depicted. Rather, the exponential decay curves predict the

Figure 6.3 Normalized Decay Profiles for Stoichiometric Oxidation of Acetic Acid in Supercritical Water, Showing Induction Times. Curves are exponential fits to data points.
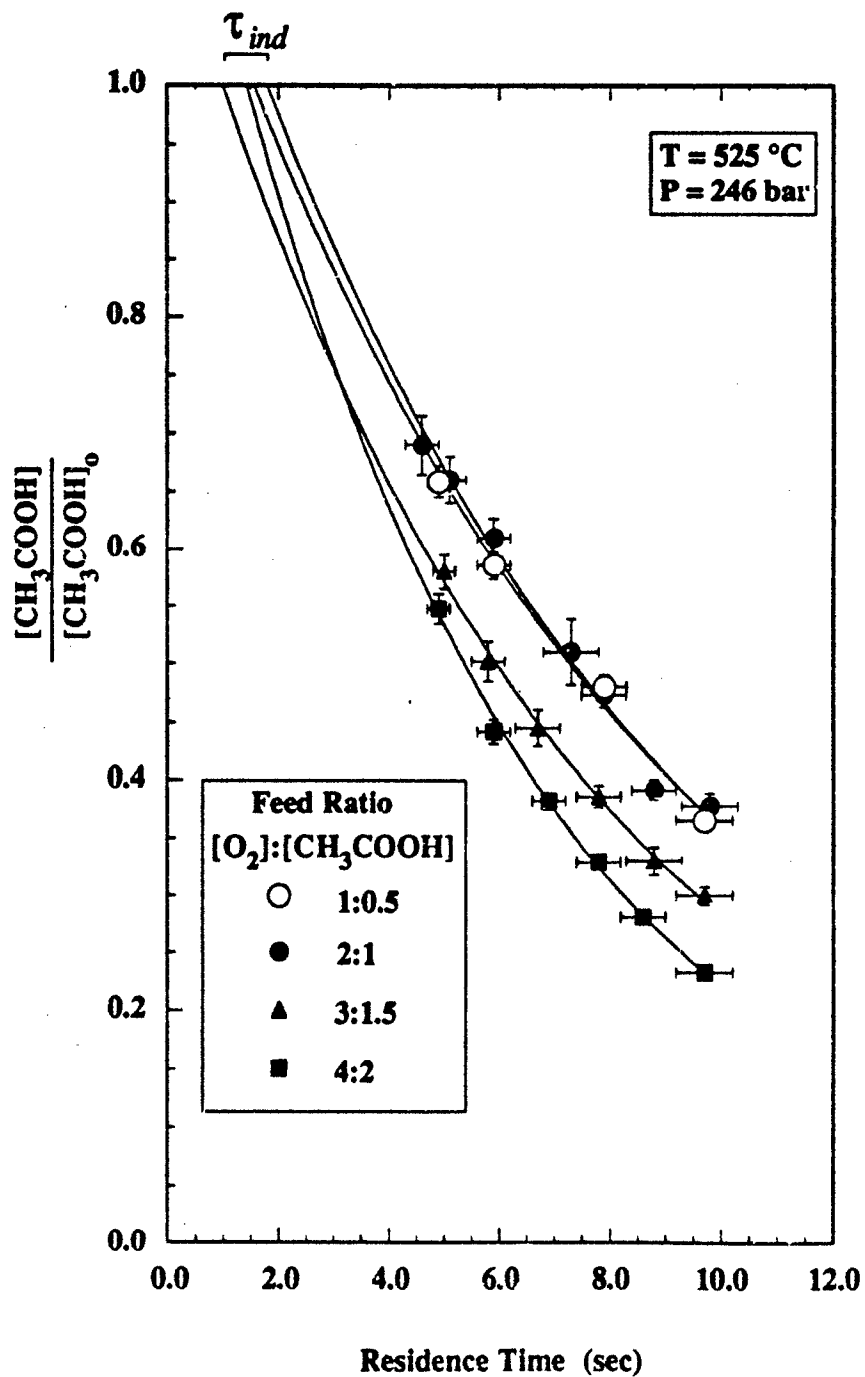
initial concentration at time $t \approx 1$ to 2 seconds. This delayed ignition of the reaction is known as an "induction time." Again, all data sets exhibit induction times. Derived decay constants and induction times are shown in Table 6.3. Intervals shown are 95% confidence intervals and were determined using a modified Monte Carlo technique (Press *et al.*, 1986) described in Section 4.4.

Another form of Figure 6.3 may show more clearly the exponential decay as well as the extrapolation to time $t = 0$. For each data set, a kinetic rate constant can be defined:

$$k' = - \frac{1}{C_i} \frac{dC}{dt} = - \frac{d \ln C_i}{dt} \tag{6.8}$$

where C_i is the concentration of species i (acetic acid, for our purposes). For non-exponential decay, k' is a function of time. For first-order decays, k' is single-valued and is equal to the exponential decay constant. The Figure 6.3 data are replotted in Figure 6.4 using a logarithmic ordinate, $\ln (C_i / C_{io})$, to linearize the decays. Again, all data sets exhibit exponential decay and extrapolation to $\ln ([CH_3COOH]/[CH_3COOH]_o) = 0$ results in estimates of induction times. Note that the three lower concentration data sets appear to have the same decay constant and have slopes within regression error (the 1:0.5 and 2:1 feeds are almost indistinguishable), but the highest feed concentration (4:2) has a decay constant (k') that is statistically different. The induction time seems to decrease slightly with increasing feed concentrations, but increases for the most concentrated feed. However, there is large error associated with induction time and a conclusive analysis cannot be made.

Table 6.3 Apparent Induction Times and Decay Constants for Acetic Acid Oxidation at 246 bar and 525±2 °C. 95% confidence intervals are presented.

Initial Conditions (10^{-3} mol/L)	k' (sec^{-1})	τ_{ind} (sec)	Average Feed Ratio $[O_2]$:$[CH_3COOH]$
$[O_2]_o$ = 1.09±.02 $[CH_3COOH]_o$ = 0.50±.01	.12±.01	1.5±.6	2.19±.04
$[O_2]_o$ = 1.09±.02 $[CH_3COOH]_o$ = 0.98±.01	.09±.01	1.1±.6	1.11±.02
$[O_2]_o$ = 2.08±.04 $[CH_3COOH]_o$ = 0.98±.01	.12±.01	1.7±.5	2.13±.05
$[O_2]_o$ = 3.15±.04 $[CH_3COOH]_o$ = 1.44±.02	.14±.02	0.8±.7	2.19±.04
$[O_2]_o$ = 3.86±.04 $[CH_3COOH]_o$ = 0.99±.01	.17±.01	1.2±.4	3.91±.06
$[O_2]_o$ = 3.90±.05 $[CH_3COOH]_o$ = 2.02±.02	.17±.02	1.3±.6	1.93±.02

Figure 6.4   **Normalized Decay Profiles for Stoichiometric Oxidation of Acetic Acid in Supercritical Water at 525 °C and 246 bar, Showing Induction Times.** Conditions as in Figure 6.3, but concentration ordinate is on a logarithmic scale. Lines are linear fits to data, indicating exponential decay.
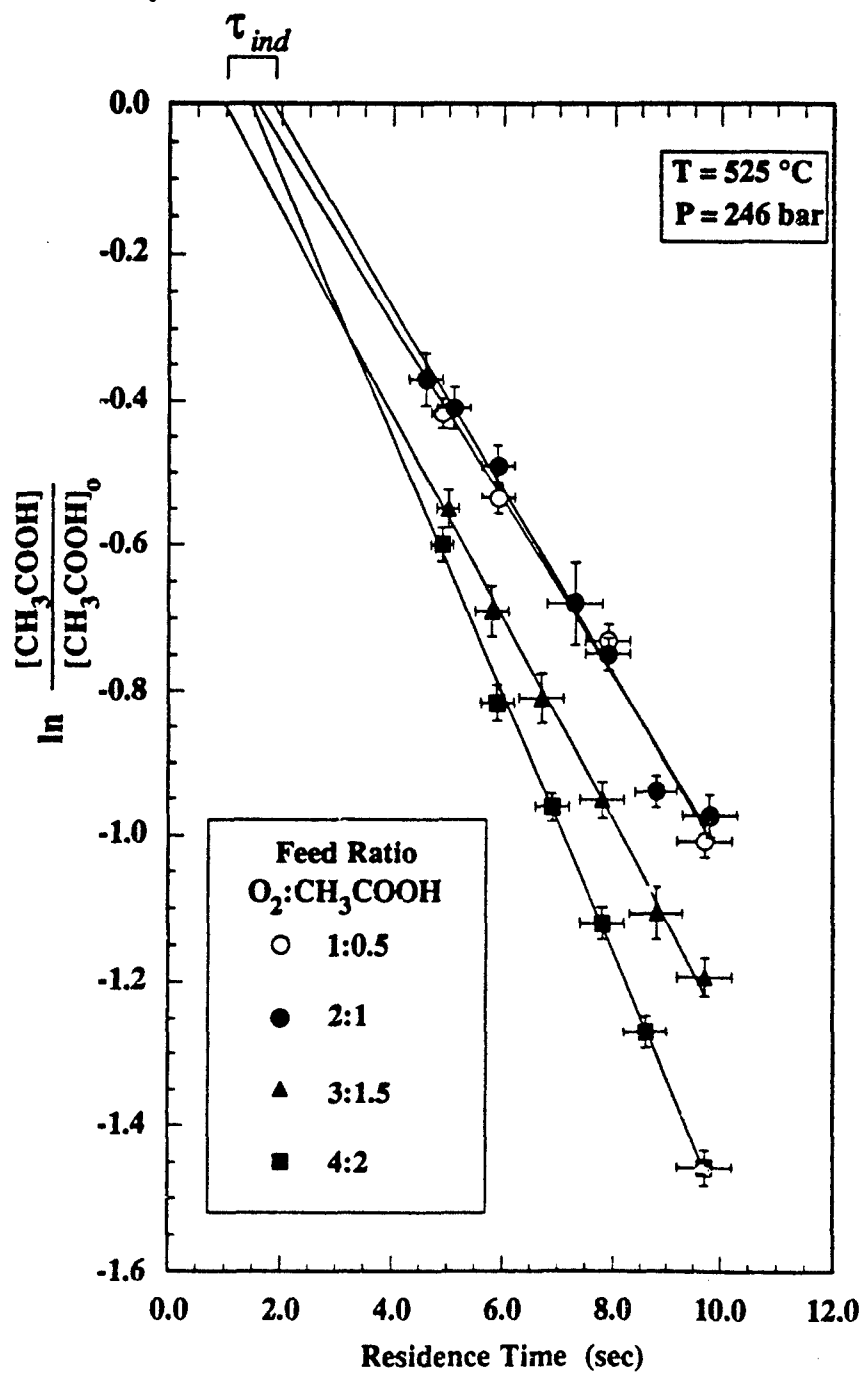
One other observation is worth mention and almost indisputable. A definitive trend observed is that as acetic acid and oxygen concentrations are stoichiometrically increased, overall conversion is increased. This can be seen by comparing data in Figure 6.3 at a specific residence time. In general, the more concentrated mixtures have the lower $[CH_3COOH]/[CH_3COOH]_o$ ratios, which translates into higher conversions $(X = 1 - \{[CH_3COOH]/[CH_3COOH]_o\})$. This aspect runs counter to results found by Holgate (1993) in similar studies of hydrogen oxidation in supercritical water, where conversions decreased with increasing stoichiometric concentrations.

The presence of an induction time is indicative of a complex reaction mechanism and severely interferes with modeling of global reactions. The rate form of Equation 6.2 assumes the reaction is initiated at $t = 0$. Experimental evidence suggests that the reaction does not begin until t ≈ 1 to 2 seconds for acetic acid oxidation in supercritical water, and that induction time itself may be a function of other experimentally-controlled variables. Ignition delay results in differing k (rate constant) values. The regressed rate form cannot replicate this behavior, and the induction time effect is subsumed in the rate equation. The scatter in ln k seen at 525 °C in Figure 6.2 can be attributed to the variation in k due to the induction time. Similarly, the regressed expression found in Equation 6.5 (or any other regression of similar form) is less accurate due to this anomaly.

Another confounding effect regarding induction time is the inability to measure ignition delay in our plug-flow reactor. Whereas mixing times are extremely short (Holgate, 1993) relative to reactor residence times (which are relatively well defined),

the mere presence of a mixing zone undoubtedly affects induction times. Ignition can also be significantly effected by minor concentration variations during mixing (Yetter *et al.*, 1985).

Two additional series of experiments were conducted to better characterize the reaction order with respect to oxygen. Seven experiments were conducted in which the initial oxygen concentration was twice that required for complete oxidation of acetic acid to CO_2 (oxygen to acetic acid ratio of 4:1). Similarly, seven runs were conducted in which the initial oxygen concentration was one-half the stoichiometric requirement (1:1). Although oxygen-lean, these experiments were never oxygen-limited in that conversion of acetic acid at the longest residence time was only 55%. Results of these investigations are plotted in Figure 6.5, along with an analogous series of experiments conducted at stoichiometric feed (2:1), originally shown in Figures 6.3 and 6.4. The acetic acid profiles are normalized with respect to initial concentrations and the curve fits are exponential. Figure 6.6 linearizes normalized profiles logarithmically and shows straight-line fits to the data. In addition to the excellent straight-line behavior, both figures show the presence of an apparent induction time. Also note that each profile exhibits a somewhat different decay rate. Kinetic decay constants and induction times from the acetic acid profiles for the data sets are summarized in Table 6.2. The decay constant under fuel-rich (1:1) conditions decreases relative to that under stoichiometric conditions. The fuel-rich induction time may be somewhat shorter, but still subject to considerable error, and approximately 1 to 2 seconds. The oxygen-rich profile depicts a correspondingly higher decay constant relative to stoichiometric feed. If the global

Figure 6.5 Normalized Decay Profiles for Oxidation of Acetic Acid in Supercritical Water at 525 °C and 246 bar, Showing Induction Times. Curves are exponential fits. Error bars represent 95% confidence intervals.
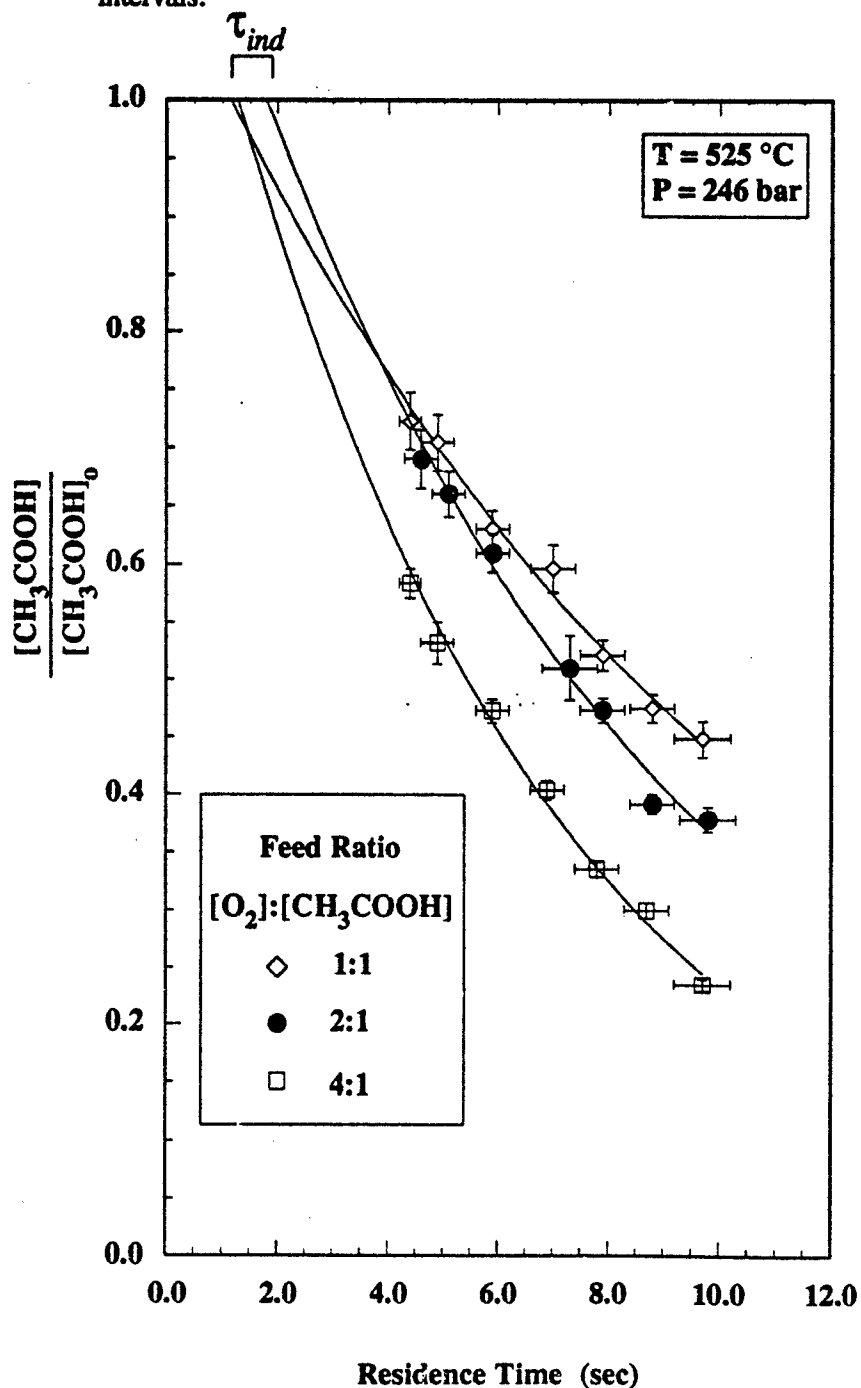
Figure 6.6   Normalized Decay Profiles for Oxidation of Acetic Acid in Supercritical Water at 525 °C and 246 bar, Showing Induction Times. Conditions as in Figure 6.5, but concentration ordinate is on a logarithmic scale. Lines are linear fits to data, suggesting exponential decay. Error bars represent 95% confidence intervals.
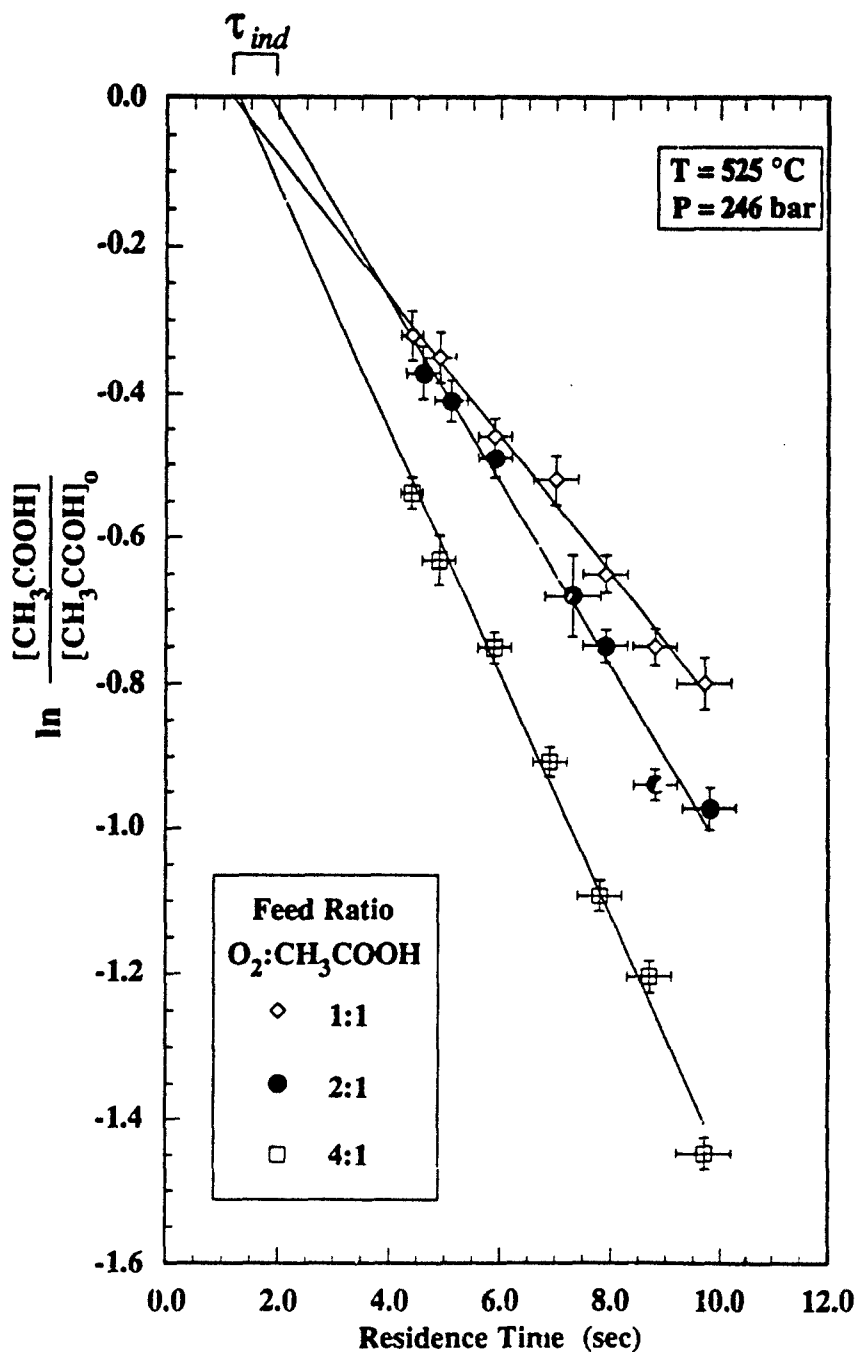
reaction rate is independent of oxygen concentration, the decay constant should be the same since the inlet organic concentrations, temperature, pressure, and residence times were essentially the same for comparable experiments in the same reactor system. The difference in profiles can only be explained by some level of oxygen dependence. These profiles substantiate the oxygen dependence of acetic acid destruction in accordance with Equation 6.5. Oxygen-rich (fuel-lean) induction time is still around 2 seconds, suggesting that ignition time may be independent of the oxygen to acetic acid feed ratio. This is in agreement with similar work conducted by Holgate (1993) involving oxidation of carbon monoxide in supercritical water.

6.6 Initial Conditions Effects on Products

Four sets of experiments were conducted at nominally stoichiometric concentrations at 525 °C and 246 bar. Plots of feed and identifiable product concentrations with respect to reactor residence time are plotted in Figures 6.7 through Figure 6.10. Numerical data are given in Table 10.3 of the Appendix.

Figure 6.7 shows the major species profiles of runs, conducted at 525 °C, 246 bar, with nominally stoichiometric feed concentration of O_2 and acetic acid (2.08×10^{-6} mole/cm^3 and 0.98×10^{-6} mol/cm^3 respectively). Again, the acetic acid and oxygen profiles are well fit by exponential decay (curve not shown). Although not recognizable with the portrayed scaling, extrapolation of an exponential curve to time t $\approx$ 0 seconds results in an ordinate intercept slightly above the initial concentrations indicated. This can be attributed to the induction time discussed (and more visually evident) in Section 6.5. Carbon monoxide and methane exhibit a small net increase in concentration while

Figure 6.7 Major Species Profiles for Stoichiometric Acetic Acid Oxidation in Supercritical Water at 525 °C and 246 bar. $[O_2]_0 = (2.08 \pm 0.4) \times 10^{-3}$ mol/L, $[CH_3COOH]_0 = (0.98 \pm .01) \times 10^{-3}$ mol/L. Error bars represent 95% confidence intervals.

Figure 6.8 Major Species Profiles for Stoichiometric Acetic Acid Oxidation in Supercritical Water at 525 °C and 246 bar. $[O_2]_o = (1.09 \pm 0.2) \times 10^{-3}$ mol/L, $[CH_3COOH]_o = (0.50 \pm .01) \times 10^{-3}$ mol/L. Error bars represent 95% confidence intervals.

Figure 6.9 Major Species Profiles for Stoichiometric Acetic Acid Oxidation in Supercritical Water at 525 °C and 246 bar. $[O_2]_o = (3.15 \pm 0.4) \times 10^3$ mol/L, $[CH_3COOH]_o = (1.44 \pm .02) \times 10^{-3}$ mol/L. Error bars represent 95% confidence intervals.

Figure 6.10 **Major Species Profiles for Stoichiometric Acetic Acid Oxidation in Supercritical Water at 525 °C and 246 bar. $[O_2]_o = (3.90 \pm 0.5) \times 10^{-3}$ mol/L, $[CH_3COOH]_o = (2.02 \pm .02) \times 10^{-3}$ mol/L. Error bars represent 95% confidence intervals.**
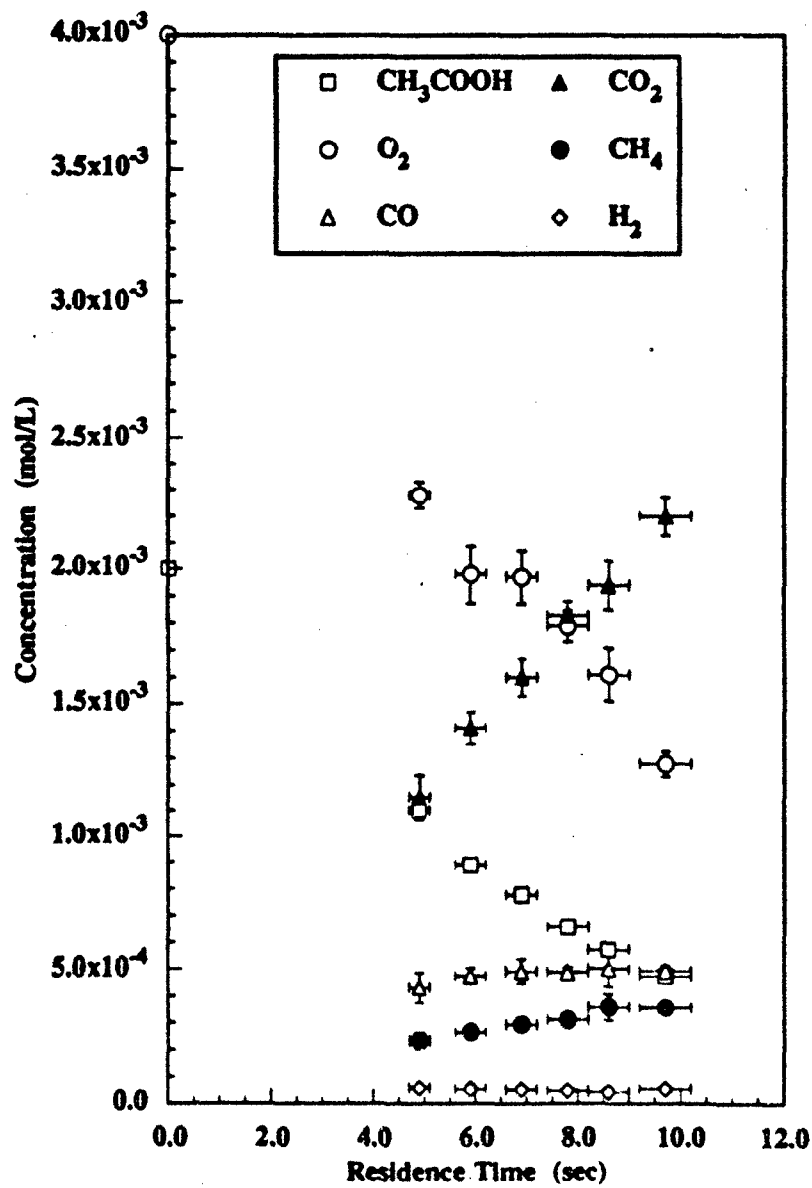
CO_2 concentration shows a rapid rise from 45% of the total carbon reacted at t = 4.6 seconds to nearly 62% of total carbon reacted at t = 9.8 seconds. Note that overall hydrogen concentration is relatively constant and low. This implies that hydrogen oxidation offsets the rate at which H_2 is formed from the water-gas shift and/or any acetic acid oxidation. Other stoichiometric feeds (Figures 6.8 - 6.10) show similar trends.

More information can be gleaned in a comparison of the most concentrated and least concentrated stoichiometric feeds. As would be expected, respective product profiles for the 3:1.5 and 2:1 stoichiometric feeds lie in between the limits defined by the nominally 4:2 and 1:0.5 feeds. Figure 6.11 compares acetic acid and oxygen decay for the 4:2 and 1:0.5 runs, with the upper profile of each compound representing the more concentrated (4:2) feed. The decays are distinctly different, reflecting complex kinetics and a change in induction time.

Effect of initial concentration on gaseous product distribution can be seen in Figures 6.12 and 6.13. Whereas the CO production has little net gain beyond 6 seconds reactor residence time, CO_2 production increases rapidly. Similarly, the four-fold increase in initial concentrations gives markedly higher methane production (Figure 6.13). Hydrogen, while produced in greater quantities, still appears to reach an equilibrium concentration level within the first four seconds of the reactor and undergoes little net change through ten seconds.

The effects of varying initial oxygen concentration while keeping acetic acid feed concentration constant can be seen by comparing sets of runs in which oxygen feed was increased four-fold, while CH_3COOH feed concentration remained essentially constant.

Figure 6.11 **Comparison of Acetic Acid and Oxygen Profiles for Stoichiometric (1:0.5 and 4:2) Acetic Acid Oxidation in Supercritical Water at 525 °C and 246 bar.** Actual average $[O_2]_o:[CH_3COOH]_o$ feed concentrations are $([1.09 \pm 0.2]:[0.50 \pm .01]) \times 10^{-3}$ mol/L for the lower profile of each species and $([3.90 \pm 0.5]:[2.02 \pm .02]) \times 10^{-3}$ mol/L for the higher profile of each species. Error bars represent 95% confidence intervals.
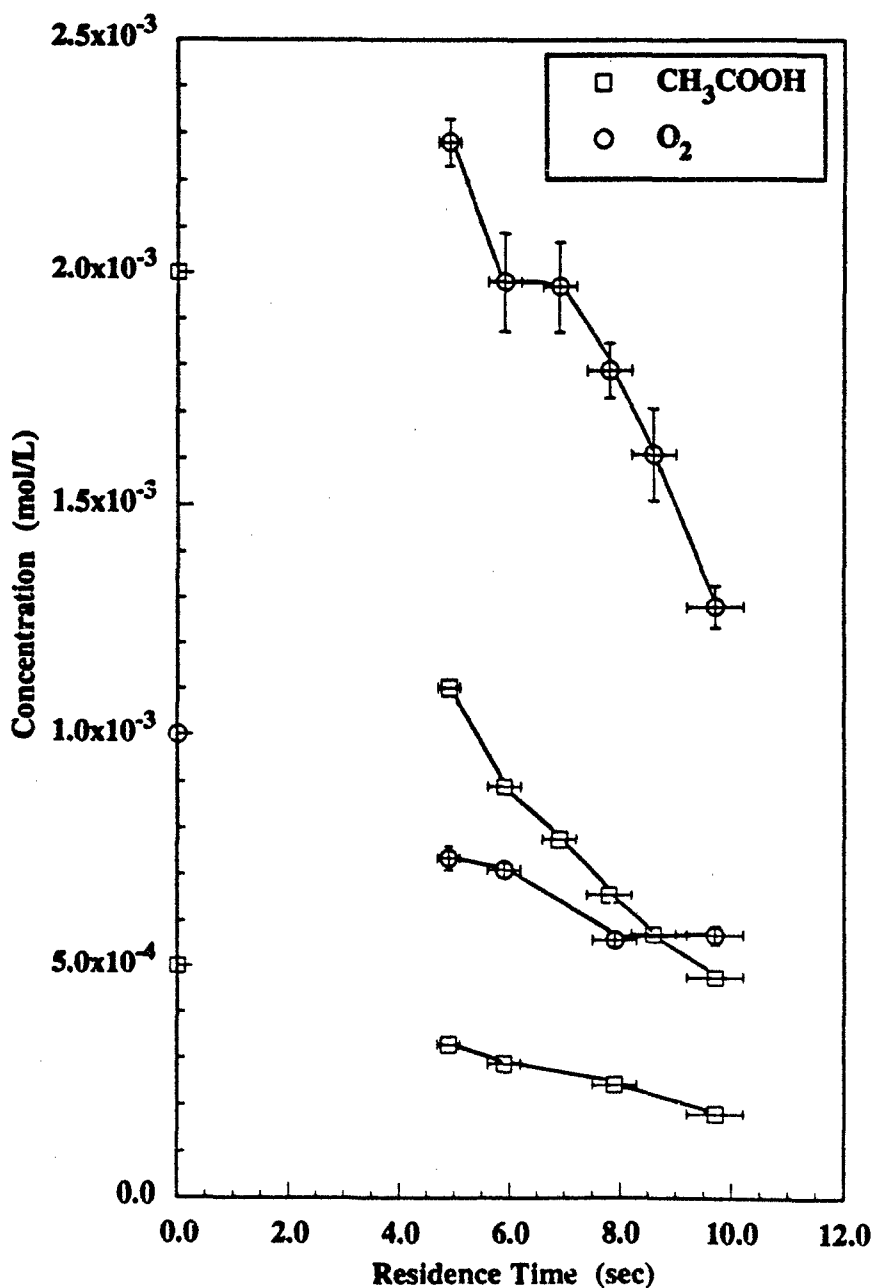
Figure 6.12 Comparison of Carbon Monoxide and Carbon Dioxide Profiles for Stoichiometric (1:0.5 and 4:2) Acetic Acid Oxidation in Supercritical Water at 525 °C and 246 bar. Actual average $[O_2]_o$:$[CH_3COOH]_o$ feed concentrations are ($[1.09\pm0.2]$:$[0.50\pm.01]$) $\times10^{-3}$ mol/L for the lower profile of each species and ($[3.90\pm0.5]$:$[2.02\pm.02]$) $\times10^{-3}$ mol/L for the higher profile of each species.
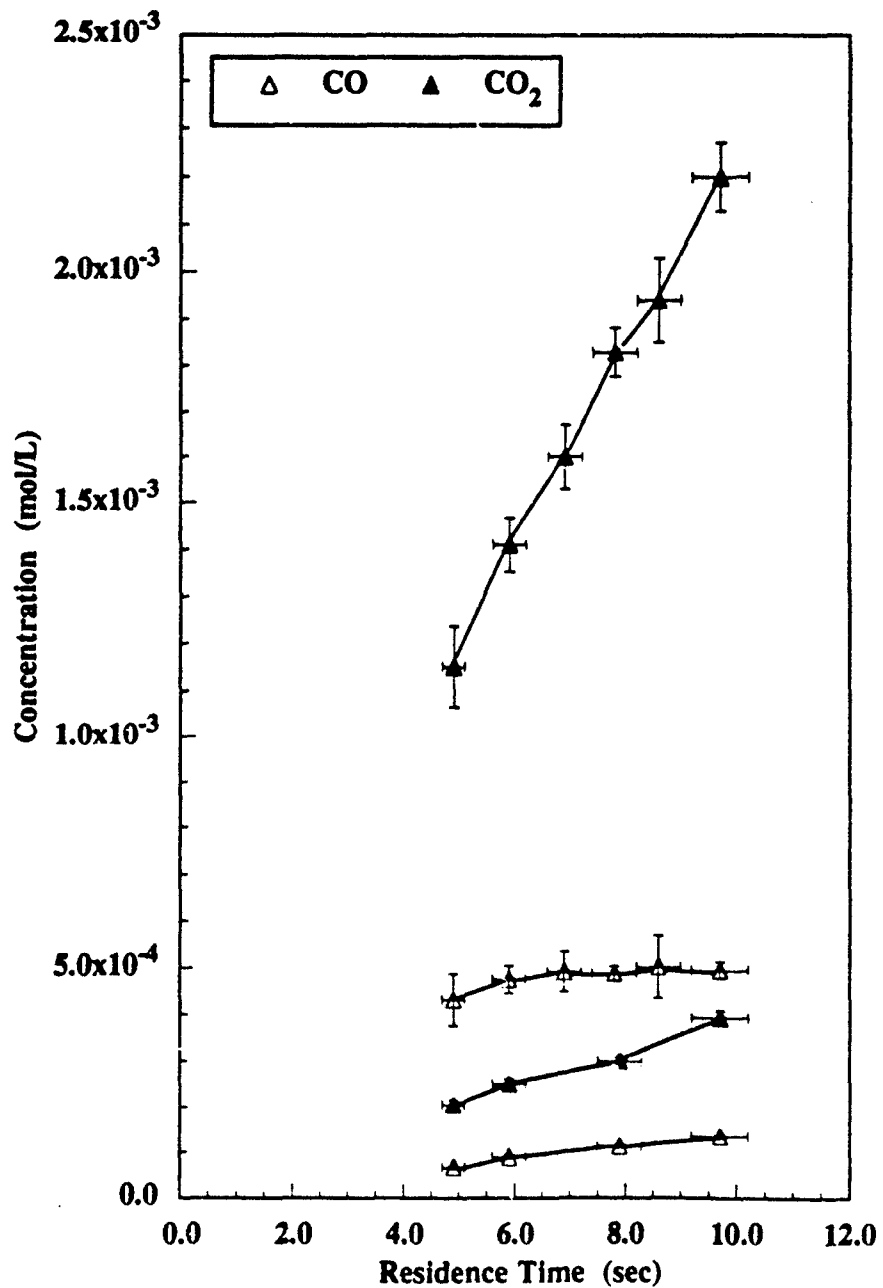
Figure 6.13 **Comparison of Methane and Hydrogen Profiles for Stoichiometric (1:0.5 and 4:2) Acetic Acid Oxidation in Supercritical Water at 525 °C and 246 bar.** Actual average $[O_2]_o$:$[CH_3COOH]_o$ feed concentrations are ($[1.09 \pm 0.2]$:$[0.50 \pm .01]$) $\times 10^{-3}$ mol/L for the lower profile of each species and ($[3.90 \pm 0.5]$:$[2.02 \pm .02]$) $\times 10^{-3}$ mol/L for the higher profile of each species. Error bars represent 95% confidence intervals.
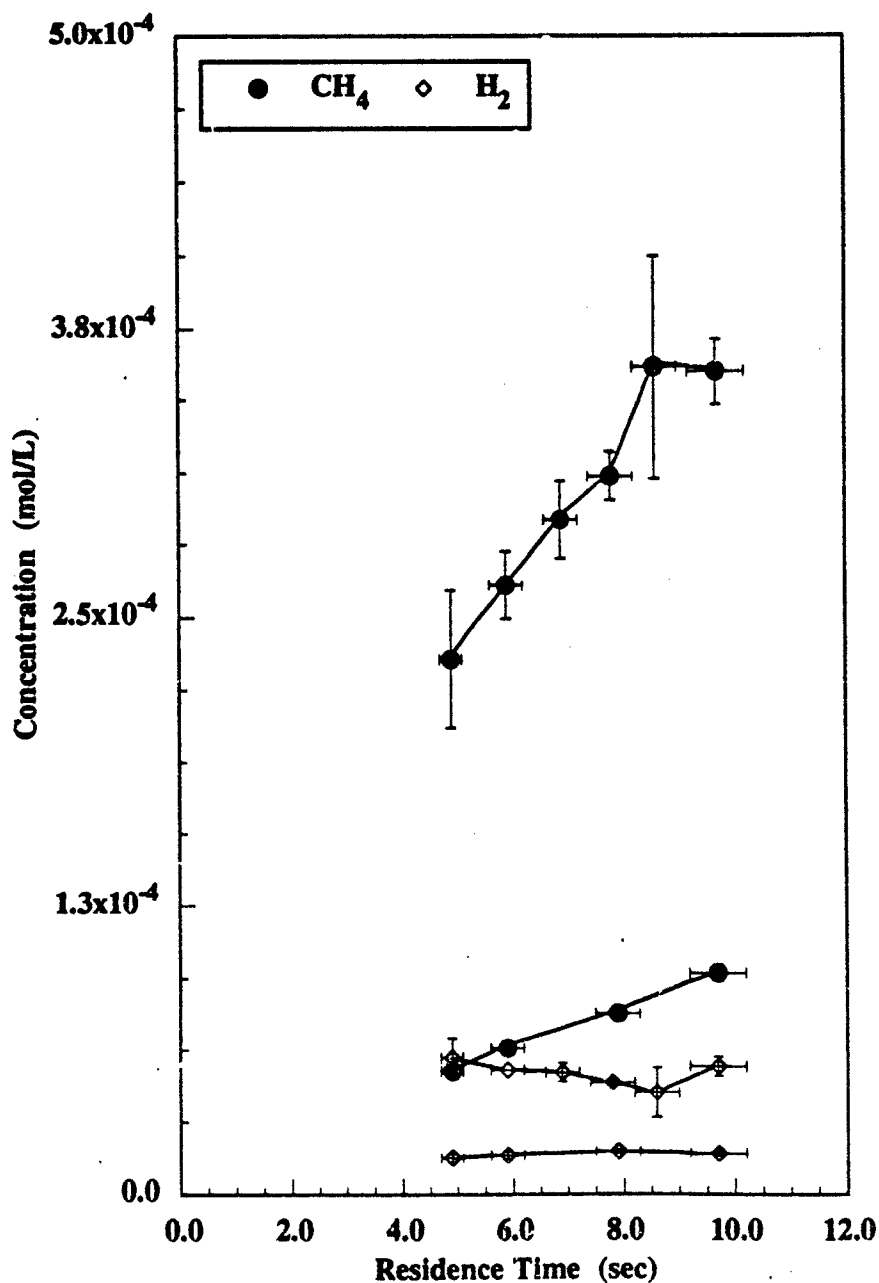
Figure 6.14 and 6.15 display reactant and gaseous product profiles for this oxygen variation. Plotting both series of runs on the same scaling gives Figure 6.16 (O_2 decay profile of the 4:1 run omitted to enhance detail of lower concentration compounds). The oxygen dependence of acetic acid oxidation in supercritical water is profoundly evident in the shift of the acetic acid decay profile. Product concentrations of methane and CO seem to be significantly less effected by increased oxygen feed concentration. Overall, hydrogen concentrations appear unaffected by the change in O_2 feed under these experimental conditions.

Liquid product variations due to varying oxygen feed concentrations are shown in figure 6.17. All runs were conducted at 525 °C, 246 bar, 9.9 seconds residence time, and $[CH_3COOH]_o = 1 \times 10^{-6}$ mol/cm^3, with O_2:CH_3COOH ratios as indicated. Though not obvious from the figure, conversion of acetic acid was 76%, 63%, and 55% for the oxygen-rich, stoichiometric, and oxygen-lean feeds, respectively. The unidentified compound with peak elution time of ~4.7 minutes significantly decreases with increased oxygen feed. Similarly, the compound with peak elution time of ~5.0 minutes decreases, to below detectable limits in the 4:1 feed. Although unidentified, these compounds elute in the same time frame as maleic (dual peaks at ~4.8 and 5.8 minutes) and oxalic (~5.2 minutes) acids, and may be similar in structure. Conversely, the unidentified compound eluting at 17.7 minutes increases with oxygen feed. As will be seen later, this compound is also consistently found in oxidation of methylene chloride.

Figure 6.14 **Major Species Profiles for Oxygen-Lean Acetic Acid Oxidation in Supercritical Water at 525 °C and 246 bar.** $[O_2]_o = (1.09 \pm 0.2) \times 10^{-3}$ mol/L, $[CH_3COOH]_o = (0.98 \pm .01) \times 10^{-3}$ mol/L. Error bars represent 95% confidence intervals.
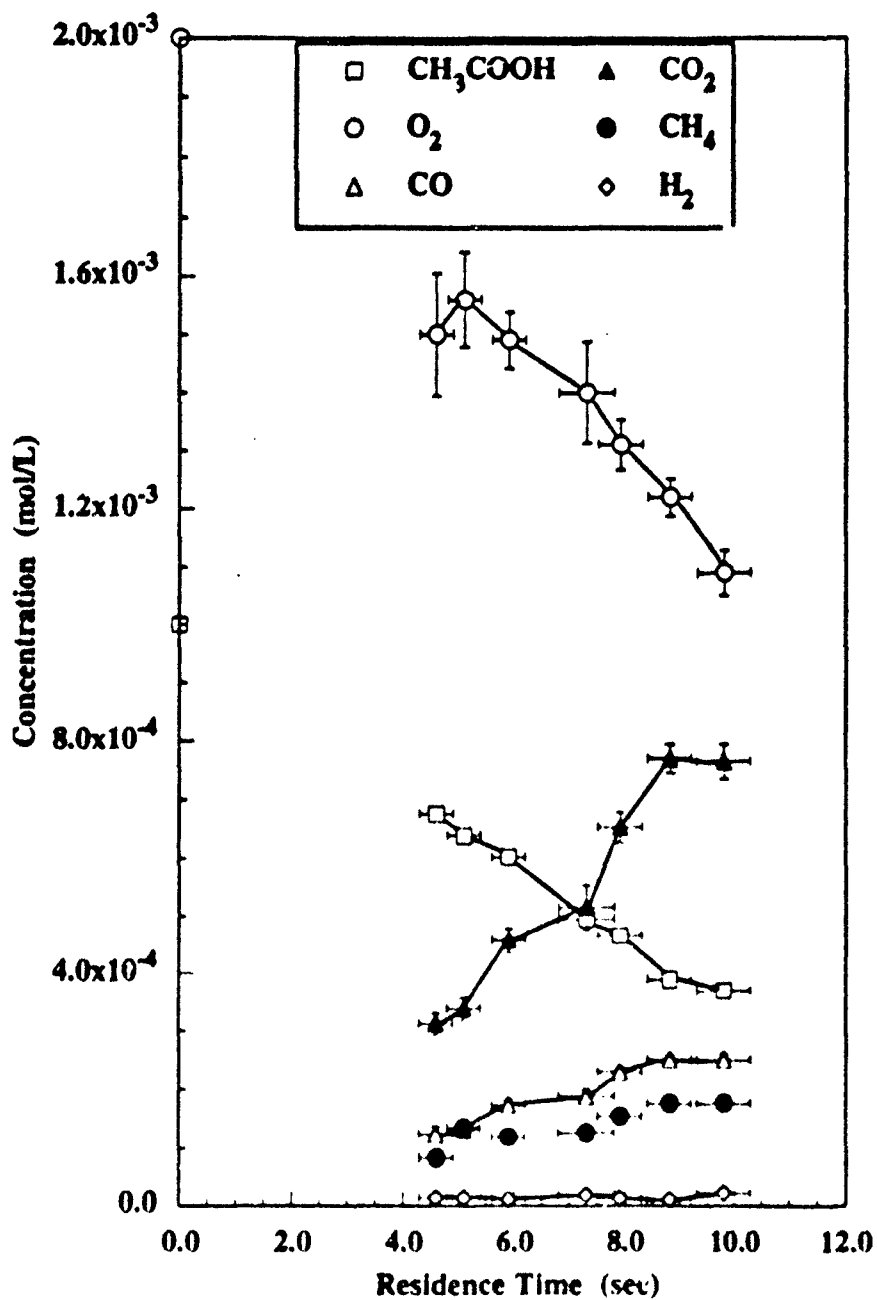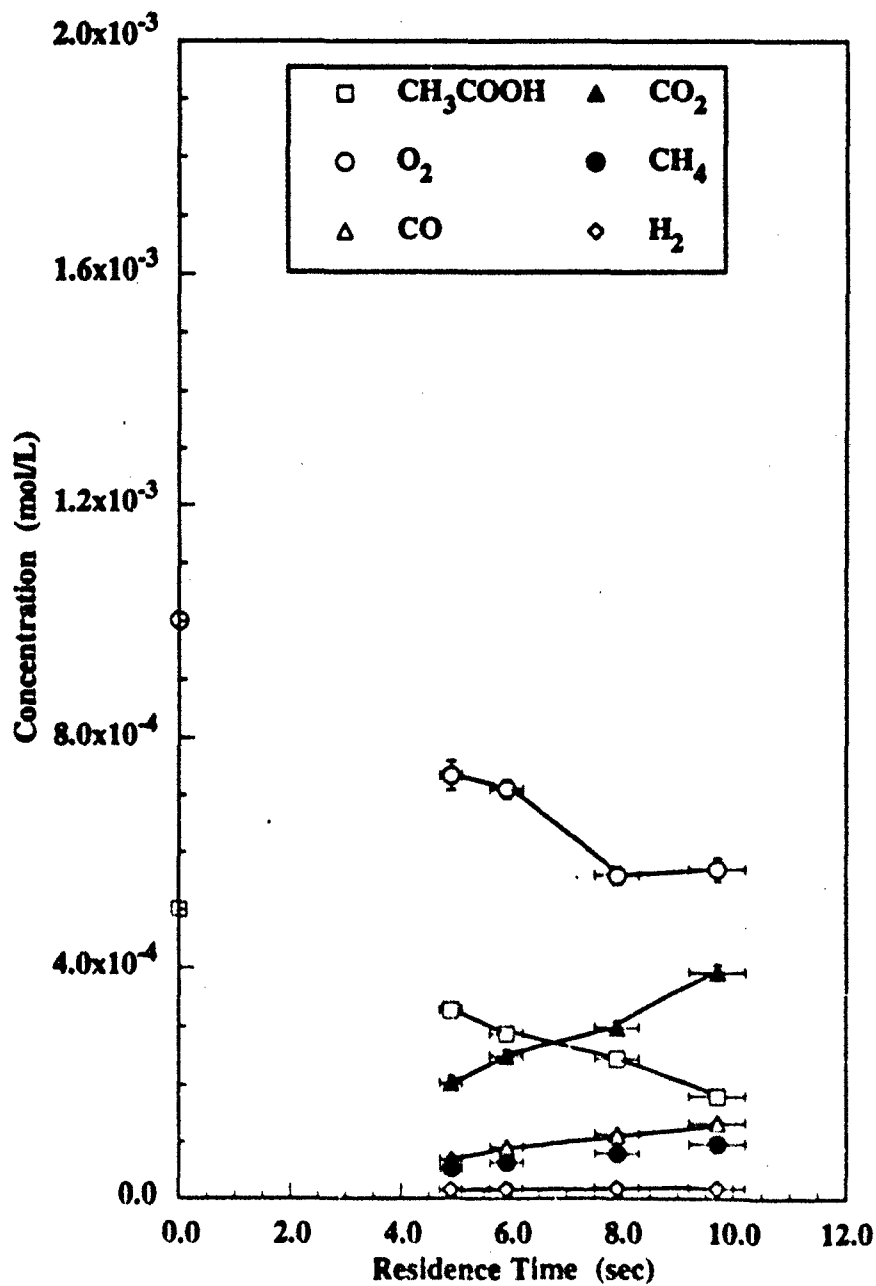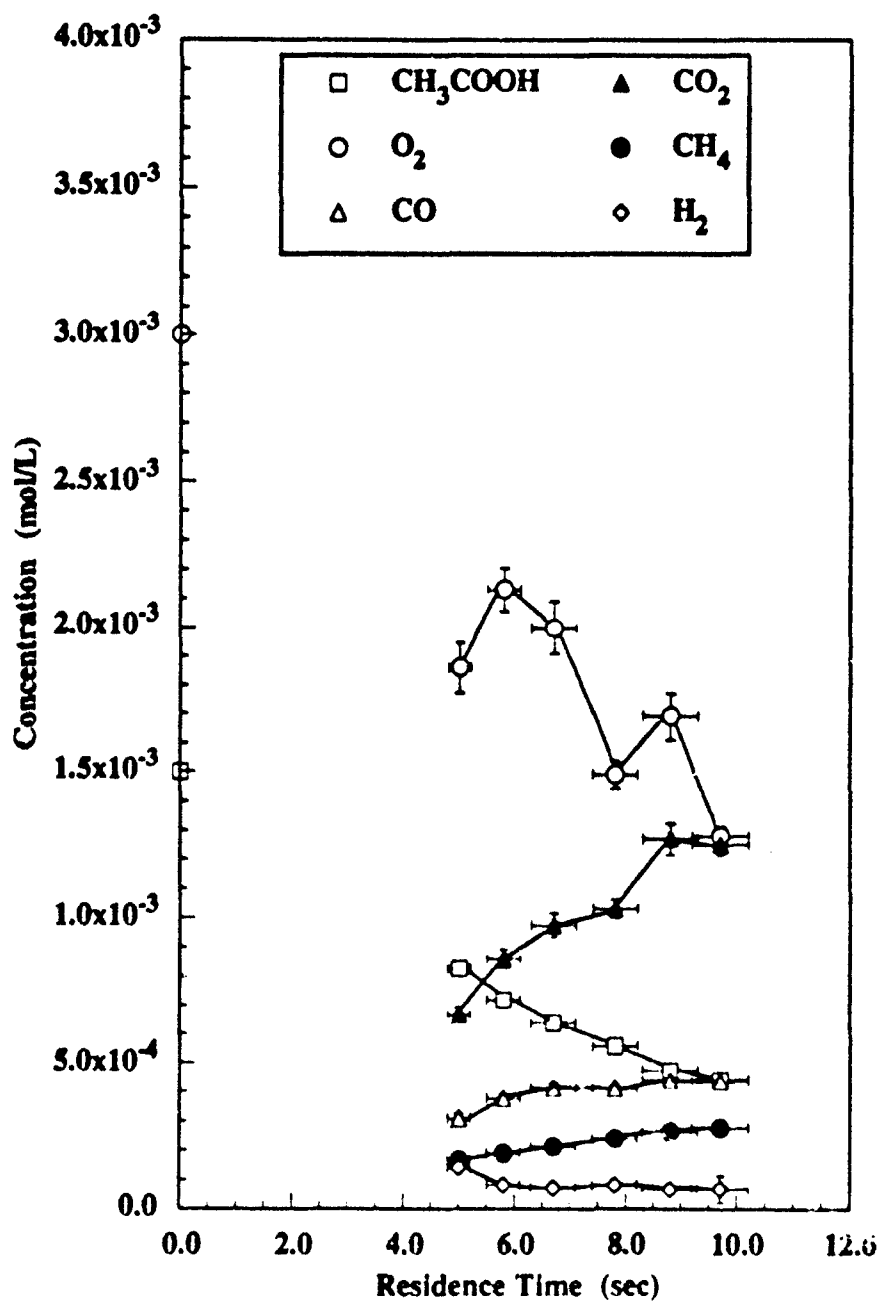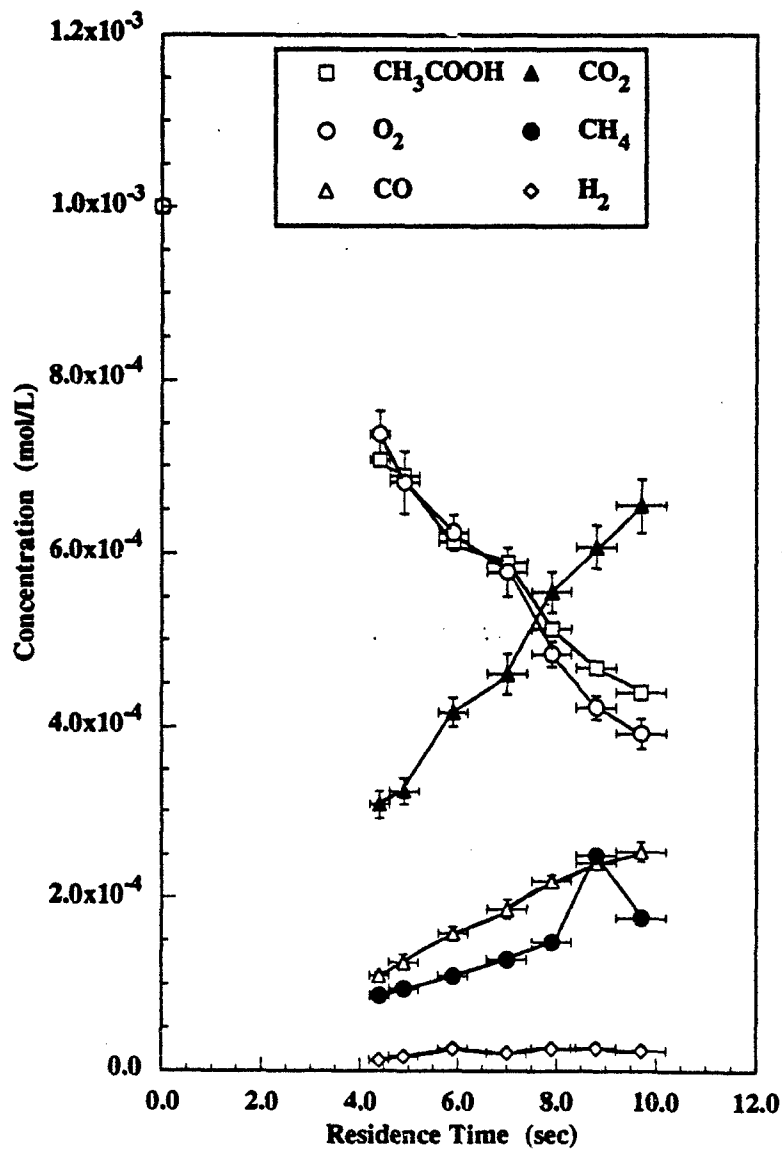
Figure 6.15 Major Species Profiles for Oxygen-Rich Acetic Acid Oxidation in Supercritical Water at 525 °C and 246 bar. $[O_2]_o = (3.86 \pm 0.4) \times 10^{-3}$ mol/L, $[CH_3COOH]_o = (0.99 \pm .01) \times 10^{-3}$ mol/L. Error bars represent 95% confidence intervals.
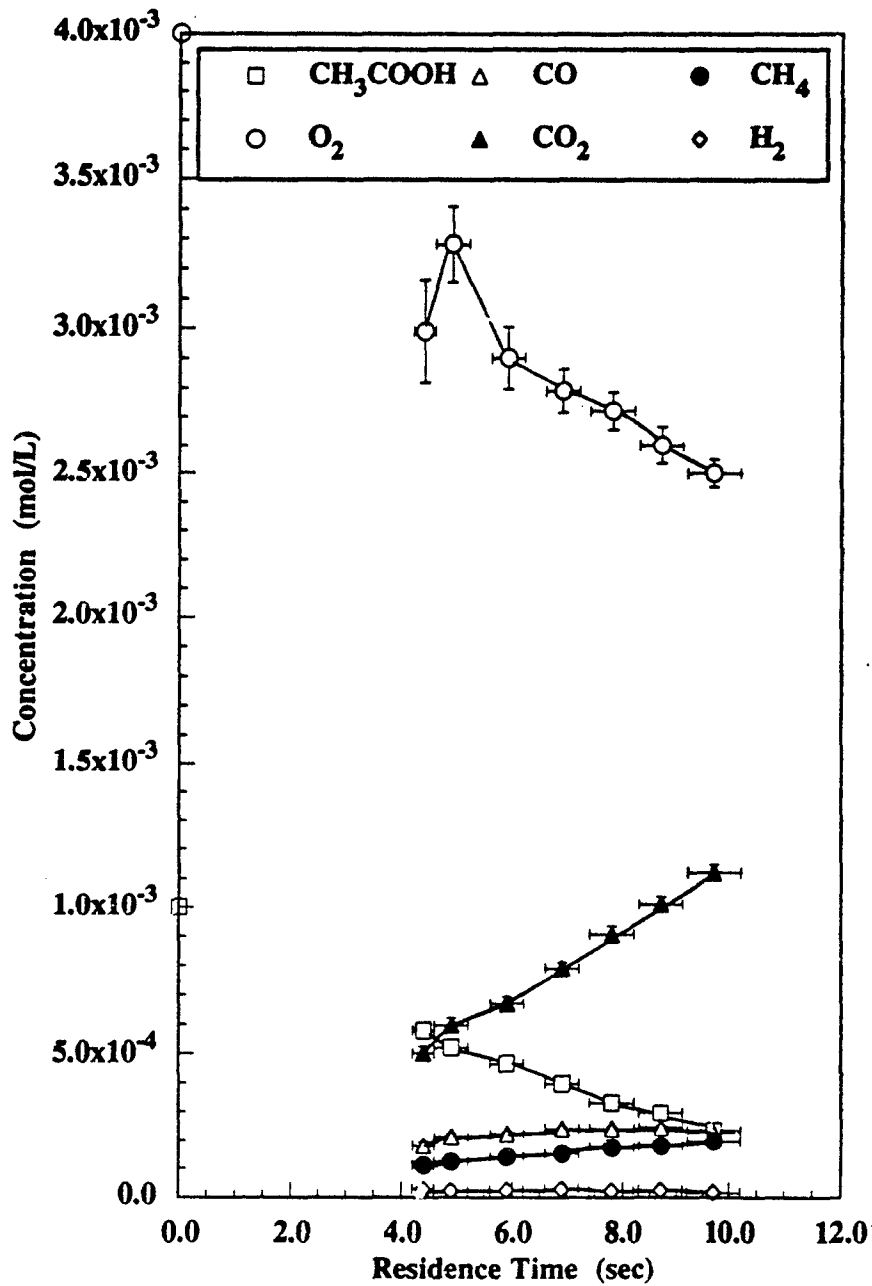
Figure 6.16 **Combined Major Species Profiles for Oxygen-Lean and Oxygen-Rich Acetic Acid Oxidation in Supercritical Water at 525 °C and 246 bar. (Figures 6.14 and 6.15 combined) Error bars represent 95% confidence intervals.**
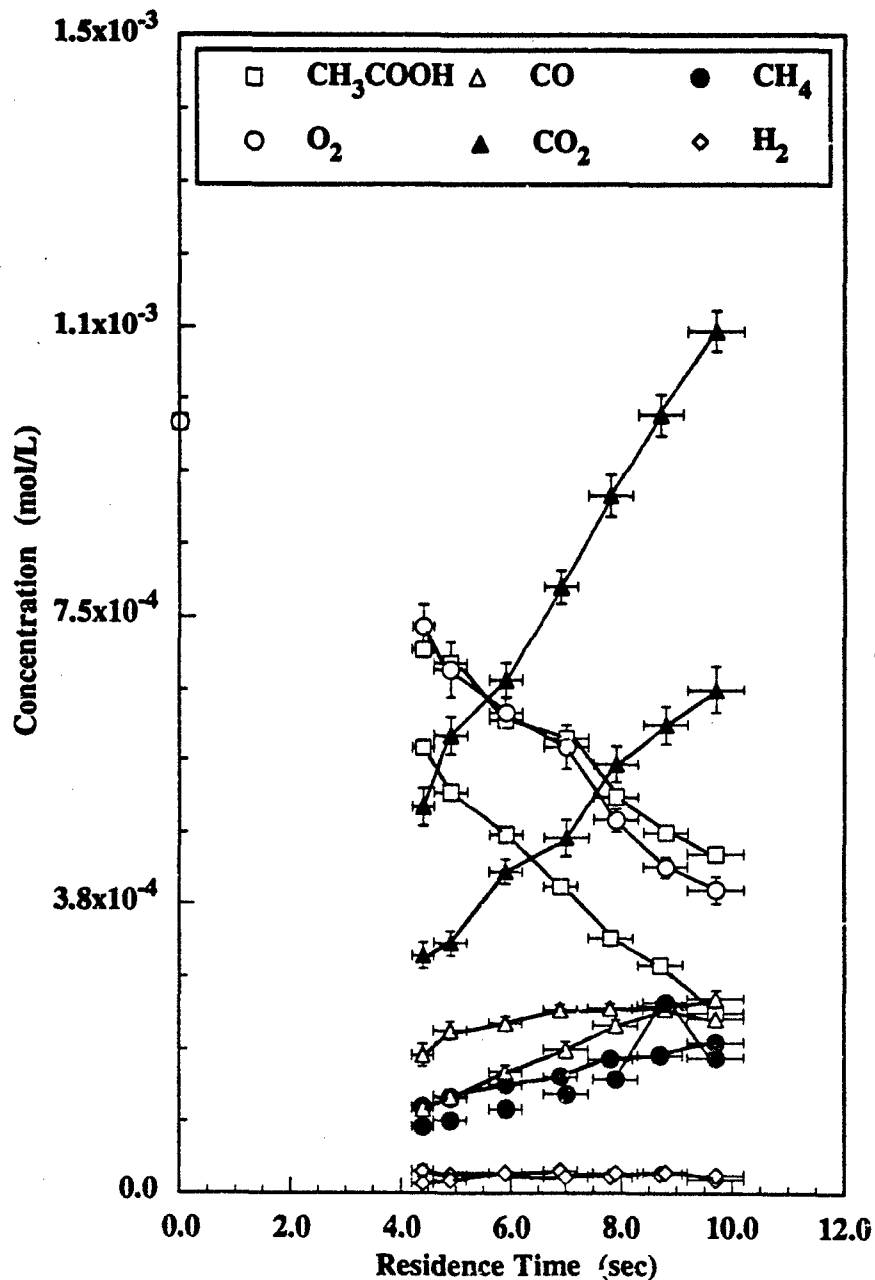
Figure 6.17 **Liquid Effluent Chromatograms from Acetic Acid Oxidation with Varying Initial O_2 Concentrations.** Experimental conditions: 525 °C, 246 bar, 9.9 seconds residence time, and $[CH_3COOH]_0 = 1 \times 10^{-6}$ mol/cm³, with O_2:CH_3COOH ratios as indicated.
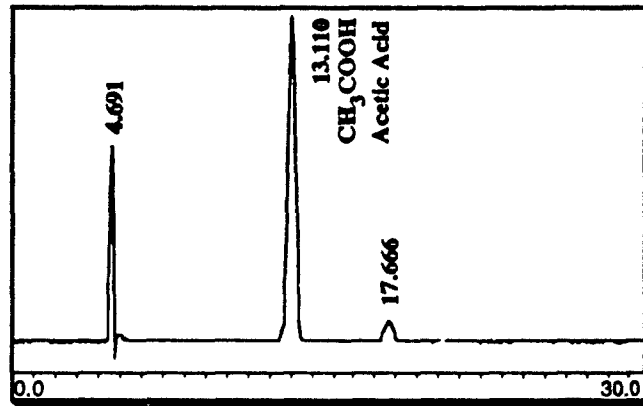
Run 280, Sample #1 (Oxygen-Rich, 4:1)
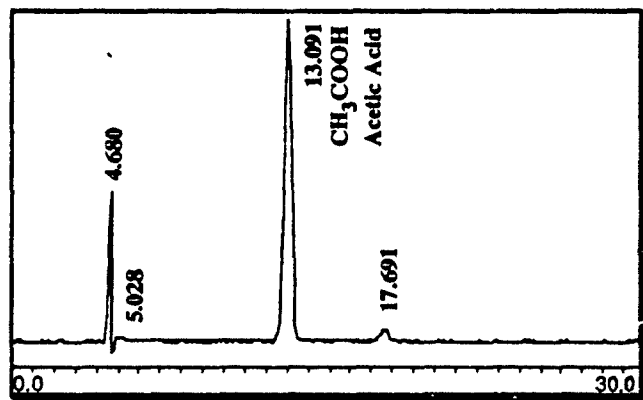
Run 265, Sample #1 (Stoichiometric, 2:1)
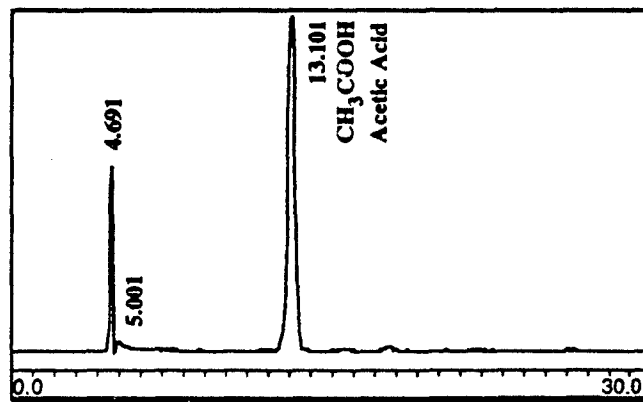
Run 271, Sample #2 (Oxygen-Lean, 1:1)

6.7 Pressure (Density) Effects

A limited series of experiments was conducted to determine the effects of operating pressure on the rate of acetic acid oxidation. These experiments were conducted similarly to Holgate's (1993) evaluation of pressure effects on hydrogen and carbon monoxide oxidation. Two series of experiments were carried out, at four and six seconds residence time, respectively. All reactions were conducted at 550 °C and nominal stoichiometric reactant concentration of 1×10^{-6} mol/cm^3 acetic acid and 2×10^{-6} mol/cm^3 of oxygen. Operating pressures ranged from 159.6 ± 4.8 bar to 263.0 ± 6.2 bar. These conditions were chosen to give the widest range of conversions over the domain of experiments. The complicating effect of residence time in previous similar work (Holgate, 1993) resulted in a concerted effort to keep residence time relatively constant (four and six seconds) for these experiments.

Results of variable-pressure experiments are shown in Figure 6.18, where ln k^* is plotted versus pressure, and tabulated in Table 10.4 of the Appendix. The rate constant, k^*, is defined here as an apparent first-order rate constant having the form of the Arrhenius equation, in contrast to k, the rate constant of Equation 6.5. The pressure range investigated incorporated both supercritical and subcritical pressures, and corresponds to water densities of 0.047 to 0.084 g/cm^3, or almost a 2-fold variation. At a residence time of 6 seconds, acetic acid conversion ranged from 80 to 93%. For runs at 4 seconds residence time, conversion spanned 64 to 86%. Figure 6.18 shows the apparent first-order rate constant, k^*, increases with increasing operating pressure at a 550 °C. But this increase in the apparent first-order rate constant is not quite as

Figure 6.18 Effects of Operating Pressure (Fluid Density) on the Apparent First-Order Rate Constant, k^* , for Acetic Acid Oxidation at 550 °C. Experimental Conditions: $[CH_3COOH]_o = (0.95 \pm .01) \times 10^{-6}$ mol/cm^3; $[O_2]_o = (2.09 \pm .02) \times 10^{-6}$ mol/cm^3. 95% confidence intervals are shown.
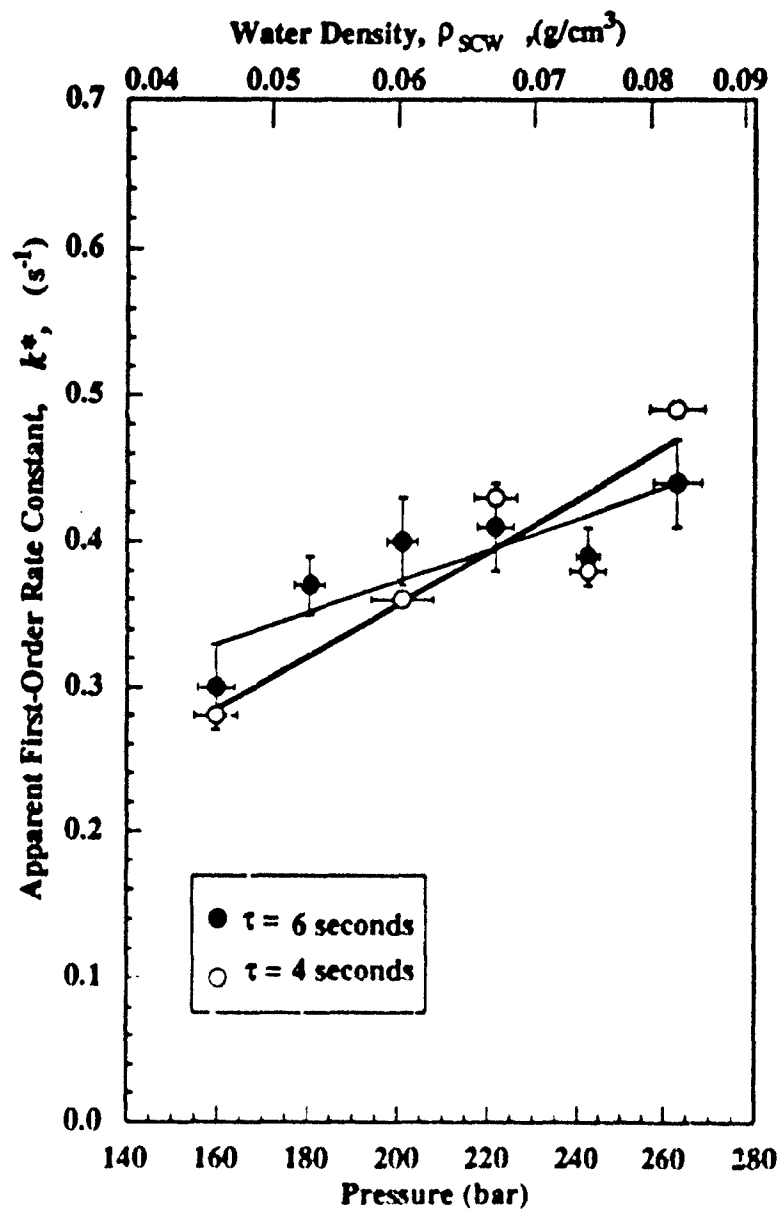
pronounced as Figure 6.18 suggests. As discussed in Section 6.5, the presence of an induction time complicates the calculation of k^*. Without an induction time and with all other experimental conditions the same, k^* should be constant, regardless of residence time. But with residence times on the order of the induction time, k^* increases with increasing residence time. This is portrayed in Figure 6.19. Although k^* might be considered constant if alternate extremes in error bars are considered, in general the trend is an increase in k^* with increasing residence time. Admittedly, the increase is slight and is much smaller than the increase seen by Holgate (1993) with hydrogen where k^* increased from 0.13 to 0.28 over residence times of about 3.4 to 5.5 seconds at 246 bar. Comparatively, acetic acid's k^* value changed from 0.12 to 0.14 over residence times of 4.9 to 9.7 seconds at 246 bar and a 4:2 oxygen to organic feed ratio. In our apparatus, variation in fluid density combined with flow restrictions imposed by the feed pump and the need to maintain a Reynolds number (Re) above the critical value of 2100 causes unavoidable variation in residence time with operating pressure. At low pressures (densities) the maximum residence time is governed by the need to maintain $Re \geq 2100$, while at high pressures, the minimum residence time is set by the maximum pump flow rate. Therefore, longer residence times seem to correspond with higher pressures as well as increased values of k^*. The pressure dependence of k^* is therefore somewhat exaggerated. Since this increase is coupled with pressure effects seen in Figure 6.17, true pressure effects are even less pronounced. The fact that all values of k^* at six seconds residence time are not greater than the corresponding experiment at four seconds may indicate that induction time is a function of pressure.

Figure 6.19 Variation of the Apparent First-Order Rate Constant, k*, with Residence Time. Experimental Conditions: $[CH_3COOH]_o = (2.02 \pm .02) \times 10^{-6}$ mol/cm^3; $[O_2]_o = (3.90 \pm .05) \times 10^{-6}$ mol/cm^3. 95% confidence intervals are shown.
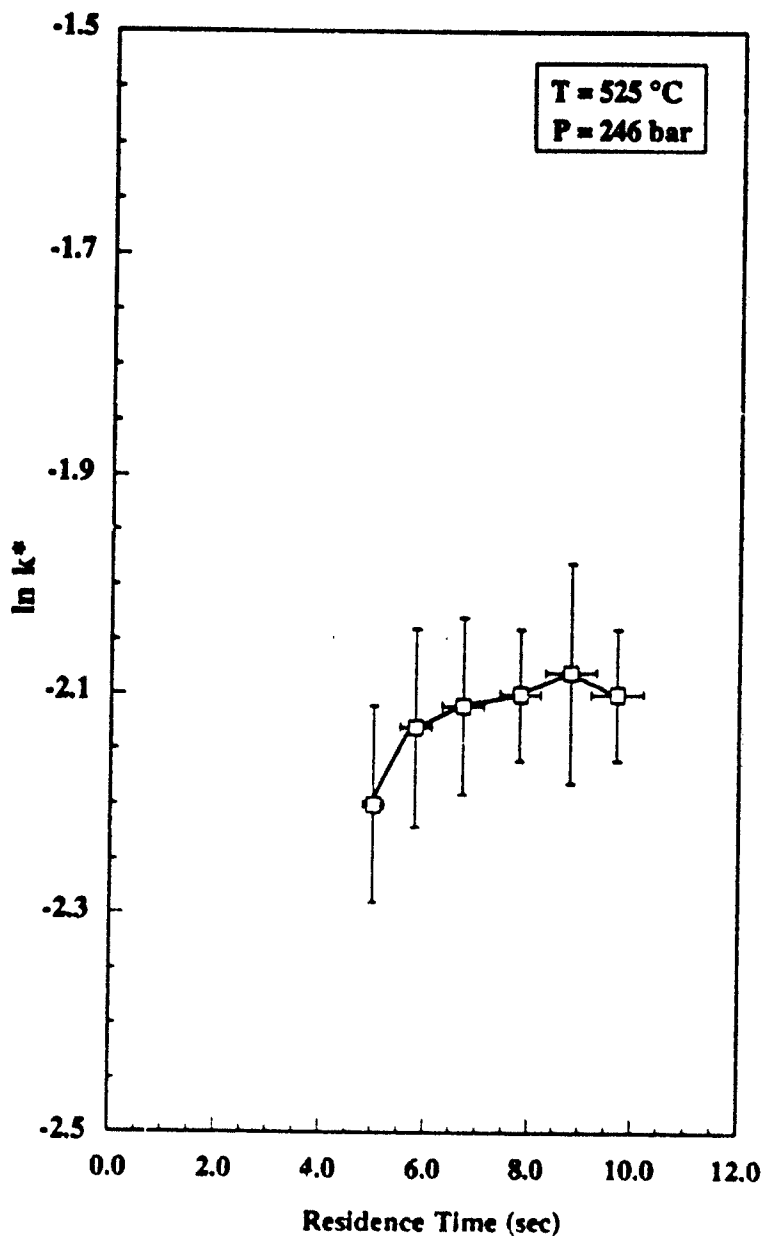
Figure 6.20 shows concentrations of the major gaseous product species in the reactor effluent as a function of pressure for a constant residence time of four seconds. Pressure variation over the conditions studied indicate virtually no effect on CH_4 concentration, while CO_2 production is slightly enhanced at the expense of CO. Still, these pressure effects are much less significant than similar pressure effect studies on carbon monoxide or hydrogen oxidation done by Holgate (1993). As partial oxidation products form, the oxidation of acetic acid occurs simultaneously with the oxidation of product intermediates (methane, carbon monoxide, etc.). The possibility that the oxidation profile of carbon monoxide differs in the presence of other compounds when all other conditions remain the same cannot be tested since CO is no doubt being created and destroyed simultaneously.

Liquid product distributions may change slightly under pressure variation, as indicated by the presence of propenoic acid eluting at ~15.5 minutes in Figure 6.21. The experiment shown gave about 80% conversion of acetic acid. A comparable experiment (314A) with pressure about 100 bar higher (160 bar versus 263 bar) gave nearly the same liquid chromatogram, but slightly increased acetic acid conversion (to 93%), and increased CH_4 yield from 12% of the gaseous effluent to 16%.

Although these few variable-pressure experiments are by no means conclusive, they seem to indicate that acetic acid oxidation kinetics are less influenced by pressure than other previously studied compounds.

Figure 6.20 Varia'ion with Operating Pressure (Fluid Density) of Major Gaseous Specl s Concentrations at 550 °C and 4 seconds Residence Time. $[CH_3COOH]_o = (0.95 \pm .01) \times 10^{-6} mol/cm^3$; $[O_2]_o = (2.09 \pm .02) \times 10^{-6}$ mol/cm^3.
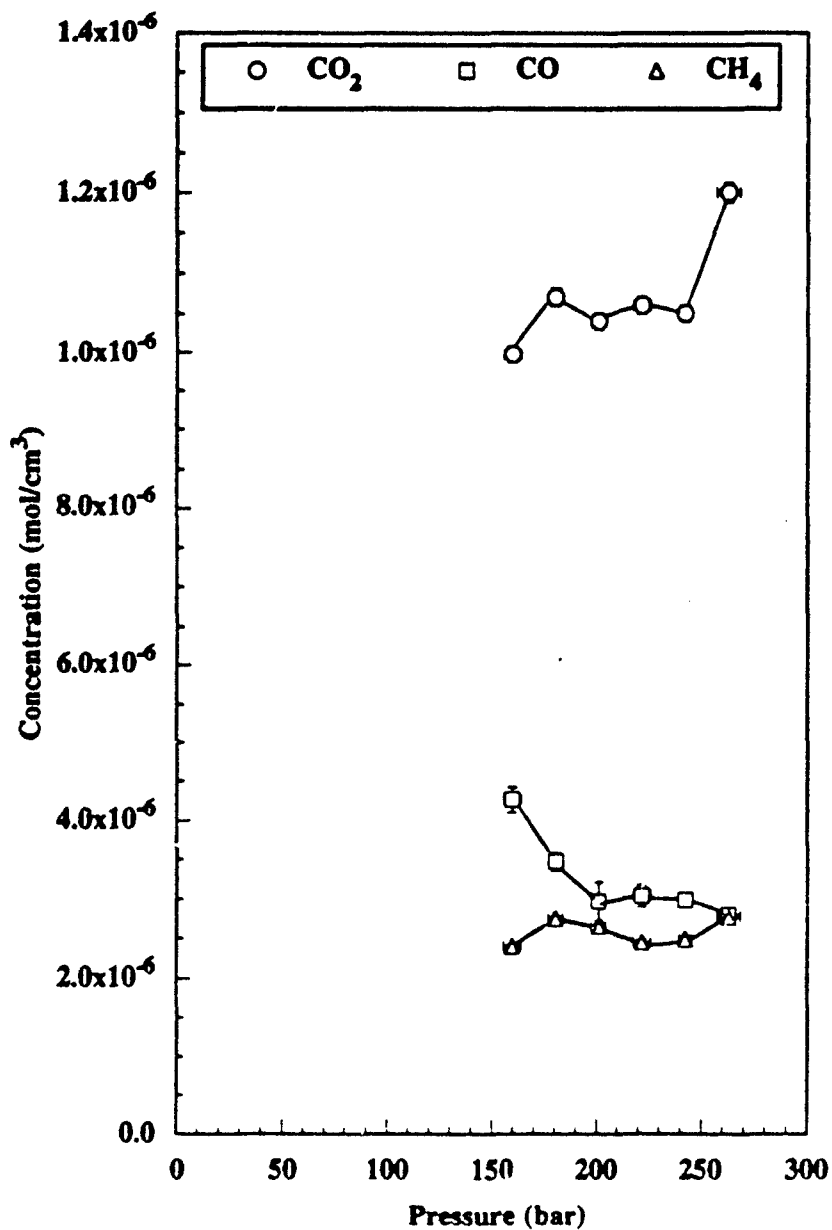
Figure 6.21 **Gas and Liquid Chromatograms of Acetic Acid Product Effluent at Subcritical Pressure.** Experimental conditions: 550 °C, 159 bar (2300 psig), 6.0 seconds residence time; $CH_3COOH]_o = (0.93 \pm .01) \times 10^{-6}$ mol/cm^3; $[O_2]_o = (2.11 \pm .02) \times 10^{-6}$ mol/cm^3. Liquid chromatogram absorbance at 210 nm.
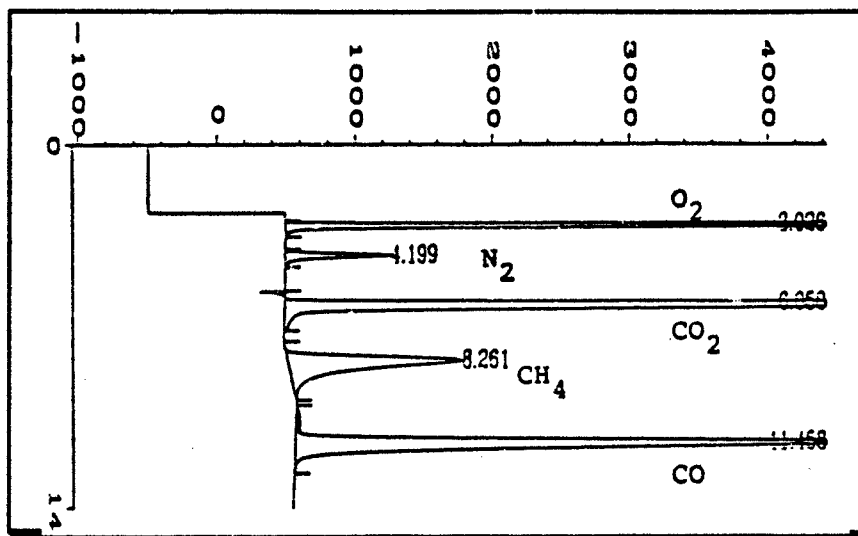
Gas Chromatogram Run 313A, Sample #6
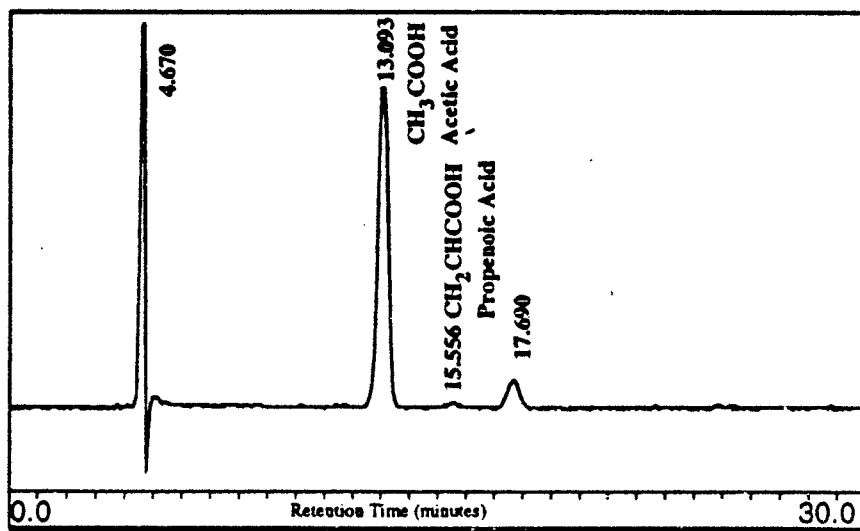
Liquid Chromatogram Run 313A, Sample #1

6.8 Acetic Acid Hydrolysis in Supercritical Water

Ten experimental runs were conducted without oxygen under pyrolysis or thermohydrolysis conditions. Although unable to introduce water totally void of oxygen, inlet O_2 concentrations in the reactor were approximately 2×10^{-8} mol/cm³ during these hydrolysis experiments. Inlet acetic acid was nominally 1×10^{-6} mol/cm³. Initially, five hydrolysis runs were conducted from 500 to 600 °C at 25 °C intervals. The remaining five hydrolysis runs were conducted two months later to substantiate the original results and determine if results were reproducible over time. One run was conducted at 475 °C while the four others were conducted at 25 °C intervals beginning at 512 °C and continuing through 587 °C. All runs were conducted at 8 seconds residence time. Although none of the experimental conditions in the first set were exactly duplicated, profiles from the second series of experiments followed the same decay profiles obtained in the first set, despite a time lapse of two months. Results are found in Table 10.1 of the Appendix.

Figure 6.22 shows that despite its reputation as one of the more refractory intermediate compounds in supercritical water reactions (Ploos van Amstel and Rietema, 1970; Skaates *et al.*, 1981; Tongdhamachart, 1990; Shanableh, 1991; Holgate 1993), acetic acid can be appreciably destroyed even in the absence of oxidant. In fact, its 35% conversion at 600 °C and 8 seconds residence time is quite good compared to some other previously studied compounds. Negligible conversion was observed for methane hydrolysis at 652 °C and residence times up to 14.8 seconds (Webley, 1989); hydrolysis of methanol was negligible (2.1%) at 544 °C and 6.6 seconds residence time (Webley,

1989, Tester *et al.*, 1992); and only 11% of ammonia was converted at 700 °C and 10.8 seconds residence time (Webley *et al.*, 1990, 1991) under oxidative conditions. Certainly the acetic acid hydrolysis and oxidation are occurring simultaneously in the presence of oxygen. This is similar to the concurrent water-gas shift and oxidative pathways present in CO oxidation in supercritical water reported by Holgate (1993). Ultimately, some credit (though perhaps small) must be given to hydrolysis when reporting the destruction efficiencies of acetic acid oxidation in supercritical water. Not only is hydrolysis aiding in the breakdown, but its products may also be undergoing hydrolysis or oxidation. Another comparison of acetic acid hydrolysis with oxidation is given in the form of a first-order Arrhenius plot in Figure 6.23.

Analysis of the liquid effluent via HPLC at 210 nm gave only unreacted acetic acid and trace amounts ($\sim 10^{-7}$ molar) of propenoic acid. The propenoic acid peak was no doubt at the limit of detection of our HPLC method as it was not always detected in every liquid sample taken from a specific experiment. Figure 6.24 compares acetic acid hydrolysis and oxidation liquid effluent chromatograms. For the run shown in Figure 6.24, hydrolysis conversion of acetic acid was ~16% (550 °C, 246 bar, 8 seconds residence time) while similar oxidation conditons gave ~98% conversion of acetic acid. The compound eluting at 17.7 minutes under oxidation conditions never appeared under hydrolysis conditions. UV analysis at 290 nm gave no peaks within 60 minutes retention time for the first few hydrolysis runs and hence was discontinued.

The major products of acetic acid hydrolysis were gaseous. However, at lower temperatures (conversions), the effluent gas flow rate was below the lower limit

Figure 6.22 Comparison of Acetic Acid Hydrolysis and Oxidation Conversion at 246 bar and 8 seconds Residence Time. For hydrolysis, $[CH_3COOH]_o$ $=(1.00\pm.01)\times10^{-6}$ mol/cm^3; $[O_2]_o = (2.19\pm.02)\times10^{-8}$ mol/cm^3. For oxidation, $[CH_3COOH]_o = (0.99\pm.01)\times10^{-6}$ mol/cm^3; $[O_2]_o = (2.09\pm.02)\times10^{-6}$ mol/cm^3. 95% confidence intervals are shown.
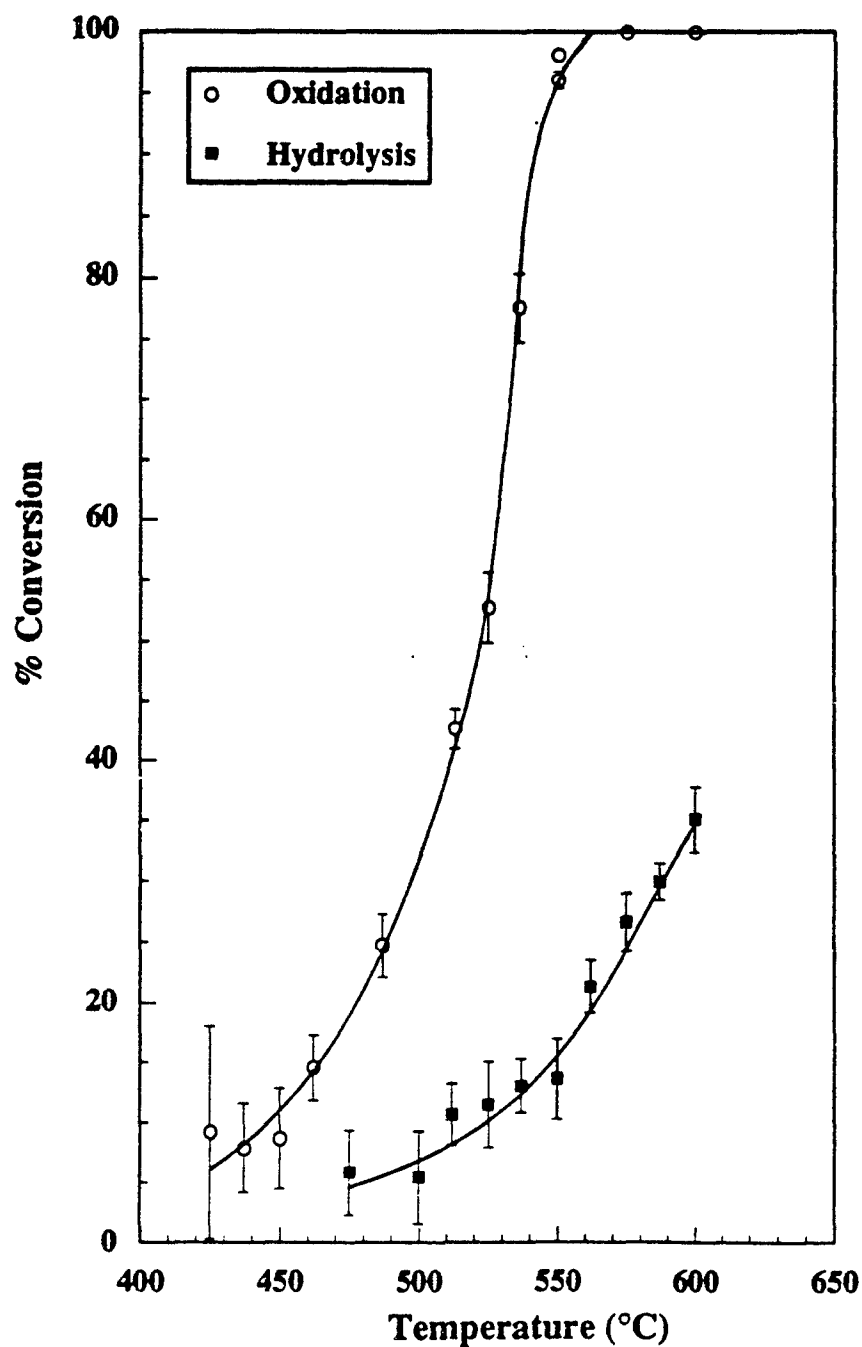
Figure 6.23 Comparison of Acetic Acid Hydrolysis and Oxidation First-Order Arrhenius Plots at 246 bar and 8 seconds Residence Time. For hydrolysis, $[CH_3COOH]_o = (1.00 \pm .01) \times 10^{-6}$ mol/cm^3; $[O_2]_o = (2.19 \pm .02) \times 10^{-6}$ mol/cm^3. For oxidation, $[CH_3COOH]_o = (0.99 \pm .01) \times 10^{-6}$ mol/cm^3; $[O_2]_o = (2.09 \pm .02) \times 10^{-6}$ mol/cm^3. 95% confidence intervals are shown.
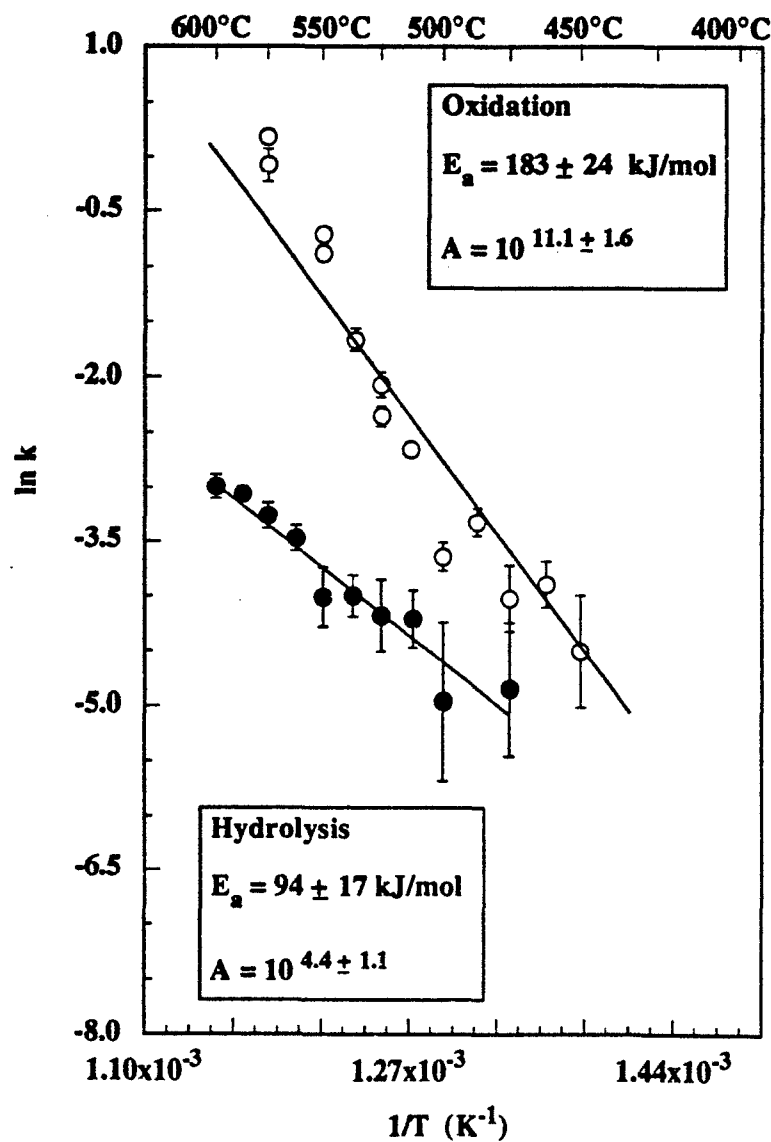
Figure 6.24   Comparison of Liquid Effluent Chromatograms in Acetic Acid Hydrolysis and Oxidation Experiments. Experimental conditions: 550°C, 246 bar, 8 seconds residence time, with $[CH_3COOH]_o = (1.00 \pm .03) \times 10^{-6} mol/cm^3$ and $[O_2]_o = (2.03 \pm .07) \times 10^{-6}$ mol/cm^3 for oxidation.
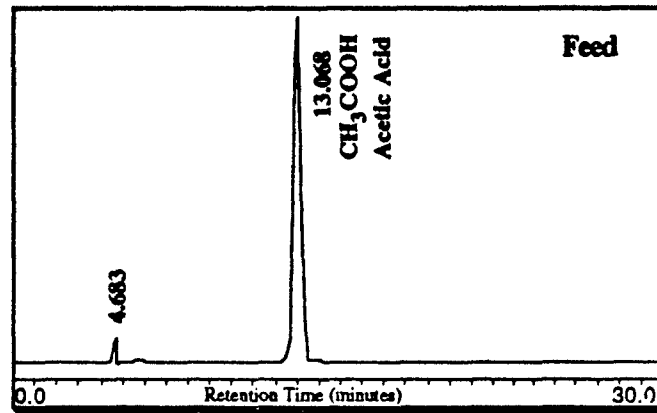
Run 246A & 247A, Feed
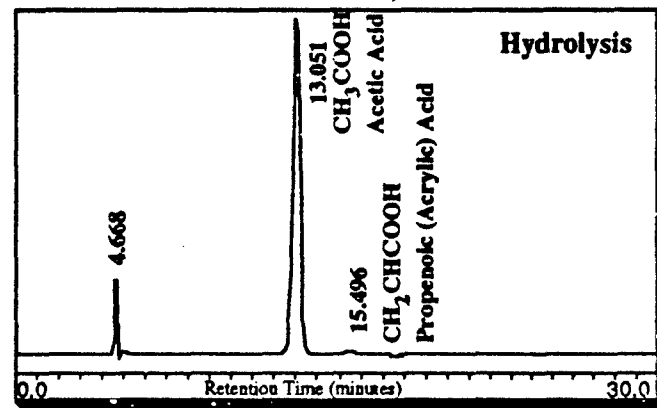
Run 246A, Sample #2
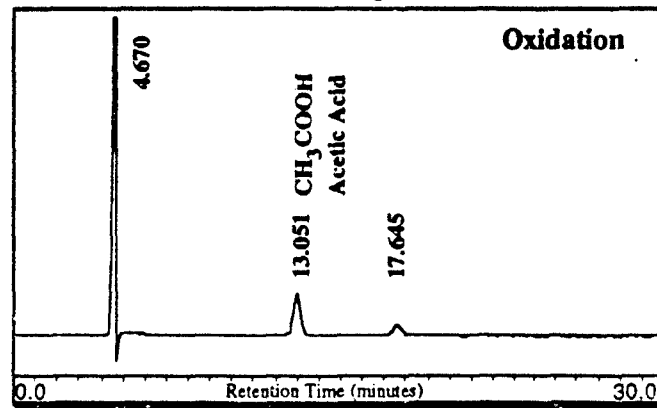
Run 247A, Sample #2

Figure 6.25 **Major Species Profiles for Acetic Acid Hydrolysis in Supercritical Water at 8 seconds Residence Time and 246 bar. $[O_2]_o = (2.19 \pm .02) \times 10^{-5}$ mol/L, $[CH_3COOH]_o = (1.00 \pm .01) \times 10^{-3}$ mol/L.**
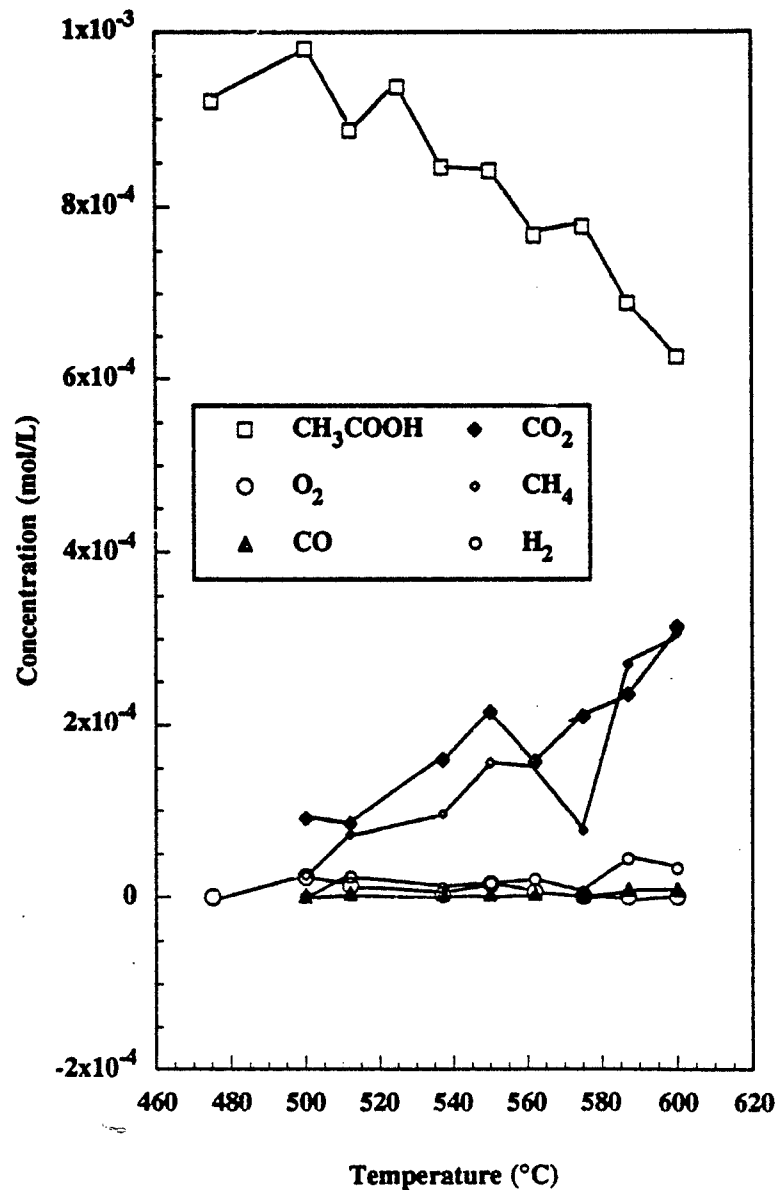
($\sim$0.3 ml/min) of measurability for our apparatus. At low (<15%) conversion, although CO_2 and CH_4 were the major products, their proportional compositions were not easily reproducible, hence the somewhat erratic carbon balance closures in Table 10.1. At higher gas flow rates ($\geq$ 0.5 ml/min), gaseous composition was reproducible, but based on only three to four dual gas samples as opposed to the normal six samples taken. Acetic acid and product gas profiles are shown in Figure 6.25. At temperatures above 550 °C, CH_4 and CO_2 were produced in nearly equal amounts, accounting for >95% of gas-phase products. Gases accounted for 76.0±16.6% of the carbon reacted at 512 °C and generally increased to 93.8±7.5% of carbon reacted at 600 °C. CO accounted for 1 - 2% of the carbon balances, and less than 1% of the total gas. Trace amounts of hydrogen, on order of 10^{-8} mol/cm^3 were also detected, accounting for less than 1% of the gaseous products. Other gases specifically tested for but not detected were ethane, ethylene, and acetylene. Minute amounts of nitrogen (from air dissolved in the aqueous feeds and possibly introduced in transferring the gas sample from the sampling port to the GC) and helium (used to pressurize the feeds) were also detected.

An assumed first-order regression of the limited hydrolysis runs gave suprisingly good results, with a rate expression of:

$$R_{[CH_3COOH]} = 10^{4.4\pm1.1} \exp(\frac{94\pm17}{RT}) \, [CH_3COOH] \qquad (6.8)$$

The correlation coefficient (r^2), adjusted for degrees of freedom was 1.00. Although the assumed first-order linear regression seems plausible (Figure 6.23), this regression must be considered suspect with the relatively few data on which it is based. A catalytic

mechanism model may be more appropriate, but was not attempted in this work. Any model verification will require more experiments over a wider variability of temperature, concentrations and residence time.

Chapter 7

Experimental Studies of Methylene Chloride Hydrolysis and Oxidation in Supercritical Water

7.1 Motivation

Halogenated hydrocarbons represent an important class of hazardous waste. Among the halogenated hydrocarbons, chlorinated derivatives find broad application as vital intermediates in the chemical industry. Chlorinated hydrocarbons are industrially important in the manufacture of plastics, agricultural chemicals, solvents, and medicines. But because of their widespread use, chlorinated hydrocarbons are a substantial component of halogenated wastes. Many are volatile, and, like other halogenated hydrocarbons, chlorinated organics are considered water contaminants. Growing concern over the effect of chlorinated compounds on the environment has led to concerted efforts to reduce their use.

As a significant class of hazardous wastes, chlorinated hydrocarbons are excellent candidates for destruction via SCWO. In particular, methylene chloride (dichloromethane, CH_2Cl_2) is structurally one of the more elementary chlorinated organics that is also a real-world contaminant. Its C1 carbon structure and simple C-Cl bonds make it an excellent choice as a model compound for careful study of reaction kinetics in a supercritical water environment.

7.2 Literature Review

Methylene chloride (CH_2Cl_2), has a formula weight of 84.92 and at ambient conditions it is a clear, colorless, volatile liquid with a boiling point of 39.8 °C at a pressure of

1 bar. Though only slightly soluble in water (1.32 g/100 mL of water at 25 °C), it is completely miscible with chlorinated solvents and itself is an excellent solvent for many aromatics, polymers, resins, waxes, and fats. Its solvency and nonflammability make it well suited to a wide variety of industrial uses. Methylene chloride is one of the least toxic chlorinated methanes, being less toxic than methyl chloride, chloroform, or carbon tetrachloride. (Anthony, 1978).

Its reputation as a contaminant in water, off-gases, and residues has led to investigation of its removal by vapor stripping, adsorption on activated charcoal, and distillation (Rossberg *et al.*, 1987). But even removal must result in eventual recycling or destruction of the compound. Incineration can be difficult because halogenated hydrocarbons have lower heats of combustion than ordinary hydrocarbons and therefore have lower flame temperatures. These lower temperatures can result in incomplete combustion products as well as molecular halogens that are difficult to remove from flue gas (Liepa, 1988). Incineration of chlorides is corrosive, as well. Catalytic oxidation of chlorinated compounds can result in poisoning of the catalyst. Consequently, higher temperatures and more catalyst may be needed, increasing the destruction costs.

Chlorinated hydrocarbon destruction has been previously investigated in both the near-critical and critical regimes. Most study has been focused on destruction efficiency, defined as the difference in the concentration of contaminant in the feed and effluent streams, divided by the concentration of contaminant in the feed stream. With wet oxidation, Randall and Kopp (1980) reported that initial concentrations of 5.0 g/L of pentachlorophenol and 12.41 g/L of 2-chlorophenol were destroyed to greater than 99%

efficiency at 320 °C and one hour oxidation time. Dietrich (1985) observed bench-scale wet-air oxidation destruction in excess of 99% for solutions of chloroform, 1,2-dichloroethane, carbon tetrachloride, and 1-chloronaphthalene at 275 °C and 60 minutes residence time. However, some chlorinated aromatics (i.e., chlorobenzene, 1,2-dichlorobenzene) were less than 75% destroyed under similar conditions, even in the presence of a potential catalyst. Destruction of numerous chlorinated organics in supercritical water have been reported by Thomason (1990), Thomason and Modell (1984), Modell (1985, 1989) and MODAR, Inc., in both pilot and bench-scale supercritical oxidation. Among those halogens undergoing ≥99.99% destruction efficiency were aroclors (polychlorobiphenyls), chlorinated Dibenzo-*p*-dioxins, hexachlorocyclohexane, *methylene chloride*, tetrachloroethylene and 1,1,1-trichloroethane.

Other than the reported destruction efficiencies cited above, reference to methylene chloride studies in supercritical water is scarce. However, non-catalytic and catalytic studies of methylene chloride oxidation have been done and are of interest for comparative purposes. In thermal oxidation by chromium oxide (1C) catalyst, Young (1982) obtained a rate expression that was first order in dichloromethane, but of undetermined order for oxygen, with an activation energy of about 72 kJ/mol in the temperature range 350 - 500 °C and at near-atmospheric pressures. A rough correction for the presence of water vapor gave a rate expression that was 0.97 order for dichloromethane, 0.09 order for oxygen, and -0.33 order in water. The unusual order for water clearly indicated that water inhibited the rate of reaction under the

aforementioned operating conditions. Catalytic oxidation of chlorides using chromia supported on γ-alumina was investigated by Liepa (1988). He found CH_2Cl_2 conversions were slightly lower than those measured for other chlorinated methanes at similar conditions (340 - 440 °C, atmospheric pressure and 0.2-0.4 second residence time). Most notable about catalyzed methylene chloride oxidation on chromia was the significantly lower amount of CO_2 formed compared to other chlorinated methanes. Other products included CO, H_2O, and HCl, with smaller amounts of Cl_2, and trace amounts of $CHCl_3$. The presence of other chlorinated hydrocarbons (CH_3Cl, C_2HCl_3, CCl_4) apparently inhibited dichloromethane oxidation rates (Liepa, 1988).

7.3 Experimental Results

The study of methylene chloride hydrolysis and oxidation in supercritical water marked the first time a chlorinated compound had been investigated in our lab. It also proved to be the first time there has been physical evidence of possible corrosion.

Thirty-seven CH_2Cl_2 oxidation and six CH_2Cl_2 hydrolysis experiments were conducted in supercritical water. Three oxidation experiments (Runs 335, 338, 360) were discarded because oxygen feed was depleted early in one experiment (#338) and an error in organic feed preparation in the other two. The remaining 34 oxidation runs were conducted at a constant pressure of 246 bar to provide a comparable data base to previous kinetic experiments in our laboratory (Helling and Tester, 1987, 1988; Webley and Tester, 1991; Webley *et al.*, 1990, 1991; Holgate, 1993) This pressure is typical of proposed operating pressures for the SCWO process (Tester *et al.*, 1993). Temperatures ranged from 450 -575 °C, although 23 of the oxidation experiments were carried out at

525 °C and seven at 500 °C to study concentration and density effects. Reactor residence times spanned 4.4 to 10.8 seconds. Feed concentrations of methylene chloride ranged from 2.01×10^{-6} mol/cm^3 (~ 0.21 weight %, or 1.5 ppmv) to 7.22×10^{-7} mol/cm^3 (~ 0.07 weight %, 0.5 ppmv), while inlet oxygen concentrations varied between 2.02×10^{-8} mol/cm^3 ("oxygen free" hydrolysis) and 2.08×10^{-6} mol/cm^3 (the highest oxygen concentration in the oxidation experiments). These concentrations resulted in inlet molar oxygen-to-methylene chloride ratios from 0.019 (hydrolysis) to 2.21 (oxygen-rich), where the stoichiometric oxidation ratio is 1.00. Conversions ranged from 38.3 $\pm$ 8.8% to complete methylene chloride destruction (within analytical detection limits).

A search for an accurate method in which to employ the available analytic techniques (thermal conductivity/flame ionization gas chromatography and high performance liquid chromatography) was complicated by the necessity to detect a diverse range of partial oxidation and hydrolysis products at ambient conditions. These included low molecular weight liquid organics, chlorinated liquid organics, gaseous hydrocarbons, and significant amounts of chloride products that ionize in aqueous solution (namely, HCl). After consideration of alternative methods of analysis, we determined to continue with the analytical procedures outlined in Section 4.2. Gas chromatography proved reliable in analyzing the gaseous products that consisted of CO, CO_2, O_2 (from unreacted feed), and contaminant N_2 (from air entrained in solution and perhaps introduced in sample collection) and He (used in organic saturator pressurization). As with our analysis of products from the glucose and acetic acid oxidation experiments (see Sections 5.3 and 6.6), no spurious peaks were ever observed in any of the 200-plus gaseous

samples analyzed, supporting the notion that negligible chlorine or chlorinated gases were formed as products in either hydrolysis or oxidation of methylene chloride. The same HPLC system, column and method were used to detect liquid effluent products. This allowed us to take advantage of the known retention times of approximately 50 previously tested organics (Tables 5.1 and 6.2) in determining the identification of any non-chlorinated products in the liquid effluent. Additionally, chlorinated products in the liquid effluent were determined in a similar manner. Chlorinated compounds tested as possible products are listed with their respective retention times for our analytical method in Table 7.1 Although the HPLC column used was not optimally designed for detection of chlorinated products, the method employed proved sensitive and reproducible in detecting chlorinated hydrocarbons. No apparent column degradation or significant pressure change was noticed throughout the course of experiments. The relatively slow mobile phase flow rate (0.5 ml/min) proved necessary in preventing peak overlap, but resulted in relatively long retention times for chlorinated products. Specifically, the slowest eluting product peak had a residence time of about 87 minutes. This long analytical time combined with the number of liquid samples taken (3 per experiment, plus the feed solution) caused some liquid effluent samples not to be analyzed on the same day as produced, but all samples were analyzed within 24 hours of sampling. Liquid samples were kept in amber, screw-cap sealed glass bottles (120 ml) in a darkened refrigerator (~6 °C) until analysis. The bottle caps were not teflon lined, so the possibility that reaction between effluent and the cap lining cannot be ruled out, although no perceptible

Table 7.1 Chlorinated Compounds Tested as Possible Liquid-Phase Products. Absorbance at 210nm using High Performance Liquid Chromatography.

Compound	Formula	Retention Time (minutes)
Carbon Tetrachloride	CCl_4	81.0
Chloroform	$CHCl_3$	48.6
1,2 Dichloroethane (Ethylene Dichloride)	$C_2H_4Cl_2$	36.4, 86.7
1,1 Dichloroethylene	$C_2H_2Cl_2$	53.4
cis-1,2 Dichloroethylene	$C_2H_2Cl_2$	51.2
trans-1,2 Dichloroethylene	$C_2H_2Cl_2$	45.6
Methylene Chloride (Dichloromethane)	CH_2Cl_2	31.7
Tetrachloroethane	$C_2H_2Cl_4$	81.3
Tetrachloroethylene	C_2Cl_4	39.1
1,1,2 Trichloroethane	$C_2H_3Cl_3$	52.0
Trichloroethylene	C_2HCl_3	86.4

chromatogram differences were noted between stored samples and samples that were immediately analyzed.

However, two other observations were noted. Over the time frame in which the methylene chloride hydrolysis and oxidation experiments were conducted (22 March - 22 April 1993), the peaks of the products with longer (>30 minutes) retention times drifted as much as ±0.2 minutes. Fortuitously, this did not seem to pose any identification problems, though, as chlorinated peaks tested were well separated at the previously mentioned flow rate. Additionally, the calibration of methylene chloride slowly drifted, such that 2 recalibrations of methylene chloride were used during the course of experiments. As a test of reproducibility, periodically a feed solution would be injected two or three times successively. This technique gave the same concentration reading ±3% (a larger error than seen for a similar technique with acetic acid) although one reading deviated 5% from an initial analysis. For this reason, all initial feed concentrations were conservatively estimated to have an associated error of ±10%. Liquid effluent concentration error was calculated to be within two standard deviations of the average of the three liquid samples collected during each experiment. Errors were propagated as described in Section 4.4.

As mentioned in Section 6.3, in some experiments, the measured liquid effluent flow rate deviated from the expected (calibrated) flow. The inlet concentrations were therefore corrected using the same proportioning as mentioned in Chapter 6. In most of the methylene chloride experiments, total effluent flow was within ±1% of the expected flow rate, with the largest actual flow deviating 3% above the expected flow. As with

the acetic acid experiments, this effect, coupled with our ability to verify the organic (methylene chloride) feed solution to at least ±10% of the desired concentration, caused the reactor inlet concentrations (and O_2:CH_2Cl_2 feed ratios) to vary slightly from the target values.

Six hydrolysis experiments were conducted over a temperature range of 450 - 575 °C at a reactor residence time of six seconds, 246 bar of pressure, and with a reactor inlet methylene chloride concentration of 1×10^{-6} mol/cm³. Of the six experiments, the actual inlet methylene chloride concentration for Run #334 was significantly below the desired conditions (7.47×10^{-7} mol/cm³ versus the sought 1×10^{-6} mol/cm³) and can not be directly compared with other hydrolysis results. Methylene chloride hydrolysis conversions ranged from 42.36±6.98% to 76.06±4.53%. Detailed discussion of hydrolysis results are found in the next section. Tabulated hydrolysis results are found in Table 10.5 of the Appendix. All propagated errors are to 95% confidence.

Oxidation conditions and results are also tabulated in the Appendix (Tables 10.6 and 10.7). Data presented are shown with a 95% confidence interval. For easier comparison, Table 10.7 regroups the data by feed ratios and reactor temperatures; it does not contain any new data. Section 7.5 describes the results of nonlinear regression of the data to a global rate form, while Section 7.6 discusses decay profiles. The influence of initial concentrations on product distribution is found in Section 7.7.

Conversion of methylene chloride under hydrolysis conditions at 450 °C, 246 bar and 6 seconds residence time was significant (47.1±6.0%), indicating that preheating

may have played an important role in methylene chloride destruction.

Corrosion was physically evident for the first time in our reactor system. After experimental runs, the liquid effluent would no longer be clear when the feed was changed to pure water. Liquid effluent discoloration varied from a light, cream-colored solution to a darker, reddish-brown precipitate when the feed was switched from oxygen and organic to a pure water feed. Although not noticed in the first three experiments in which inlet CH_2Cl_2 was doubled from 1×10^{-6} mol/cm^3 to 2×10^{-6} mol/cm^3, the liquid effluent became distinctly tainted with a pale yellow color during oxidation. This phenomena was the first observation of possible corrosion during actual oxidation. Additionally, the exit temperature thermocouple, located at the end of the reactor where corrosive conditions may be most severe (high acidity, high temperature), failed. It is not known whether this failure was attributable to cumulative degradation over the course of several months, or mainly due to more severe conditions created by the oxidation of methylene chloride. The replacement thermocouple may also be giving indications of degradation. The effect of these processes on kinetics is unknown. A detailed presentation on observed corrosion is reported in Section 7.8.

7.4 Methylene Chloride Hydrolysis in Supercritical Water

Conversion results from limited hydrolysis studies are plotted with corresponding oxidation runs in Figure 7.1. Tabulated hydrolysis data is given in Table 10.5 of the Appendix (Chapter 10). Some interesting characteristics of methylene chloride behavior in supercritical water are revealed in the plot of conversion versus reactor temperature. High destruction efficiency of methylene chloride can be achieved, even in the virtual

Figure 7.1   Methylene Chloride Hydrolysis and Oxidation Conversion in Supercritical Water. Reactor pressure of 246 bar with residence time of 6 seconds. $[CH_2Cl_2]_o = 1 \times 10^{-6}$ mol/cm^3 for hydrolysis and oxidation; $[O_2]_o = 1 \times 10^{-6}$ mol/cm^3 for oxidation. 95% confidence intervals are shown.

$\tau = 6.0$ sec
P = 246 bar

○ Oxidation
■ Hydrolysis

% Conversion
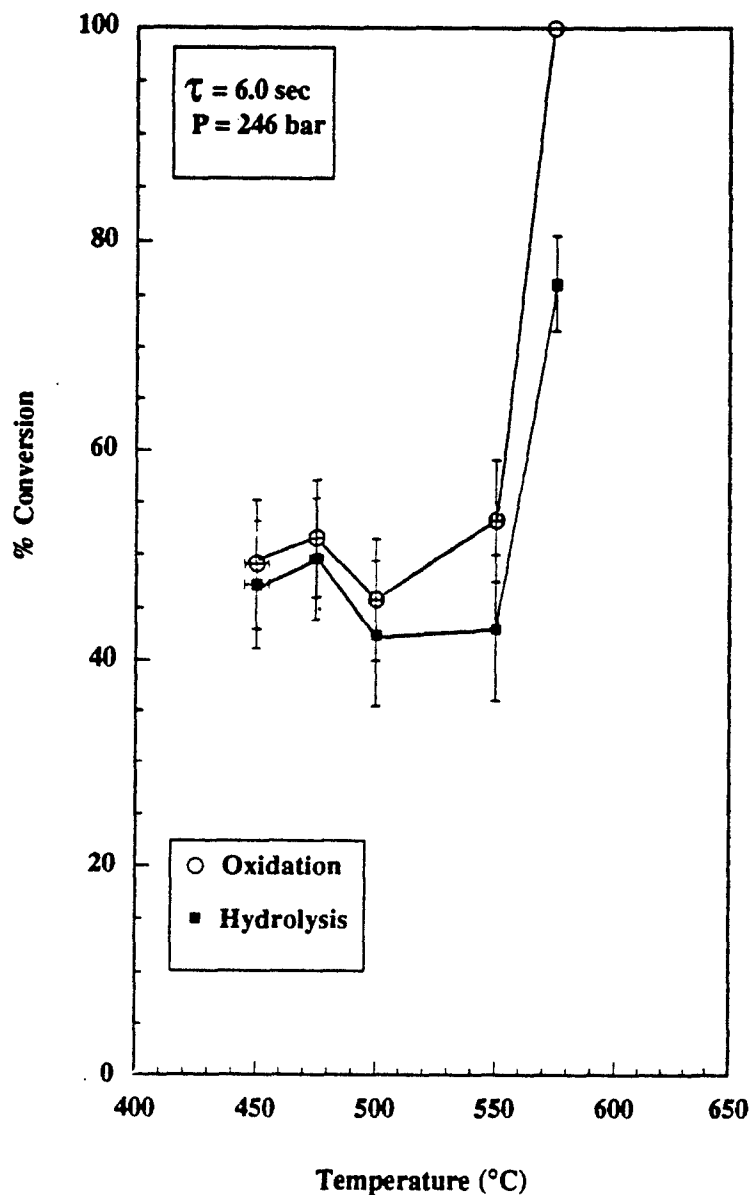
Temperature (°C)

absence of oxygen, as evidenced by the 76% conversion observed at 246 bar, 575 °C, and six seconds residence time. Significant conversion (>40%) is seemingly achievable at temperatures as low as 450 °C. Figure 7.1 suggests that even with oxygen present, hydrolysis accounts for most of the CH_2Cl_2 destruction over the temperature range of 450 to 550 °C . Oxygen seems to be influencing CH_2Cl_2 destruction very little as conversion remains essentially constant over this range; preferential oxidation of CH_2Cl_2 hydrolysis products may preclude direct oxidation of CH_2Cl_2. But the data in this region are perplexing, suggesting that CH_2Cl_2 conversion is relatively unaffected by a temperature increase of about 100 °C, in the range 450 - 550°C. This phenomenon seems quite suspect, requiring additional hydrolysis data in this temperature region before any meaningful conclusions can be made. Another confounding effect is the influence corrosion products may have had on kinetics. The first evidence of discolored effluent was made during startup of an oxidation experiment immediately following the conclusion of the series of runs in which hydrolysis measurements were taken.

Gaseous products were comprised almost entirely of H_2 and CO. Negligible (<1% by volume) amounts of CO_2 were formed. Figure 7.2 shows typical gas and liquid chromatograms for CH_2Cl_2 hydrolysis at 575 °C, 246 bar, and a residence time of six seconds. The gas chromatogram was obtained from the GC using helium as the carrier gas. The injected volume was approximately 200 μL. The limit of detectability for hydrogen on this GC is about 50 μl (He and H_2 have similar thermal conductivities; see Section 4.2). The mere presence of the hydrogen peak (at ~2.4 minutes) is indicative of its significant concentration in the sample, and the peak size indicates that

Figure 7.2 Gas and Liquid Chromatograms for CH_2Cl_2 Hydrolysis at 575 °C, 246 bar, and Residence Time of 6 Seconds. $[CH_2Cl_2]_o = 1 \times 10^{-6}$ mol/cm³, $[O_2]_o = 1 \times 10^{-6}$ mol/cm³.
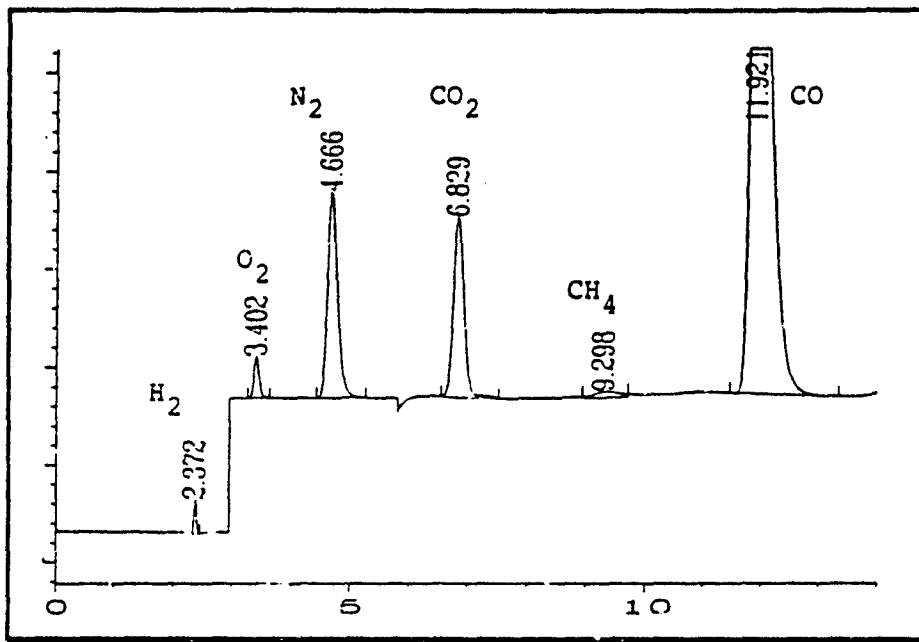
Hydrolysis Gas Chromatogram
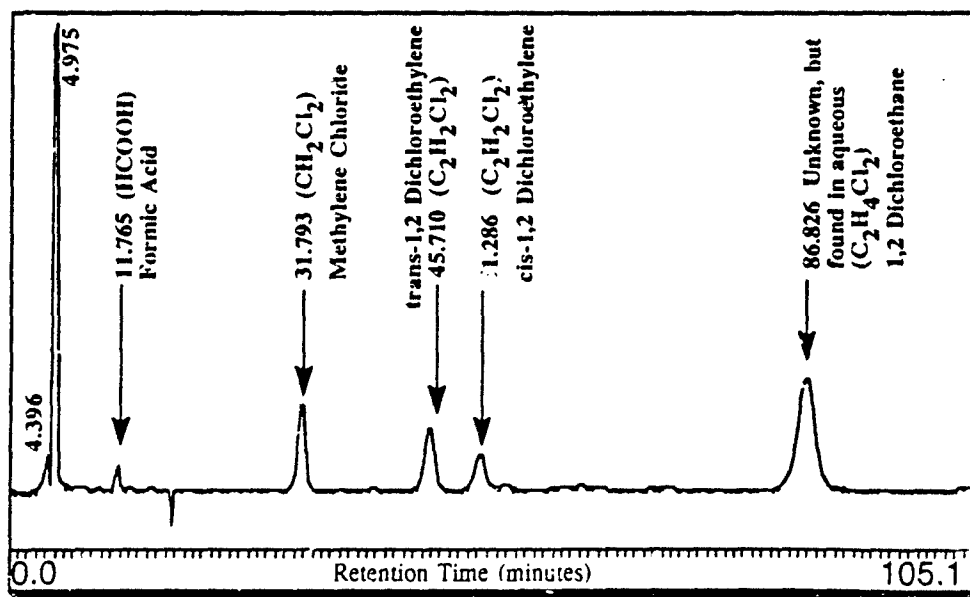
Hydrolysis Liquid Chromatogram

it makes up about 50% of the sample volume. Actual quantification of hydrogen is done with another GC using nitrogen as the carrier gas (Section 4.2). Oxygen and nitrogen in the hydrolysis sample most likely come from two sources. Air is slightly soluble in water and cannot be prevented from entering the reactor in minute amounts via the aqueous feeds. Also, the sample may have been contaminated with air as it was transported directly from the sampling port to the GC. In the gas chromatogram shown (Figure 7.2), N_2 accounts for about 5 % of the volume and O_2 is <1% of the sample volume. The $N_2:O_2$ ratio is not indicative of the composition of air, since the oxygen portion of the air dissolved in the feeds undoubtedly were consumed during hydrolysis (due to the presence of air, some minor oxidation will occur during hydrolysis). CO_2 makes up about 5% of this sample, about half the amount produced from the same inlet concentration (1×10^{-6} mol/cm^3) of acetic acid (CH_3COOH) during hydrolysis at the same temperature and pressure (CH_2Cl_2 hydrolysis reactor residence time was 6 seconds, versus 8 seconds for CH_3COOH). The methane (9.298 minutes retention time) produced was about 0.5% of the sample volume and was not detected in any other hydrolysis experiments. However, it was consistently detected in all six samples taken during this run at 575 °C. A surprisingly high amount (33% of the gaseous product, by volume) of CO was produced in this run. Even at 450 °C, 17% of the gaseous effluent was CO. Comparatively, CO made up only about 2% of the gaseous effluent produced in acetic acid hydrolysis over virtually the same temperature range. Gaseous product profiles as a function of reactor temperature are depicted in Figure 7.3. Figure 7.4 indicates that the majority of the gas formed under oxidative conditions may be actually attributable

Figure 7.3 Major Gaseous Product Profiles for Methylene Chloride Hydrolysis in Supercritical Water at 246 bar and 6 seconds Residence Time. $[CH_2Cl_2]_o = 1 \times 10^{-3}$ mol/L.
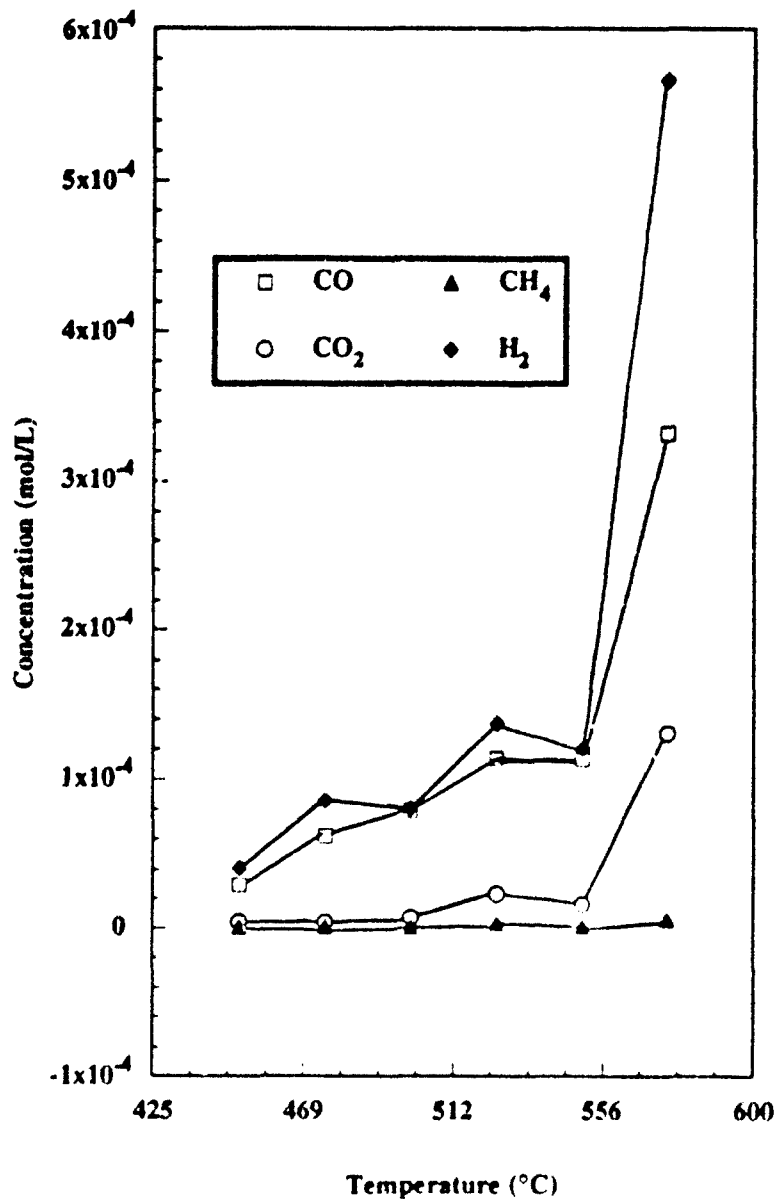
**Figure 7.4**   **Percent of Reacted Carbon that Appears as Gas Phase Product in Methylene Chloride Hydrolysis and Oxidation in Supercritical Water.** Reactor pressure of 246 bar and residence time of 6 seconds. $[CH_2Cl_2]_o = 1 \times 10^{-6}$ mol/cm^3 for hydrolysis and oxidation; $[O_2]_o = 1 \times 10^{-6}$ mol/cm^3 for oxidation. Exponential fits for clarity only.
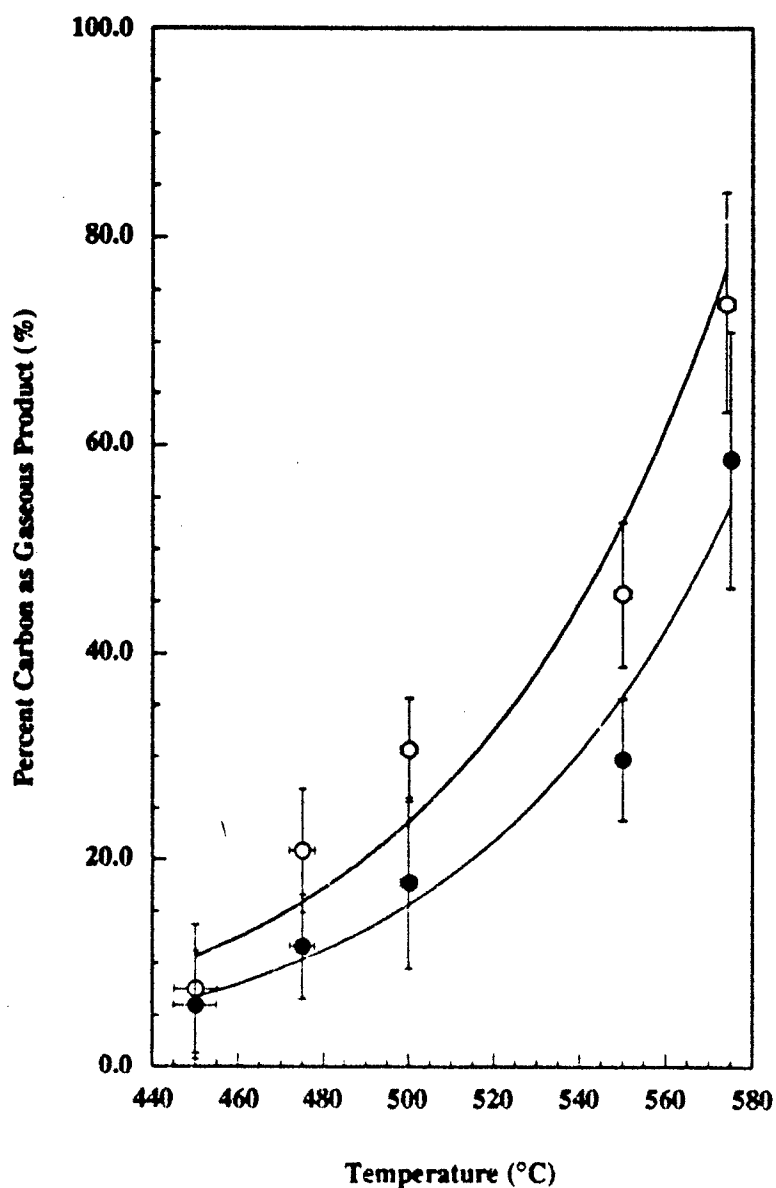
to hydrolysis. The percent gasification represents the portion of reacted carbon that is measured in the gas phase. However, these data points were results from the same set of experiments that implied CH_2Cl_2 conversion changed little over a 100 °C temperature rise, and must be subjected to further verification.

The analysis of the liquid-phase products of methylene chloride hydrolysis was difficult. The task was complicated in that many "pure" chlorinated compounds gave multiple peaks upon analysis in aqueous solution. Identification of these multiple peaks became necessary in order to categorize "unknown" peaks found in the analysis of the liquid-phase product effluent. An excellent example is that of 1,2 dichloroethylene. Initial analysis gave three peaks with retention times of 45.6, 51.2, and 53.6 minutes, each peak with appreciable magnitude. Eventual resolution identified the peaks as *trans*-1,2 dichloroethylene, *cis*-1,2 dichloroethylene, and 1,1 dichloroethylene, respectively. In addition to undergoing reaction in water, many compounds are light-sensitive, undergoing photolysis over a period of time. Like our analysis of glucose products described in Section 5.3, some compounds that seem viable product candidates were not readily available, commercially. As previously mentioned, peak retention times did drift slightly (about ±.2 minutes), causing us to re-analyze some pure compounds to make absolutely positive identification that an observed peak was indeed a previously identified compound, and not a new peak with a very similar retention time. Our list of about 50 previously tested organics proved of less help than we anticipated, as most effluent compounds (likely chlorinated) eluted at retention times not seen before. A look at the hydrolysis liquid chromatogram in Figure 7.2 shows we had limited success in

identifying hydrolysis liquid-phase products.

As many as five peaks were observed to elute between 3.0 and 5.5 minutes over the course of experiments. Two are shown in Figure 7.2. Unfortunately, these peaks often merge into one another and are of varying magnitudes, such that reproducibility and separation are very difficult. Formic acid (~11.8 minutes retention time) was present in all hydrolysis experiment liquid effluent. It was more concentrated in the run at 450 °C than in the chromatogram shown, but remained relatively constant over the entire temperature range investigated. CH_2Cl_2 (~31.8 minutes) was never completely destroyed by hydrolysis under our experimental conditions. Cis- and trans-$C_2H_2Cl_2$ always appeared together when present (one did not appear without the other), but were not detectable in the hydrolysis liquid effluent at 500 °C and below. A major shortcoming in our analytic work was the inability to identify the compound with an elution time of approximately 86.7 minutes. This product was not present in the hydrolysis run at 450 °C, but did form in the hydrolysis liquid effluent at 475 °C and above. Compared to the other peaks in the chromatograms, it is almost always the largest, which infers it absorbs well at 210 nm (2100 Å), but may not imply a relatively large amount is present. During our testing of possible chlorinated products, we learned that this compound is formed when pure 1,2 dichloroethane is mixed with water. Two peaks, listed in Table 7.1, elute when aqueous 1,2 dichloroethane is analyzed, one of which is this unidentified compound. Despite additional analytic support from Merrimac College, North Andover, Massachusetts (Dr. K. C. Swallow) and the MIT Core Analytical Laboratory (Dr. Arthur Lafleur and Elaine Plummer) in attempting to isolate

and identify this compound, its identity as of this writing (May 1993) is still unknown. This compound does *not* appear to be 1,2 dichloroethane, due to its relatively long elution time. Additionally, calibrating this peak as 1,2 dichloroethane results in unreasonable carbon and chlorine balances in our experiments. However, we think this compound is primarily responsible for the overall low carbon and chlorine balances found in Tables 10.5 through 10.7. Particularly frustrating is the fact that this compound is an even more prominent product in the oxidation of CH_2Cl_2. Based on other tested compound elution times, we think this unidentified compound is multi-chlorinated and probably contains a $C=C$ bond. Identification of this compound is part of the ongoing research by the supercritical water research group at MIT, and material presented in this work will be updated once this compound is identified. It is imperative to note that the mass balances presented in Tables 10.5 - 10.7 are based solely on the carbon products in the gaseous phase and chloride concentrations determined from the liquid phase. Identification of the chlorinated and non-chlorinated liquid products came too late for additional calibration and analytical work to be included in this study. Cursory examination of those products with known identities in the liquid-phase effluent indicates that their concentrations may be such that their inclusion in material balances may give little improvement. Major improvement in carbon and chlorine closures may not occur until identification of the peak with the 86.7 minute elution time.

As alluded to, the chromatogram shown is also the chromatogram with the most peaks of all the hydrolysis experiments. Even without identification of all liquid effluent products, one aspect is strikingly evident. Supercritical water, typically thought of as a

destructive environment, does have the potential to provide a medium for constructive, additive chemical synthesis under thermohydrolysis or pyrolytic mechanisms. The observation that 1,2 dichloroethylene is detected only above 500 °C and exhibits an overall increase in concentration at higher temperatures (575 °C) reveals a production of more complex molecules from methylene chloride is possible. Identification of the 86.6 minute peak may further substantiate this observation.

7.5 Derivation of Global Rate Expression

Justification in describing our apparatus as an isothermal plug-flow reactor and pertinent assumptions have already been addressed in Section 6.4.

The reaction rate is assumed to be in the form of a global rate expression,

$$R_{CH_2Cl_2} = k \; [CH_2Cl_2]^a \; [O_2]^b \qquad (7.1)$$

with the rate constant k in the Arrhenius form

$$k = A \; \exp(E_a /RT) \qquad (7.2)$$

Total oxidation of methylene chloride proceeds as:

$$CH_2Cl_2 + O_2 \rightarrow CO_2 + 2HCl$$
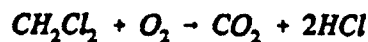
Applying this stoichiometry to the isothermal, plug-flow equation (Equation 6.1), the following equation is derived:

$$[CH_2Cl_2]_o^{a+b-1} \; k\tau = \int_0^X \frac{dX}{(1-X)^a \; (F-X)^b} \qquad (7.3)$$

with: $[CH_2Cl_2]_o$ = initial concentration at reactor inlet

$$F = [O_2]_o / [CH_2Cl_2]_o$$

X = methylene chloride conversion

while τ and k are as previously defined.

A nonlinear multivariable regression program employing a modified Marquardt method (Press *et al.*, 1986) was used to obtain best-fit values of the rate parameters A, E_a, a, and b. Of the thirty-four oxidation experiments, at least five (Runs 325, 327, 329, 331, and 333) experiments were found to have no statistically different effect on conversion of methylene chloride than hydrolysis at corresponding conditions. These results were also suspect (as discussed in Section 7.5), because CH_2Cl_2 conversion varied little over the range 450 to 550 °C, and therefore these five runs were not included in the oxidation regression; correlation was based on the remaining 29 experiments. As observed by Liepa (1988) under catalytic oxidation of gas phase methylene chloride, substantial selectivity to carbon monoxide as opposed to carbon dioxide was observed. Consequently, it was more appropriate to use an S (stoichiometric ratio) value not for complete conversion of the organic to CO_2, but for partial oxidation to the intermediate, CO. For reasons detailed in Section 10.1, S was given the value of ½, commensurate with partial CH_2Cl_2 oxidation:

$$CH_2Cl_2 + \tfrac{1}{2}O_2 \rightarrow CO + 2HCl$$
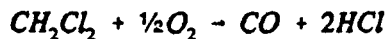
With temperature as the predicted variable (see Chapter 10), the best fit expression is

$$R_{CH_2Cl_2} = 10^{7.9\pm2.1} \exp(\frac{-135\pm30}{RT}) [CH_2Cl_2]^{0.87\pm0.19} [O_2]^{0.07\pm0.08} \qquad (7.4)$$

Units for the rate is mole/cm^3 s^{-1}, concentration is in mol/cm^3, and activation energy is in kJ/mol. All parameter are given with a 95% confidence interval and were determined by an ANOVA routine (Press *et al.*, 1986). Since the parameter *b*, the reaction order with respect to oxygen, was not statistically significant at this level of confidence, *b* was eliminated from the rate expression and the remaining parameters regressed again. The new, 3-parameter rate expression became:

$$R_{CH_2Cl_2} = 10^{8.2\pm2.3} \exp(\frac{-140\pm32}{RT}) [CH_2Cl_2]^{0.93\pm0.20} \qquad (7.5)$$

Now notice that *a*, the hydrogen reaction order, is also not statistically distinct from a value of 1.0 at this 95% confidence interval. With assumed first-order behavior, Equation 7.3 reduces to:

$$k = -\ln (1-X)/\tau \qquad (7.6)$$

Setting $a = 1$, a third regression of the pre-exponential and activation energy parameters gives:

$$R_{CH_2Cl_2} = 10^{8.5\pm2.1} \exp(\frac{-142\pm32}{RT}) [CH_2Cl_2] \qquad (7.7)$$

Note that the regressed Arrhenius parameters A and E_a of the three rate forms found in

Equations 7.4, 7.5, and 7.7 fall within the 95% confidence interval of each other. The small variability of A and E_a among the three rate forms indicates these parameters' independence of the reaction orders. The correlation coefficient (r^2) for all three rate forms was 0.74, with F-statistics of 29, 39, and 79 for Equations 7.4, 7.5, and 7.7, respectively. The somewhat low correlation coefficient may be partly due to the regression encompassing only two temperatures (twenty-three experiments at 500 °C and six experiments at 535 °C). Statistically, the extra parameters in Equations 7.4 and 7.5 did not improve the accuracy of the global rate expression; thus Equation 7.7 sufficiently correlates the experimental data.

Figure 7.5 shows the Arrhenius plot obtained from all the oxidation data reported in Tables 10.5 - 10.7 of the Appendix (Section 10). These data represent the combined action of hydrolysis and oxidation, as both occur simultaneously. Error bars represent a 95% confidence interval. The straight line shown represents the best-fit rate expression of Equation 7.7, based on regression of 29 open-circle data points in the two "stacks" of data. The five data points withheld from regression are depicted by darkened circles. Note that the darkened circle at 500 °C is almost totally masked by the stacking of data points. These were the first series of oxidation experiments conducted and their profile on the Arrhenius plot is suspicious. Note that they indicate that the reaction rate constant remains essentially unchanged in the temperature range 450 to 550 °C. With all other reaction conditions held constant, this underscores the fact that each experiment gave virtually the same conversion ($\sim 50\%$) over this 100 °C temperature range. As with hydrolysis, this seems quite incredulous, since the rate of reaction depends exponentially

Figure 7.5   Assumed First-Order Arrhenius Plot for Methylene Chloride Oxidation in Supercritical Water at 246 bar.   Linear least squares fit is shown, corresponding to Equation 7.7. Data represent the combined effect of hydrolysis and oxidation, which occur simultaneously.   Error bars represent 95% confidence intervals.
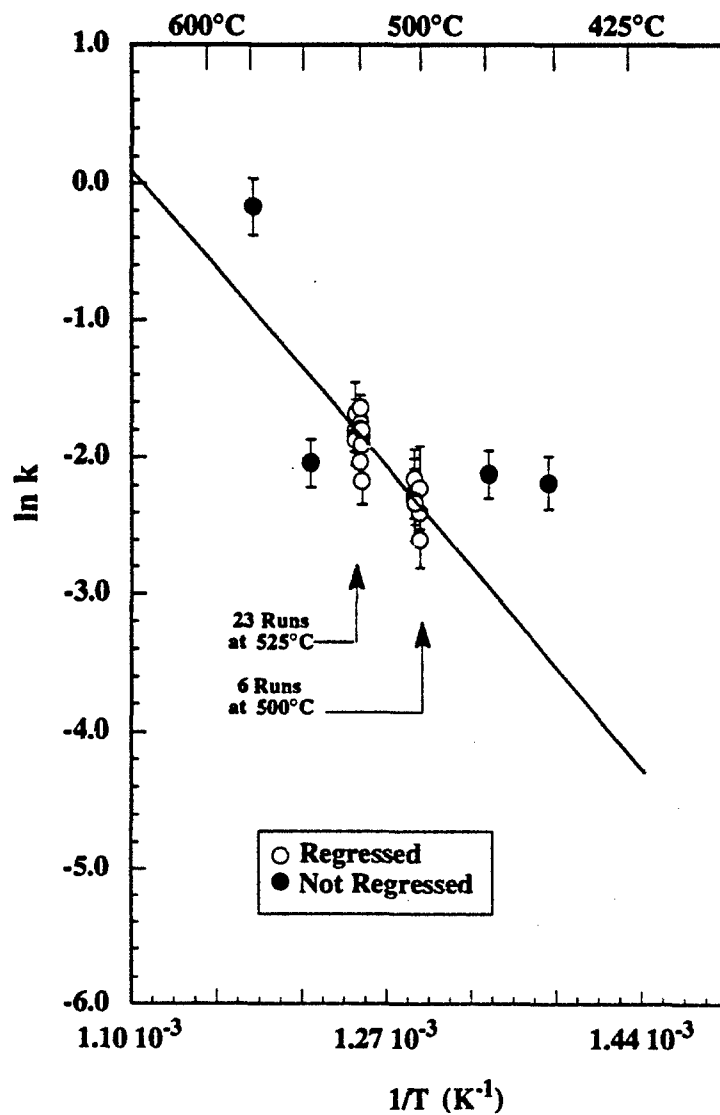
on temperature through the rate constant, k. Inclusion of these data points in the nonlinear multivariable regression is therefore deferred until verification of the data by subsequent investigators (see Chapter 9, Recommendations). Inclusion of these data in the regression still gives values within the window of error for each parameter in Equation 7.4, but the values of the 95% confidence intervals virtually doubles, and the correlation coefficient (r^2)adjusted for degrees of freedom decreases from 0.74 to 0.30.

Two other characteristics of the Arrhenius plot are worth mention. A general increase in the size of the error bars is expected at lower conversions (temperatures), as was observed in the acetic acid results (Figure 6.1) and explained in Section 10.1. This trend is not evident in Figure 7.5, because conversion at the lower temperatures (450 - 500 °C) is still relatively high (~50%), evidently due to hydrolysis.

The other noteworthy observance occurs in the "stacking" of data points at 500 and 525°C. The scatter of these points is clearly not due to experimental error alone, but may be partially due to an identified induction time. This phenomenon has been previously observed by Holgate (1993) in supercritical water oxidation of hydrogen and carbon monoxide, and in our previous results with acetic acid.

7.6 Apparent Induction Times and Methylene Chloride Decay Profiles

Six sets of experiments were conducted to investigate methylene chloride oxidation. The first set varied temperature from 450 - 575 °C while keeping pressure (246 bar), reactor residence time (6 seconds) and inlet feed concentrations (stoichiometr., $[CH_2Cl_2]_o$ = 1×10^{-6} mol/cm^3 and $[O_2]_o$ = 1×10^{-6} mol/cm^3) constant. The next three sets of experiments were conducted at 525 °C and 246 bar. Of these three, one set was

conducted at a stoichiometric ratio (1:1) of feeds with $[CH_2Cl_2]_o = 1 \times 10^{-6}$ mol/cm^3 and $[O_2]_o = 1 \times 10^{-6}$ mol/cm^3, varying residence time from 4.3 to 9.8 seconds. The two other sets of experiments, conducted to help verify global reaction order with respect to oxygen, were conducted at oxygen to methylene chloride feed ratios of 2:1 (oxygen-rich) and 0.5:1 (oxygen-lean), respectively. Reactor inlet methylene chloride concentrations were kept at $[CH_2Cl_2]_o = 1 \times 10^{-6}$ mol/cm^3 and residence time was varied. The fifth set of experiments were conducted at 500 °C and 246 bar with stoichiometric feeds of $[CH_2Cl_2]_o = 1 \times 10^{-6}$ mol/cm^3 and $[O_2]_o = 1 \times 10^{-6}$ mol/cm^3. The last set of runs kept a stoichiometric feed ratio, but increased both feed concentrations to 2×10^{-6} mol/cm^3. This series of experiments was halted after 3 runs due to visible signs of corrosion during oxidation (Section 7.8). These conditions were chosen to give a wide range of both residence time and conversion, as constrained by our apparatus.

A normalized plot of CH_2Cl_2 decay under stoichiometric, oxygen-rich and oxygen-lean initial feed concentrations is shown in Figure 7.6. The utility and derivation of such a plot was discussed in Section 6.5. All series of experiments appear to follow exponential decay. As observed in oxidation of other organic compounds (i.e., hydrogen, carbon monoxide, acetic acid) in supercritical water, extrapolation of these decay curves to initial concentration ($[CH_2Cl_2]/[CH_2Cl_2]_o = 1$) suggests the presence of an induction time (τ_{ind}). The Figure 7.6 data are replotted in Figure 7.7 using a logarithmic ordinate, ln (C_i/C_{io}), to linearize the decays. Again, all data sets exhibit exponential decay, and extrapolation to ln $([CH_2Cl_2]/[CH_2Cl_2]_o) = 0$ results in estimates of induction times. Note that the three concentration data sets appear to

Figure 7.6   Normalized Decay Profiles for Stoichiometric Oxidation of Methylene
Chloride in Supercritical Water, Showing Induction Times. Curves are
exponential fits to data points. Error bars show 95% confidence intervals.
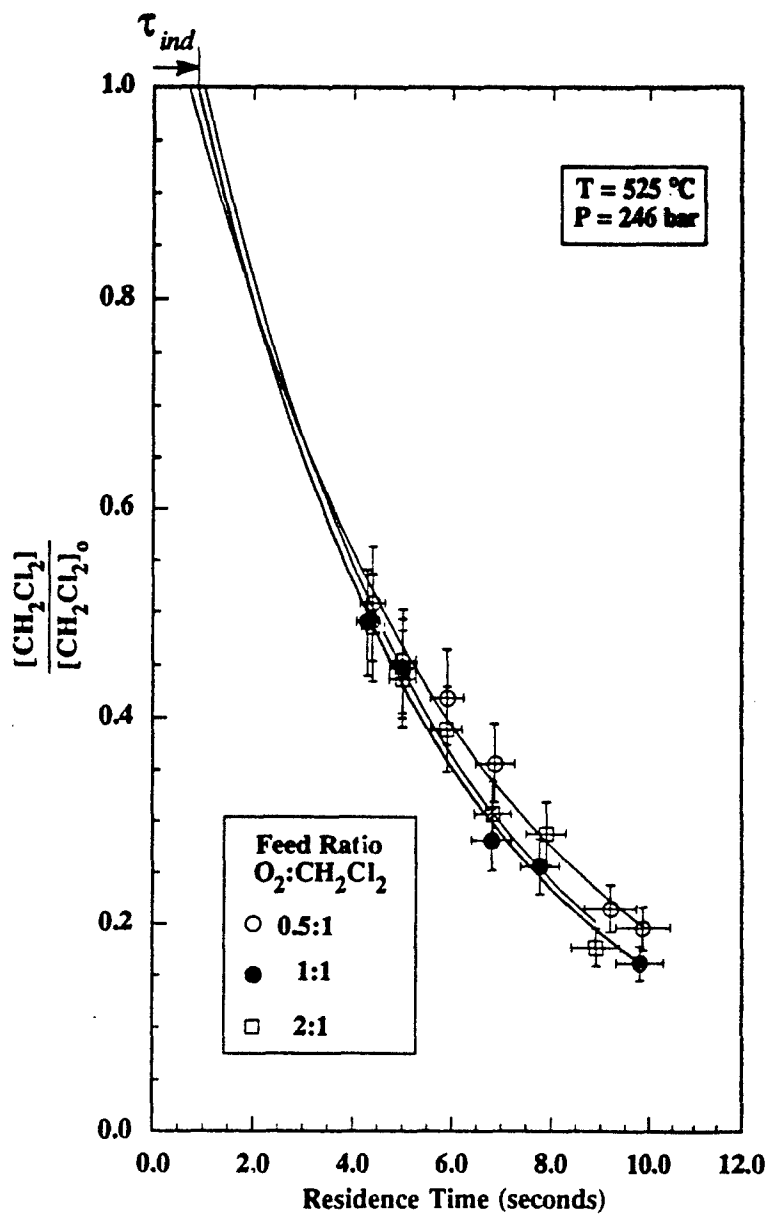
have the same decay constant and have the same slope within regression error. There is large error associated with induction time, and a conclusive analysis about how oxygen concentration effects τ_{ind} cannot be made, although the plot suggests it has little effect.

Figures 7.6 and 7.7 help confirm the derived global rate expression in Equation 7.7, in that a change in oxygen feed concentration by a factor of four (from 0.5×10^{-6} mol/cm^3 to 2×10^{-6} mol/cm^3) had little effect on the reaction rate. In fact, observation that the linear fits do not lie on the exact same path may be more attributable to our ability to reproduce experimental conditions between corresponding runs, rather than a result of the effect of oxygen.

Finally, we should remember that if the data in the first (temperature variant) series of experiments holds true, the observed decay of CH_2Cl_2 is due more to hydrolysis than oxidation. The oxidation data shown here are *global* observations and show the combined effect of oxidation and hydrolysis. Derived decay constants and induction times are summarized in Table 7.2.

In analyzing the experimental data for stoichiometric oxidation at 500 °C with varying residence time, we obtained somewhat confusing results. As with previous experiments, the data fit an exponential decay curve well. But in a plot of C_i/C_{io} versus residence time, the exponential decay curve extrapolated to ($[CH_2Cl_2]/[CH_2Cl_2]_o$) ≈ 0.85 at $t = 0$. This suggests that only 85% of the original feed was present at the reactor inlet (if the exponential decay holds throughout the reactor). This is quite plausible, considering preheating may have caused some degradation of CH_2Cl_2. But why was this effect evident at 500 °C and not during any of the three previous series of

Figure 7.7 Normalized Decay Profiles for Stoichiometric Oxidation of Methylene Chloride in Supercritical Water at 525 °C and 246 bar, Showing Induction Times. Conditions as in Figure 7.6, but concentration ordinate is on a logarithmic scale. Lines are linear fits to data, indicating exponential decay. Intervals shown are to 95% confidence.
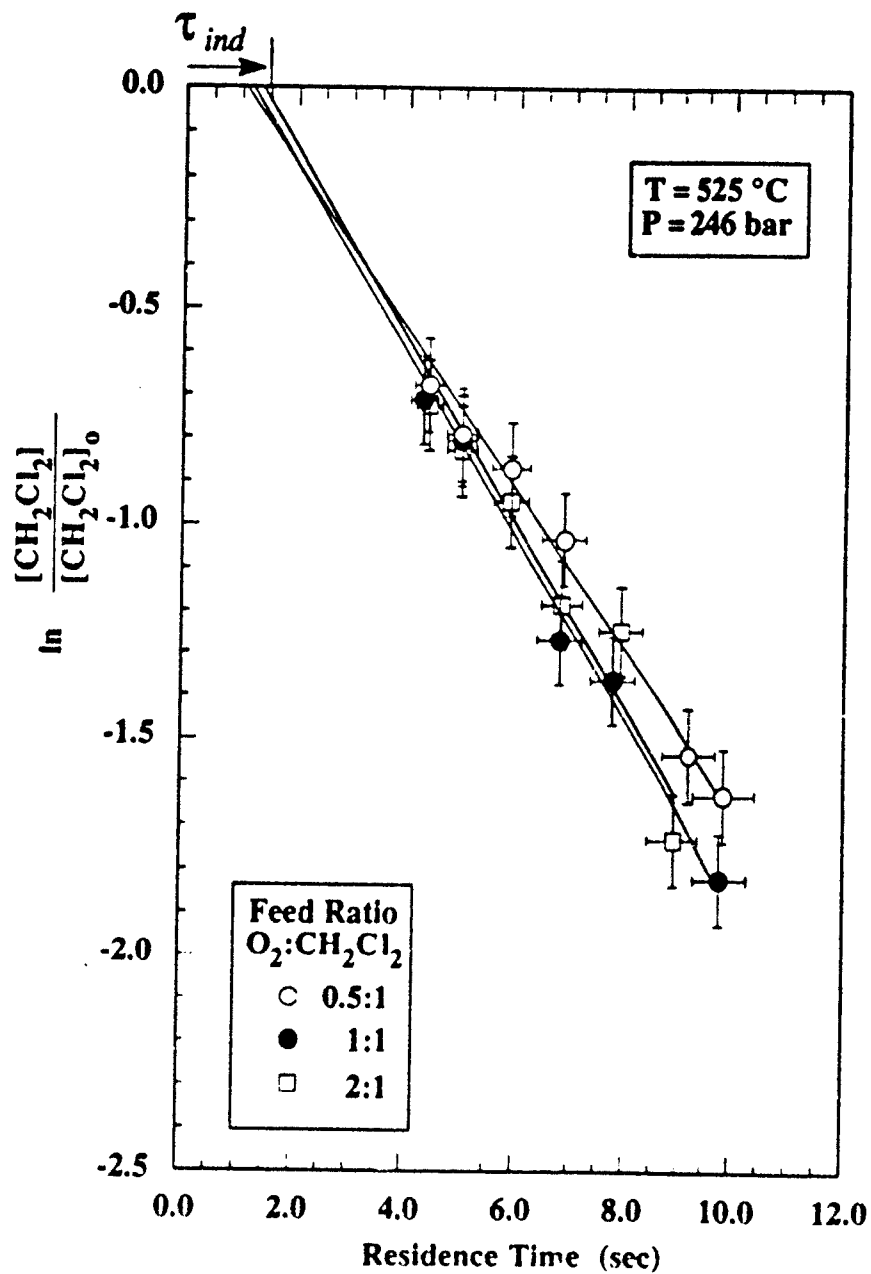
Table 7.2 **Apparent Induction Times and Decay Constants for Methylene Chloride Oxidation at 246 bar and 525 °C.** Intervals represent 95% confidence levels.

Initial Conditions (10^{-3} mol/L)	k' (sec^{-1})	τ_{ind} (sec)	Average Feed Ratio $[O_2]:[CH_2Cl_2]$
$[O_2]_o$ = 0.58±.01 $[CH_2Cl_2]_o$ = 1.03±.04	.18±.03	0.7±1.0	0.56±.03
$[O_2]_o$ = 1.09±.01 $[CH_2Cl_2]_o$ = 0.96±.04	.20±.03	0.8±.9	1.13±.06
$[O_2]_o$ = 2.05±.05 $[CH_2Cl_2]_o$ = 0.97±.04	.20±.03	1.0±.9	2.11±.12
$[O_2]_o$ = 1.07±.03* $[CH_2Cl_2]_o$ = 0.96±.22*	.07±.02*	-2.5±2.8*	1.12±.24*
$[O_2]_o$ = 2.06±.03† $[CH_2Cl_2]_o$ = 1.99±.03†	.14±.09†	-2.0±46.9†	1.00±.11†

* Reactor Temperature T = 500 °C
† Based on only three data points

experiments at 525 °C? Preheater heat transfer and water density change is such that at higher sand bath temperatures, the organic feed will reach a higher temperature prior to entering the reactor inlet compared to lower sand bath temperatures (Holgate, 1993). However, the feed will be at these higher temperatures for a shorter period of time than at a lower sand bath setting. This phenomena may have had some effect on our observed results. As seen in Figure 7.8, the slope of the linear fit at 500 °C is lower than its comparable series of runs conducted at 525 °C. This is as would be expected, since higher temperatures should produce faster reaction rates (steeper slopes), considering that the reaction rate constant, k, depends exponentially on temperature. But unlike previous observations of methylene chloride oxidation, the intercept at ln $([CH_2Cl_2]/[CH_2Cl_2]_0) = 0$ does not give physically achievable results. The most likely explanation for this unexpected intercept may be experimental error. The arrows in Figure 7.8 graphically portray the limits in the error of the slope, based on data error bars (the data point at $\tau = 8$ seconds was not included in this illustration). Induction time $\tau = 0$ (and greater) clearly falls within the window of error of the slope. Table 7.2 shows, the error associated with this intercept is quite large relative to the absolute value of the intercept, and τ_{ind} may very well be zero within experimental error (Section 4.4). A similar trend seemed to be forming for our last series of runs (2:2 stoichiometric feed) which was discontinued after evidence of corrosion. This series of experiments did not warrant a plot, since it had only three data points. It is unknown what effect corrosion may have had on kinetics. Further investigation is needed into kinetics under these conditions as well as calculation of preheater effects.

Figure 7.8   **Normalized Decay Profiles for Oxidation of Methylene Chloride in Supercritical Water at 525 °C and 500 °C with Pressure of 246 bar. Concentration ordinate is on a logarithmic scale. Nominal feed concentrations are 1×10^{-6} mol/cm^3 for both O_2 and CH_2Cl_2. Lines are linear fits to data, suggesting exponential decay. Error bars represent 95% confidence intervals. Arrows indicate approximate 95% limit of confidence on the slope of the line through data at 500 °C.**
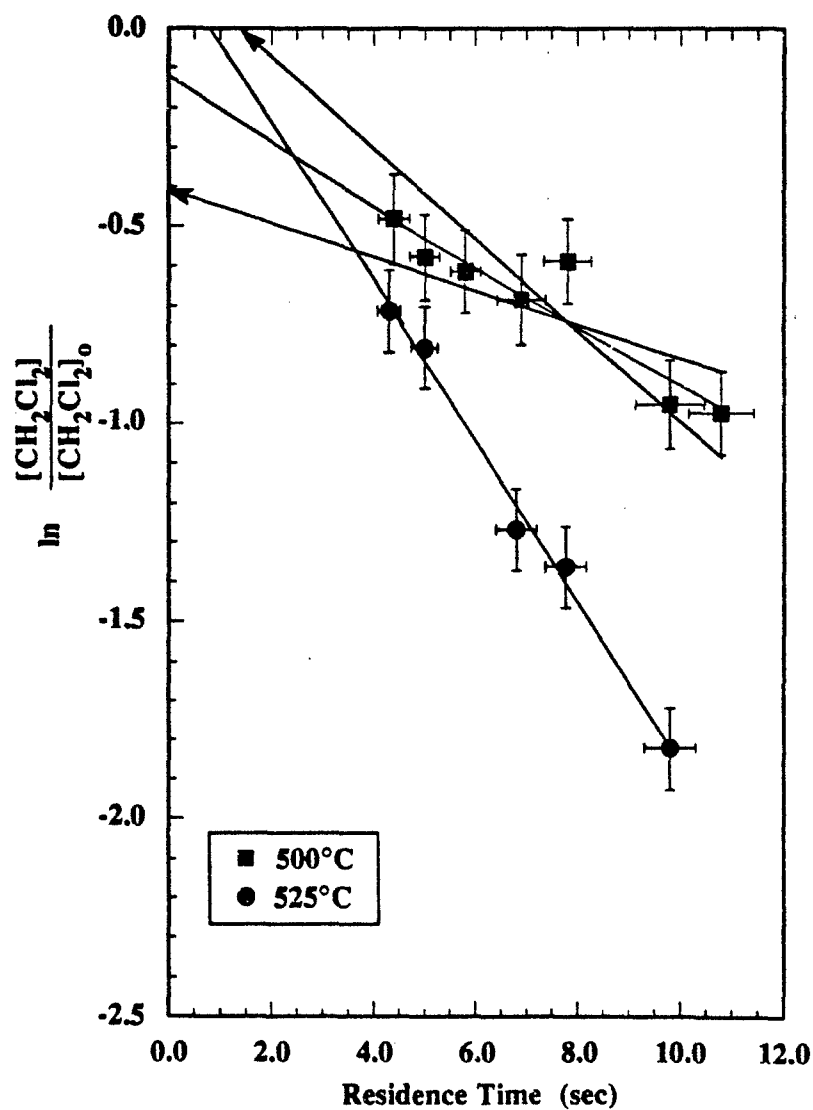
7.7 Initial Conditions Effects on Products

Figure 7.9 shows how major (CO and CO_2) gaseous product yields are influenced when initial oxygen feed is increased by a factor of four, with all other experimental variables (pressure, temperature, residence time, initial CH_2Cl_2 concentration) held constant. The increase in CO_2 is accompanied by a corresponding decrease in CO. This is consistent with the slight oxygen dependence of CO oxidation in supercritical water found by Holgate (1993). Also note that the rate of CH_2Cl_2 decay remains essentially unchanged.

Figures 7.10 and 7.11 compare liquid effluent chromatograms from various initial feed conditions. Each chromatogram is representative of the analysis seen in other experiments of its series. Identification of liquid products was difficult, as discussed in Section 7.4. Still, some positive identifications were made, and work continues as of this writing (May 1993) to resolve all peaks. A table of currently identified peaks is found in Table 7.3.

Note the relative consistency in all chromatograms. Multiple, merged peaks were still evident between 2.5 - 5.5 minute elution times, with the peak at approximately 5.0 minutes showing the most absorbance. Formic acid (11.8 minutes) was present in all samples, as was the unidentified compound (86.7 minutes) found in hydrolysis. The continual presence of the peak at 17.7 minutes is of particular note in that this compound was also present in acetic acid oxidation in supercritical water. It is therefore not likely to be a chlorinated compound, and is also not one of the 50 or so organics tested. *Cis-* and *trans*-1,2 dichloroethylene are, as in hydrolysis, always present together. In the

Figure 7.9   Gaseous Product Profiles for Oxidation of Methylene Chloride in Supercritical Water at 525 °C with Pressure of 246 bar.

Nominal feed concentrations are 1×10^{-6} mol/cm^3 for CH_2Cl_2 with O_2:CH_2Cl_2 ratios as indicated. Lines are linear fits for clarity only. Error bars represent 95% confidence intervals.
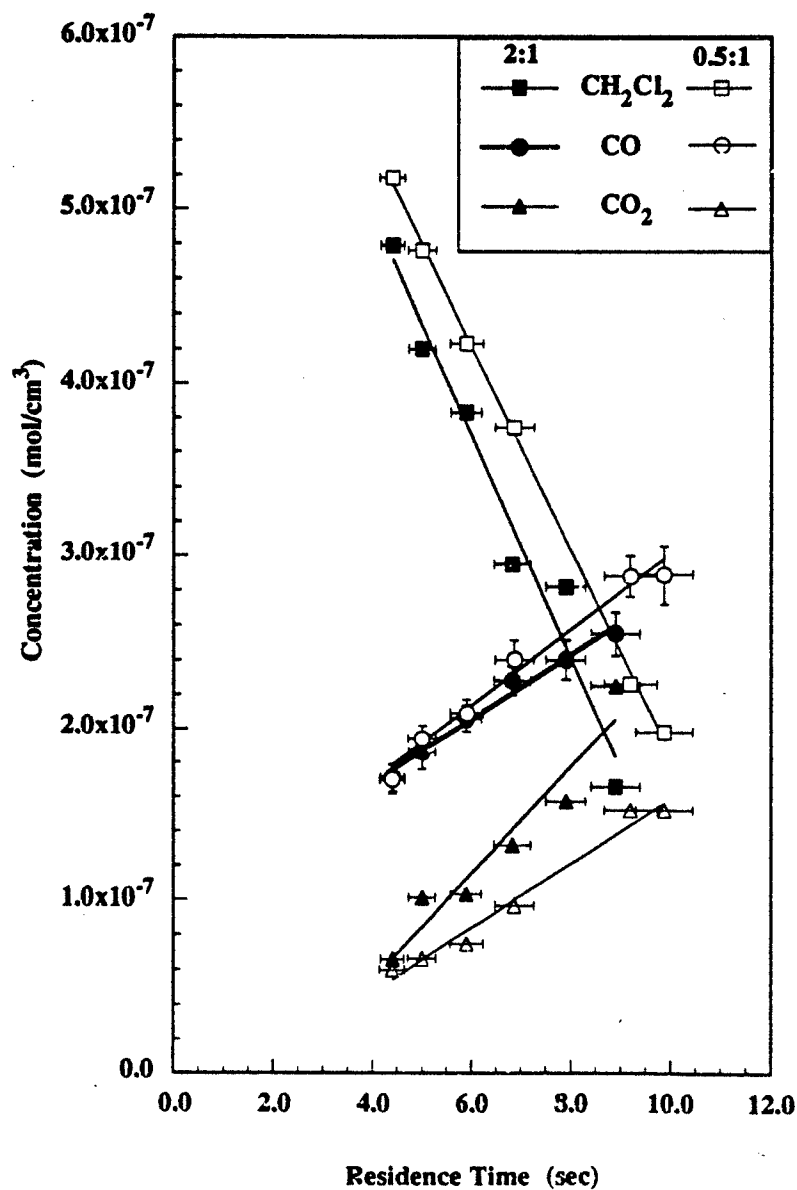
Figure 7.10 **Reactor Liquid Effluent Chromatograms.** Reactor conditions of 525 °C, 246 bar, reactor residence time of 7 seconds, and $[CH_2Cl_2]_o = 1 \times 10^{-6}$ mol/cm^3 with $[O_2]$:$[CH_2Cl_2]_o$ feed ratios as indicated.
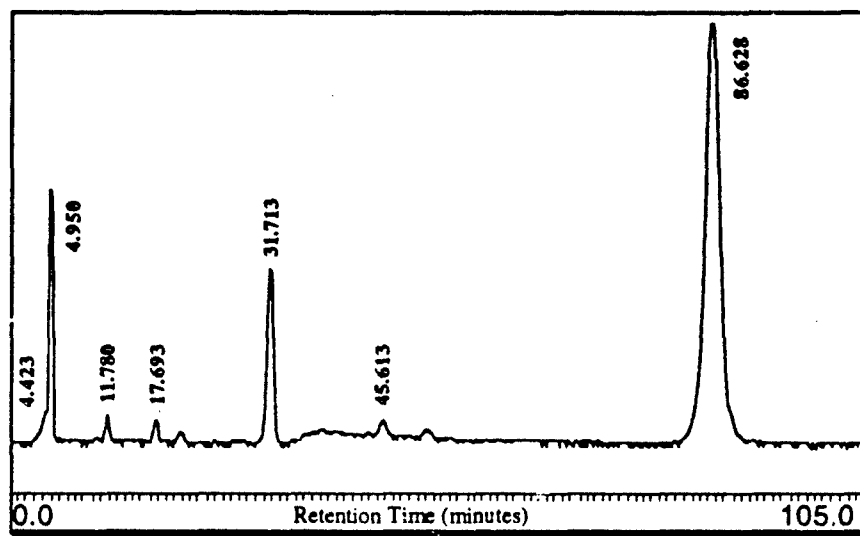
Run 349A, Sample #2 (0.5:1)
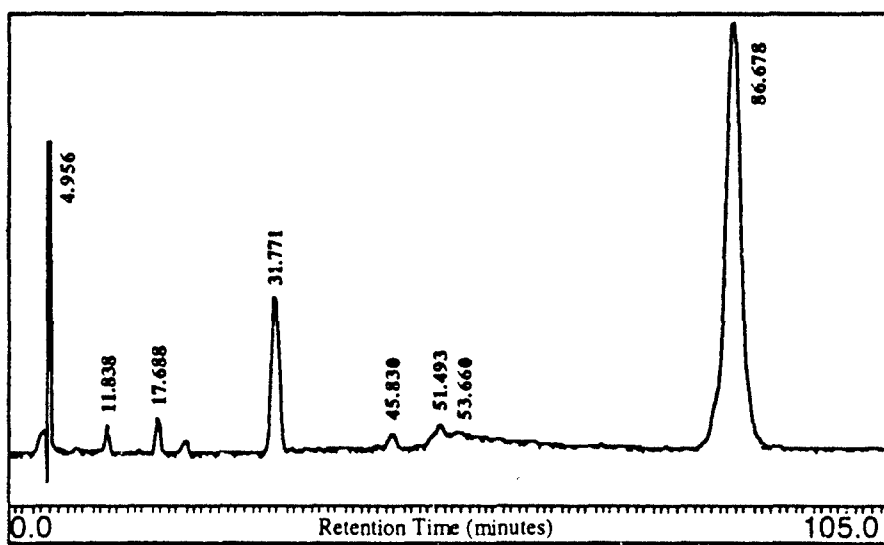
Run 337, Sample #3 (1:1)

Figure 7.11 **Reactor Liquid Effluent Chromatograms.** Reactor conditions for Run #343: 525 °C, 246 bar, reactor residence time of 7 seconds, with $[CH_2Cl_2]_o = 1 \times 10^{-6} mol/cm^3$ and $[O_2]_o = 2 \times 10^{-6} mol/cm^3$; reactor conditions for Run #361: 525 °C, 246 bar, reactor residence time of 8 seconds, with $[CH_2Cl_2]_o = 2 \times 10^{-6} mol/cm^3$ and $[O_2]_o = 2 \times 1\Gamma \cdot mol/cm^3$.
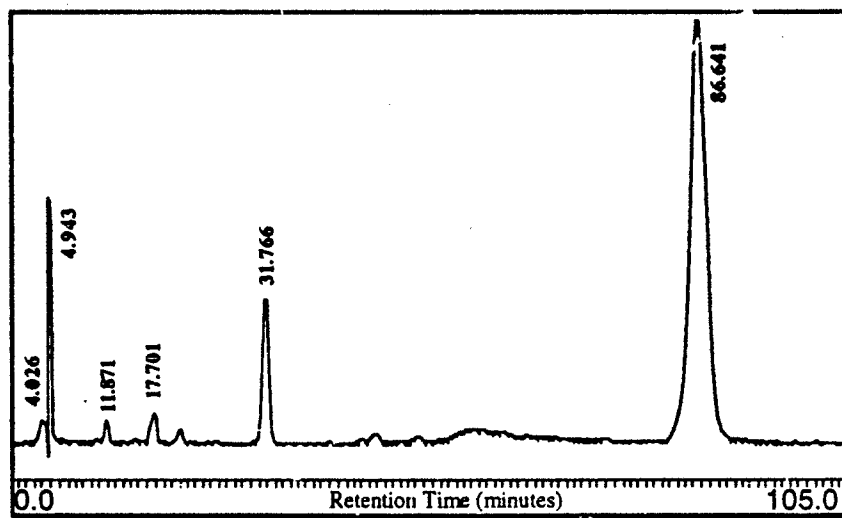
Run 343, Sample #2 (2:1)
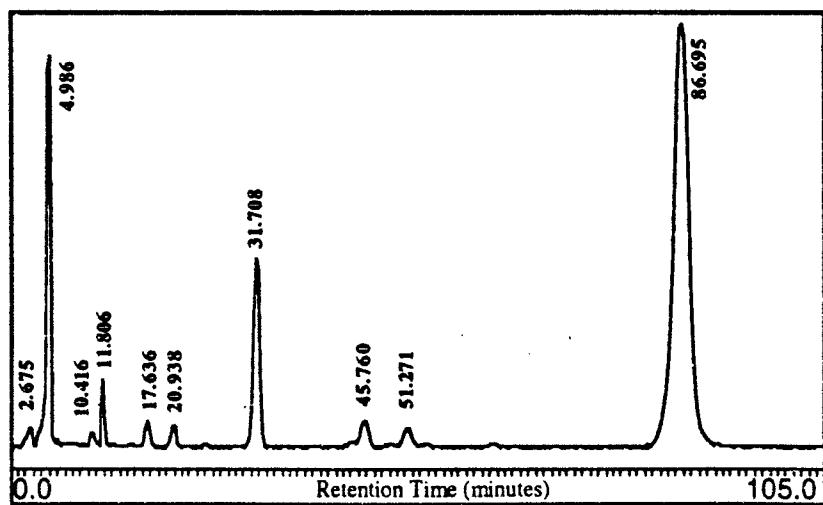
Run 361, Sample #3 (2:2)

Table 7.3   **Major Liquid Effluent Products from Methylene Chloride Hydrolysis (Oxygen-Free) and Oxidation Runs in Supercritical Water.** Based on liquid chromatography absorbance at 210 nm.

Retention Time (minutes)	Compound	Formula	Products of Hydrolysis?	Products of Oxidation?
4.9	Unknown		X	X
5.2	Oxalic Acid	HOOCCOOH		✓
10.4	Acetol	CH_3COCH_2OH		✓
11.8	Formic Acid	HCOOH	X	X
17.7	Unknown			X
20.9	Propenal (Acrolein)	CH_2CHCHO		✓
31.7	Methylene Chloride	CH_2Cl_2	X	X
45.7	cis-1,2 Dichloroethylene	$C_2H_2Cl_2$	X	✓
51.2	trans-1,2 Dichloroethylene	$C_2H_2Cl_2$	X	✓
86.7	Unknown		X	X
~150	Unknown		✓	✓

X = always present
✓ = present under certain conditions

0.5:1 feed chromatogram, the *cis-* configuration was present as can be seen by a small peak at approximately 51.2 minutes, but was not categorized as a peak with our analytical method, because of it fell below the set limit of peak height. Neither *cis-* nor *trans-* were detected in the 2:1 feed, but both are still clearly present (in very minute quantities that are slightly below the limit of detection with our method). The doubling of initial CH_2Cl_2 concentration gives well defined *cis-* and *trans*-1,2 dichloroethylene peaks in the 2:2 chromatogram. One last general observation is interesting. Note the slight rise or bulge in the baselines of the 0.5:1, 1:1, and 2:1 chromatograms near the *trans*-1,2 dichioroethylene (~45 minutes) peak. This drift was observed only after experiments were well underway. In each chromatogram in which it is present, it is a very slow eluting peak from the previously injected sample. It is not a well-defined peak, but has a consistent elution time of about 150 minutes. The peak is located at different elution times on each chromatogram because time between sample injections into the HPLC varied by a few minutes. It may have actually caused the 53.6 minute peak observed in the chromatogram of the 1:1 run; the 53.6 minute peak is not found in the other chromatograms. At times this bulge masked or distorted peaks in the 40 - 55 minute elution range. It has an actual elution time of approximately 150 minutes, which was well-beyond our method which employed a 105-minute sampling time. Again, quantification of most know peaks results in small concentrations, not usually enough to effect carbon and chlorine balances significantly. Improvement in the material balances may only be profoundly improved when the compound eluting at 86.7 minutes is resolved.

Liquid effluent pH, measured by pH indicator, remained consistent at approximately 2.0 to 1.5 for all experiments, except for the 2:2 feed effluent, which measured about 1.0. Chloride ion concentration was measured for each sample via the ion-electrode method described in Section 4.2. Chloride ion concentration doubled in the liquid effluent when the reactor residence time was doubled from 4.5 to 9.0 seconds for stoichiometric, oxygen-rich, and oxygen-lean conditions.

7.8 Corrosion

After reaching desired reactor conditions for run 330, the liquid effluent flow rate dropped drastically upon changing over to organic feed. This is normally due to air trapped in the organic or oxygen side pump head and is corrected by momentarily venting the pump, whereby the flow rate returns to normal. In following this corrective procedure, a rust-like color of effluent was evident. Instead of the normally observed clear water, this solution had the color of coffee with cream. The flow returned to the normal rate, but was still slightly tainted with this contamination, for a few minutes before the liquid effluent ran clear again. This effluent was collected and subsequently analyzed. No further observations of this colored effluent were recorded. Upon startup of the reactor system the next morning, the first 100 ml of effluent were again colored. It then cleared and was not observed during the remainder of the heating up period nor during actual oxidation or hydrolysis. The next morning's startup gave similar results. An attempt was made to flush the system after the oxidation experiments for the day were concluded. Upon switching to pure water feed, the discoloration was again present. Over the next few days, discolored water was observed anytime pure water was pumped

through the system following oxidation experiments.

Within about a week of beginning the methylene chloride experiments, the Inconel-sheathed thermocouple located in the reactor exit failed. Physical inspection revealed a small hole had been created in the tubular wall of the thermocouple. It is not known whether this was specifically caused by the methylene chloride experiments, or was simply the result of many months of use and degradation.

With replacement of the thermocouple, kinetic experiments were continued. The discolored liquid effluent was seen each time pure water feed followed an oxidation experiment. No discoloration was noticed any time the organic and oxygen feeds were being pumped through the system. Pure water feed was run through the reactor system after the first runs in which methylene chloride concentration was doubled to 2×10^{-6} mol/cm^3. Again the discolored effluent was noticed, only darker and seemingly more concentrated than before. In continuing these more concentrated experiments the next day, the effluent flow began decreasing again, with no apparent system pressure changes. Venting the pumps corrected the flow initially, but subsequent flow of organic and oxidant gave effluent with a distinctly yellow tint. Additionally, the recently replaced reactor exit thermocouple seemed to be giving temperature readings about 4 °C lower than what was expected, based on temperature readings of other thermocouples in the system. Measurement and calculation of the resistivity of the thermocouple while still hot indicated that its resistivity may have dropped from its initial value, thereby giving false readings. This could be caused by a thinning of the thermocouple sheathing. We had been given prior notice that the appearance of a yellow effluent in other supercritical

water oxidation studies was indication of corrosion most likely due to small amounts of dissolved chromium. Experiments were discontinued until a more thorough analysis of the effluent could be made.

Numerous samples of the discolored water were taken. Upon standing, a precipitate settles to the bottom. This precipitate was filtered and evaluated using x-ray analysis with a scanning electron microscope. Preliminary results showed the precipitate contained significant amounts of nickel, iron, and chromium. Analysis of the yellow-tainted reactor effluent has not been completed at the time of this writing.

1. Glucose hydrolysis and oxidation. Glucose is quickly destroyed under hydrolysis and oxidative conditions in supercritical water. Both reactions produce significant gasification, although oxygen accelerates destruction of the intermediate products. Reaction kinetics were too fast under our operating conditions in our reactor apparatus to obtain a global rate expression. Major intermediate products in the liquid-phase of glucose hydrolysis and oxidation are acetic acid, acetonylacetone, propenoic acid, and acetaldehyde. Gas-phase intermediate products are carbon monoxide, methane, ethane, ethylene, and hydrogen.

2. Measurement of oxidation kinetics. The oxidation kinetics of acetic acid were examined at 246 bar and 425 - 600 °C and over an extended range of fuel equivalence ratios. Over the range studied, the reaction is nearly first-order (0.72 ± 0.15) in acetic acid and fractionally (0.27 ± 0.15) dependent on oxygen, with an activation energy of 168 ± 21 kJ/mol. Methylene chloride oxidation is first-order in CH_2Cl_2 with an activation energy of 142 ± 32 kJ/mole. Methylene chloride hydrolysis plays a significant role in the destruction of CH_2Cl_2 in supercritical water.

3. Identification of induction times. As found in previous studies of model compound oxidation in supercritical water (Holgate, 1993), acetic acid and methylene chloride exhibit a delayed reaction ignition, or induction time. This is indicative of free-radical

mechanisms and complicates global reaction modeling.

4. Effects of operating pressure. Acetic acid oxidation in supercritical water is less pressure (water density) dependent than carbon monoxide or hydrogen (Holgate, 1993). The presence of an induction time distorts the pressure effect, making reaction rates seem more pressure dependent than they truly are.

5. Corrosion. Methylene chloride oxidation and hydrolysis in supercritical water can cause visible signs of corrosion.

Chapter 9
Recommendations

1. Enhanced experimental capabilities. Changes to the current apparatus system, or construction of a new system are necessary to widen the operating conditions (namely, concentrations and residence time). Larger diameter reactors would decrease surface effects observed by Holgate (1993). Use of higher capacity feed pumps would also require more heating capacity than currently available with the present fluidized sand bath, and more cooling capacity than the current shell-and-tube countercurrent heat exchanger.

2. Enhanced analytical capabilities. Although SCWO of compounds rapidly destroys many compounds, identification of refractory products and intermediates is needed to fully characterize reaction mechanisms. Positive identification of intermediates and products will require more sophisticated analytical techniques, such as liquid chromatography with mass spectrometry. Dedication of an analytical lab facility or analytical chemist is needed.

3. Surface area effects. A packed reactor currently available in our lab should be used to investigate what effects reactor inner walls may have played in determining oxidation kinetics of acetic acid and methylene chloride.

4 Pressure effects. More studies are needed to verify pressure effects of acetic acid oxidation in supercritical water. Pressure effect experiments are also needed to

determine methylene chloride reaction response to changes in water density (concentration).

5. *Expanded glucose experiments.* Lower operating pressures and/or temperatures are needed to quantify the global oxidation kinetics for glucose. Experiments in the subcritical regime (wet-air oxidation) may be sufficient to destroy glucose and, hence, cellulosic wastes.

6. *Additional methylene chloride studies.* Verification of the importance of hydrolysis in conversion of CH_2Cl_2 is needed, particularly over varying temperatures in the 450-550 °C temperature regime. Residence time studies at lower (~ 450 °C) temperatures and/or pressures may be needed to characterize oxidation and hydrolysis over the full range of conversion. Recalculation of carbon and chlorine balances upon identification of the liquid chromatography peak with 86.7 minute elution time should be done to determine if product effluent has been well characterized.

7. *Co-oxidation.* With a general understanding of global reaction rates and products for a growing list of model compounds, co-oxidation should be studied to investigate what kinetic effects (if any) compounds have on each other. This is more representative of the SCWO process, where mixtures rather than pure components of hazardous wastes are more likely to be processed.

8. *Studies of additional model compounds.* The database of kinetic studies and products of model compound oxidation in supercritical water should be expanded. Persistent intermediates identified should be added to a priority list of compounds to investigate. Investigation of additional model compounds containing nitrogen, sulfur, and phosphorus

heteroatoms still represent an important class of wastes that have not been adequately studied.

9. Alternative oxidants. The applicability of using other compounds as hydroxyl radical sources should be explored. Hydrogen peroxide has already been used and shows some augmentation to the oxidation process. Understanding of fundamental oxidation mechanisms could be improved through a careful study of this enhancement.

Appendices

10.1 Regression of Global Rate Parameters

Discussion of global rate parameter regression has been previously addressed by earlier investigators (Webley, 1989; Holgate, 1993). Co-worker Holgate gives particular insight into assumptions and calculations made in regressing data and his work is paraphrased here.

The functional relationship among observables in our reactor apparatus can be described by the plug-flow equation

$$\frac{\tau}{[C]_o} = \int_0^X \frac{dX}{R_c} \qquad (10.1)$$

with τ = reactor residence time

$[C_o]$ = initial organic concentration

X = conversion

R_c = rate of disappearance of C

A typical reaction rate form is

$$R_c = k \, [C]^a \, [O_2]^b \qquad (10.2)$$

with k, the rate constant, given by an Arrhenius form:

$$k = A \exp(E_a/RT) \qquad (10.3)$$

Using the definition $[C] = [C]_o(1-X)$, the plug flow equation can be rewritten: assuming the rate of disappearance of oxygen is directly proportional to the rate of disappearance of C. S is the proportionality given by the stoichiometric O_2/C ratio. F

$$k\,[C]_o^{a+b-1}\,\tau = \int_0^X \frac{dX}{(1-X)^a\,(F-SX)^b} \qquad (10.4)$$

is defined as the O_2/C feed ratio. For a reaction that is first order in organic ($a=1$, $b=0$), Equation 12.4 reduces to $k = -\ln(1-X)/\tau$. For other values of a and b, Equation 10.4 must be solved numerically.

Mathematically, Equation 10.4 is equivalent to the coupled ordinary differential equations (ODEs)

$$d[C]/dt = -k[C]^a[O_2]^b \qquad (10.5a)$$

$$d[O_2]/dt = -S\,d[C]/dt \qquad (10.5b)$$

with the initial concentrations of $[C]_o$ for the organic and $F \times [C]_o$ for oxygen initial concentration. Equation 10.5a and 10.5b can be integrated to give $[C]$ at time $t = \tau$, or X. Therefore, both Equation 10.4 and 10.5a,b describe the relationship among plug-flow reactor variables, and either the integral form or the coupled ODE form can be used for

regression purposes. However, both methods do not necessarily give the same results. Of the experimental variables (conversion X, feed ratio F, residence time τ, initial organic concentration $[C]_o$, and temperature T), X is the dependent (predicted) variable, since its value is fixed by the choosing the values of the other variables. The integral form of the plug-flow equation (Equation 10.4) cannot be used if X is the predicted variable, since X (and F) must be known to solve the equation. Using Equation 10.4 precludes using X as the predicted variable, and some other variable (say, T) must be chosen. Conversely, using Equations 10.5a and 10.5b requires X to be the chosen variable since all other quantities (T, $[C]_o$, F, τ) must be known to solve the coupled ODEs.

Since the coupled ODEs more accurately represent the physical situation, Equations 10.5a and 10.5b might be considered the preferred functional relationship. However, solving the ODEs usually requires more intense computation than the integral in Equation 10.4. Also, X may *not* be the preferable predicted variable for regression. Regression seeks to minimize the difference between predicted and observed values, regardless to the absolute magnitude of the values themselves. When variables are of the same order of magnitude, using X as the predicted variable is fine. If, however, variables vary over an order of magnitude, skewed solutions can result. For example, experimental conversions can vary by more than a factor of ten (e.g., from 5% conversion to 95%). With conversion, the absolute error in the measured value is likely to be equal to or greater at low conversions as the absolute errors at high conversions. A 2% difference in conversion at 5% conversion can be a much more serious error than

a 2% deviation at 80% conversion. Holgate (1993) describes this phenomena well:
Consider the first-order rate constant, $k = -\ln(1-X)/\tau$. Experimental data are often presented in the form of an Arrhenius plot, with $\ln k$ plotted against $1/T$; the best-fit rate expression should give a straight line through the data. The fractional error in k ($\delta \ln k$) due to error in X (δX) is given by

$$\frac{\delta \ln k}{\delta X} = \frac{-1}{(1-X)\ln(1-X)} \qquad (10.7)$$

For $X = 80\%$, an error of 2% in X gives an error of about 6% in k; but for $X = 5\%$, an error of 2% gives an error of over 40% in k! Choosing X as the predicted variable can effectively weight higher-temperature (higher conversion) data more heavily and may yield a curve fit that does not pass through all the data. Choosing k as the dependent variable, or weighting data may or may not improve the fit.

The problems associated with weighting of data can be alleviated by choosing a different predicted variable. T (through k) is the best choice for our experimental apparatus, since it is known to relatively high precision, and normally varies by less than two orders of magnitude over our range of experimental conditions. τ could be used, but it is known only to limited precision, and experiments have confirmed that reactions are less sensitive to residence time than temperature. $[C]_0$ is known to relatively high precision, but, like conversion, it can vary over a factor of ten. Therefore, the regressions in this work used Equation 10.4 with T the predicted variable.

The choice of regression approach may affect the values of the regressed parameters and their respective errors (Holgate, 1993).

Particular mention must also be made of the value for S, the stoichiometric ratio, used in both forms of the plug-flow equation. For reactions where there are no stable intermediates, S is well-defined (e.g., hydrogen oxidation). For oxidation of more complex reactants, such as glucose, acetic acid, and methylene chloride, the stoichiometric ratio is usually defined by the amount of oxygen need to completely convert the organic to CO_2 and H_2O. By this definition, $S = 6$ for glucose, $S = 2$ for acetic acid, and $S = 1$ for methylene chloride. But some organic oxidations proceed through intermediates before forming CO_2. It is therefore possible to oxidize all of the organic without completely converting them to CO_2. Using S as defined by total oxidation in either plug-flow equation is therefore inappropriate, and may lead to incorrect predictions of O_2-limited organic conversions when in fact it is the carbon monoxide conversion that is O_2-limited. The proper value for S is not that for complete conversion of the organic to CO_2, but that for complete conversion to CO and H_2O. Thornton and Savage (1990) have pointed our that in systems where the number and /or identities of the stable intermediates may not be known, it is not possible to choose a value for S prior to conducting a number of experiments under excess oxygen conditions. In vast excess, oxygen concentration remains essentially constant and the kinetic results are independent of S.

10.2 Tabulated Experimental Data

Data obtained from the hydrolysis and oxidation of acetic acid and methylene chloride are contained in the following tables. Not all measured and calculated quantities are listed for each experiment, but all experiments are included and enough data is given to allow calculation of quantities not listed, if such information is desired.

Runs designated with the suffix "A" indicate duplicates of earlier experiments; the results of the original experiment were discarded, either because mass-balance closure was poor or because experimental conditions varied significantly from their targeted values.

Table 10.1 Experimental Data for Acetic Acid Hydrolysis at 246 bar. Intervals shown are to 95% confidence.

Run No.	Temperature °C	$[CH_3COOH]_0$ $\times 10^{-6}$ mol/cm^3	$[O_2]_0$ $\times 10^{-3}$ mol/cm^3	τ seconds	Conversion %	ln k s^{-1}	Carbon Balance Closure %
246A	550±1	0.97±.03	2.12±.06	8.1±0.4	13.7±3.4	-4.01	140.0
249	575±1	1.06±.02	2.01±.05	8.1±0.4	26.7±2.4	-3.26	51.2
251	500±3	1.04±.03	2.44±.07	8.0±0.4	5.5±3.8	-4.96	103.4
253	525±1	1.06±.03	2.29±.06	8.0±0.4	11.5±3.5	-4.18	0 1
257	600±1	0.96±.03	1.92±.06	8.6±0.4	35.2±2.7	-2.99	93.8
306	475±1	0.98±.03	2.63±.07	7.7±0.4	5.9±3.5	-4.85	0.0
307	537±1	0.97±.02	2.19±.05	7.7±0.4	13.1±2.2	-4.00	101.5
308	562±1	0.98±.02	2.07±.04	7.7±0.4	21.4±2.2	-3.47	75.2
309	587±1	0.99±.02	1.91±.04	7.6±0.4	30.0±1.5	-3.06	87.3
310	512±1	0.96±.02	2.33±.06	7.7±0.4	8.0±2.6	-4.52	104.5

Table 10.2 **Experimental Data for Acetic Acid Oxidation at 246 bar. Intervals shown are to 95% confidence.**

Run No.	Temperature °C	$[CH_3COOH]_o$ $\times 10^{-6}$ mol/cm^3	$[O_2]_o$ $\times 10^{-6}$ mol/cm^3	τ seconds	Conversion %	ln k s^{-1}	Carbon Balance Closure %
247A	550±1	1.00±.03	2.03±.07	8.0±0.4	98.0±0.3	-0.71	99.1
248	475±1	1.06±.03	2.13±.08	7.9±0.4	14.1±3.6	-3.95	65.6
250	575±1	1.08±.03	2.04±.06	8.0±0.4	99.9±0.1	0.18	92.9
252	500±1	1.04±.02	2.13±.06	7.9±0.4	18.9±2.0	-3.64	73.5
254A	525±1	0.99±.02	2.07±.02	7.9±0.4	52.7±2.9	-2.35	99.8
256	450±2	0.98±.02	2.13±.07	8.2±0.4	8.7±4.2	-4.50	34.5
258	600±1	0.97±.03	2.07±.09	8.4±0.4	99.9±0.1	0.13	97.5
260	426±2	0.99±.05	2.10±.02	8.3±0.5	9.21±8.9	-4.45	10.4
261	525±2	0.96±.03	2.12±.09	5.1±0.3	33.8±3.3	-2.52	92.4
262	525±1	0.97±.05	2.10±.02	7.3±0.5	49.2±5.2	-2.38	86.4
263A	525±1	0.99±.02	2.06±.06	8.8±0.4	60.9±1.4	-2.24	98.9
264	525±2	0.98±.04	2.12±.12	4.6±0.3	31.0±4.7	-2.51	85.6
265	525±1	0.98±.03	2.12±.07	9.8±0.5	62.2±1.7	-2.31	97.6
266	525±1	0.98±.03	2.08±.07	5.9±0.3	38.5±2.3	-2.50	99.3
267	525±2	0.98±.03	1.08±.05	4.9±0.3	29.6±3.4	-2.63	93.9
268	525±1	0.98±.03	1.08±.05	8.8±0.5	52.7±2.5	-2.46	98.3
269	525±1	0.98±.03	1.10±.05	4.4±0.2	27.7±3.5	-2.61	93.1
270	525±1	0.99±.03	1.09±.05	7.0±0.4	40.4±3.1	-2.60	97.1

Table 10.2 (Continued)   Experimental Data for Acetic Acid Oxidation at 246 bar. Intervals shown are to 95% confidence.

Run No.	Temperature °C	$[CH_3COOH]_0$ $\times 10^{-6}$ mol/cm³	$[O_2]_0$ $\times 10^{-6}$ mol/cm³	τ seconds	Conversion %	ln k s⁻¹	Carbon Balance Closure %
271	525±1	0.98±.03	1.10±.05	9.7±0.5	55.1±2.4	-2.49	100.3
272	525±1	0.97±.02	1.10±.04	5.9±0.3	37.0±2.1	-2.56	94.8
273	525±1	0.98±.03	1.09±.04	7.9±0.4	47.9±2.0	-2.49	97.9
274	525±2	0.98±.03	3.86±.15	4.9±0.3	46.9±2.6	-2.04	101.4
275	525±1	0.99±.02	3.85±.11	4.4±0.2	41.6±1.8	-2.09	96.2
276	525±1	0.98±.02	3.87±.10	6.9±0.3	59.7±1.1	-2.03	100.5
277	525±1	0.98±.02	3.86±.10	8.7±0.4	70.0±0.9	-1.97	103.8
278	525±1	0.99±.02	3.86±.11	5.9±0.3	52.8±1.7	-2.06	98.9
279	525±1	0.99±.02	3.85±.11	7.8±0.4	66.4±1.0	-1.96	100.8
280	525±1	1.00±.02	3.88±.11	9.7±0.5	76.5±0.7	-1.91	101.1
281	525±1	0.098±.002	1.08±.04	7.9±0.4	72.4±1.0	-1.82	108.3
282	525±1	0.50±.01	1.06±.04	7.9±0.4	51.8±2.9	-2.39	93.6
283	525±1	2.04±.04	1.06±.04	7.9±0.4	41.5±1.8	-2.69	89.7
284	525±1	0.50±.01	1.09±.04	4.9±0.2	34.2±2.2	-2.46	96.1
285	525±1	0.49±.01	1.10±.04	5.9±0.3	41.6±1.8	-2.40	98.4
286	525±1	0.49±.01	1.09±.04	9.7±0.5	63.5±1.5	-2.26	99.3
287	525±1	2.01±.05	3.92±.12	4.9±0.2	45.5±2.5	-2.08	99.0

Table 10.2 (Continued)   **Experimental Data for Acetic Acid Oxidation at 246 bar.** Intervals shown are to 95% confidence.

Run No.	Temperature °C	$[CH_3COOH]_o$ $\times 10^{-6}$ mol/cm³	$[O_2]_o$ $\times 10^{-6}$ mol/cm³	τ seconds	Conversion %	ln k s⁻¹	Carbon Balance Closure %
288	525±1	2.01±.05	3.92±.13	5.9±0.3	55.8±1.8	-1.97	95.7
289	525±1	2.04±.05	3.89±.12	9.7±0.5	76.7±0.9	-1.90	97.5
290	525±1	2.03±.04	3.91±.10	6.9±0.3	61.8±2.4	-1.97	95.0
291	525±1	2.02±.04	3.92±.11	7.8±0.4	67.5±1.0	-1.93	96.4
292	525±1	2.03±.05	3.85±.11	8.6±0.4	71.9±0.9	-1.92	96.0
293	487±1	1.01±.02	2.03±.06	7.8±0.4	24.7±2.6	-3.32	76.7
294	462±1	0.99±.02	2.06±.06	7.7±0.4	14.6±2.7	-3.89	69.4
295	437±2	0.98±.03	2.12±.08	7.8±0.4	7.9±3.7	-4.55	58.0
296	513±1	0.97±.02	2.08±.07	7.9±0.4	42.6±1.7	-2.65	94.0
297	575±1	0.98±.03	2.10±.07	7.8±0.4	99.9±0.1	-0.08	94.7
298	550±1	0.92±.02	2.11±.06	7.8±0.4	96.1±0.7	-0.88	96.2
299	536±1	0.94±.02	2.09±.06	7.9±0.4	77.6±2.8	-1.66	98.8
300	525±2	1.43±.04	3.15±.10	5.0±0.2	42.2±2.4	-2.20	94.3
301	525±1	1.44±.04	3.14±.09	7.8±0.4	61.3±1.3	-2.10	95.3
302	525±1	1.45±.04	3.13±.09	9.7±0.5	69.6±1.1	-2.10	97.5
303	525±1	1.43±.05	3.16±.12	5.8±0.3	49.9±2.3	-2.13	99.4
304	525±1	1.43±.05	3.15±.12	6.7±0.4	55.7±2.2	-2.11	99.9
305	525±1	1.43±.05	3.16±.13	8.8±0.5	66.9±3.0	-2.08	103.0

Table 10.3 **Experimental Conditions for Acetic Acid Oxidation Product Species Profiles at 525 °C and 246 bar with Specified Residence Times and Feed Concentrations. Intervals shown are to 95% confidence.**

Initial Conditions: 525 ± 2 °C

$[O_2]_o = (1.09 \pm .02) \times 10^{-6}$ mol/cm^3

$[CH_3COOH]_o = (0.50 \pm 0.01) \times 10^{-6}$ mol/cm^3

Run #	Residence Time, s	$[CH_3COOH]_o$ $\times 10^{-6}$ mol/cm^3	$[O_2]_o$ $\times 10^{-6}$ mol/cm^3	Carbon Balance Closure, %
282	7.9 ± 0.4	$0.50 \pm .01$	$1.06 \pm .04$	93.6
284	4.9 ± 0.2	$0.50 \pm .01$	$1.09 \pm .04$	96.1
285	5.9 ± 0.3	$0.49 \pm .01$	$1.10 \pm .04$	98.4
286	9.7 ± 0.5	$0.49 \pm .01$	$1.09 \pm .04$	99.3

Table 10.3 (Continued) Experimental Conditions for Acetic Acid Oxidation Product Species Profiles at 525 °C and 246 bar with Specified Residence Times and Feed Concentrations. Intervals shown are to 95% confidence.

Initial Conditions: 525 $\pm$ 2 °C

$[O_2]_o = (2.08 \pm .04) \times 10^{-6}$ mol/cm^3

$[CH_3COOH]_o = (0.98 \pm 0.01) \times 10^{-6}$ mol/cm^3

Run #	Residence Time, s	$[CH_3COOH]_o$ $\times 10^{-6}$ mol/cm^3	$[O_2]_o$ $\times 10^{-6}$ mol/cm^3	Carbon Balance Closure, %
254A	7.9$\pm$0.4	0.99$\pm$.02	2.07$\pm$.02	99.8
261	5.1$\pm$0.3	0.96$\pm$.03	2.12$\pm$.09	92.4
262	7.3$\pm$0.5	0.97$\pm$.05	2.10$\pm$.02	86.4
263A	8.8$\pm$0.4	0.99$\pm$.02	2.06$\pm$.06	98.9
264	4.6$\pm$0.3	0.98$\pm$.04	2.12$\pm$.12	85.6
265	9.8$\pm$0.5	0.98$\pm$.03	2.12$\pm$.07	97.6
266	5.9$\pm$0.3	0.98$\pm$.03	2.08$\pm$.07	99.3

Table 10.3 (Continued)   **Experimental Conditions for Acetic Acid Oxidation Product Species Profiles at 525 °C and 246 bar with Specified Residence Times and Feed Concentrations. Intervals shown are to 95% confidence.**

Initial Conditions: 525 ± 2 °C

$[O_2]_o = (3.15 \pm .04) \times 10^{-6}$ mol/cm^3

$[CH_3COOH]_o = (1.44 \pm 0.02) \times 10^{-6}$ mol/cm^3

Run #	Residence Time, s	$[CH_3COOH]_o$ $\times 10^{-6}$ mol/cm^3	$[O_2]_o$ $\times 10^{-6}$ mol/cm^3	Carbon Balance Closure, %
300	5.0 ± 0.2	$1.43 \pm .04$	$3.15 \pm .10$	94.3
301	7.8 ± 0.4	$1.44 \pm .04$	$3.14 \pm .09$	95.3
302	9.7 ± 0.5	$1.45 \pm .04$	$3.13 \pm .09$	97.5
303	5.8 ± 0.3	$1.43 \pm .05$	$3.16 \pm .12$	99.4
304	6.7 ± 0.4	$1.43 \pm .05$	$3.15 \pm .12$	99.9
305	8.8 ± 0.5	$1.43 \pm .05$	$3.16 \pm .13$	103.0

Table 10.3 (Continued)   **Experimental Conditions for Acetic Acid Oxidation Product Species Profiles at 525 °C and 246 bar with Specified Residence Times and Feed Concentrations. Intervals shown are to 95% confidence.**

Initial Conditions: 525 ± 2 °C

$[O_2]_o = (3\ 90 \pm .05) \times 10^{-6}$ mol/cm^3

$[CH_3COOH]_o = (2.02 \pm 0.02) \times 10^{-6}$ mol/cm^3

Run #	Residence Time, s	$[CH_3COOH]_o$ $\times 10^{-6}$ mol/cm^3	$[O_2]_o$ $\times 10^{-6}$ mol/cm^3	Carbon Balance Closure, %
287	4.9 ± 0.2	$2.01 \pm .05$	$3.92 \pm .12$	99.0
288	5.9 ± 0.3	$2.01 \pm .05$	$3.92 \pm .13$	95.7
289	9.7 ± 0.5	$2.04 \pm .05$	$3.89 \pm .12$	97.5
290	6.9 ± 0.3	$2.03 \pm .04$	$3.91 \pm .10$	95.0
291	7.8 ± 0.4	$2.02 \pm .04$	$3.92 \pm .11$	96.4
292	8.6 ± 0.4	$2.03 \pm .05$	$3.85 \pm .11$	96.0

Table 10.4 Experimental Data for Acetic Acid Oxidation at 550 °C and 160 - 263 bar to Examine the Effect of Pressure/Density on Reaction Rates. Intervals shown are to 95 % confidence.

Run #	Pressure bar	$[CH_3COOH]_o$ $\times 10^{-6}$ mol/cm^3	$[O_2]_o$ $\times 10^{-6}$ mol/cm^3	τ seconds	Conversion %	ln k s^{-1}	Carbon Balance Closure %
311	242.3±2.8	0.93±.02	2.05±.05	5.9±0.3	89.9±0.6	-0.94	95.2
312	221.6±4.1	0.93±.03	2.06±.07	5.8±0.3	90.5±0.6	-0.90	95.8
313A	159.6±4.1	0.93±.04	2.11±.08	5.4±0.3	80.1±3.6	-1.21	111.2
314A	263.0±5.5	0.98±.03	2.10±.07	5.9±0.3	92.5±0.3	-0.83	96.5
315	200.9±3.4	0.94±.02	2.09±.06	5.8±0.3	90.5±0.6	-0.91	93.9
316	180.3±3.4	0.96±.02	2.10±.07	5.8±0.3	88.5±0.8	-0.99	99.2
318	263.0±6.2	0.96±.03	2.11±.08	4.0±0.2	85.6±1.3	-0.72	90.4
319	221.6±4.8	0.96±.03	2.11±.07	3.9±0.2	81.2±1.2	-0.85	94.6
321A	242.3±4.1	0.98±.02	2.09±.06	3.9±0.2	77.3±0.9	-0.98	97.8
322	200.9±6.9	0.95±.04	2.11±.10	3.8±0.2	74.9±1.5	-1.02	102.2
323	159.6±4.8	0.93±.04	2.09±.09	3.7±0.2	63.9±2.0	-1.29	116

Table 10.5   Experimental Data for Methylene Chloride Hydrolysis at 246 bar. All intervals shown are to 95% confidence. Carbon balances based only on gaseous products.

Run No.	Temperature °C	$[CH_2Cl_2]_0$ $\times 10^{-6}$ mol/cm³	τ seconds	Conversion %	ln k s⁻¹	Carbon Balance Closure %	Chlorine Balance Closure %
324	550±1	1.01±.12	5.8±0.3	43.0±7.0	-2.34	29.7	50.0
326A	500±2	1.15±.12	5.9±0.3	42.4±7.0	-2.37	17.7	45.4
328	450±5	1.17±.12	6.0±0.3	47.1±6.0	-2.24	6.0	55.0
330	575±1	1.05±.11	5.9±0.3	76.1±4.5	-1.42	58.6	72.8
332	475±3	1.16±.12	6.0±0.3	49.6±5.8	-2.16	11.6	47.1
334	525±2	0.74±.08	5.8±0.3	42.2±6.3	-2.36	44.6	74.9

Table 10.6 Experimental Data for Methylene Chloride Oxidation at 246 bar. All intervals shown are to 95 % confidence. Carbon balances based only on gaseous products.

Run No.	Temperature °C	$[CH_2Cl_2]_0$ $\times 10^{-6}$ mol/cm³	$[O_2]_0$ $\times 10^{-6}$ mol/cm³	τ seconds	Conversion %	$\ln k$ s^{-1}	Carbon Balance Closure %
325	550±2	1.01±.12	1.09±.04	5.8±0.3	53.3±5.9	-2.04	45.7
327	500±2	1.16±.12	1.07±.04	5.8±0.3	45.8±5.8	-2.26	30.7
329	450±5	1.18±.13	1.09±.05	5.9±0.4	49.1±6.1	-2.18	7.6
331	574±2	1.04±.11	1.12±.04	5.9±0.3	100.0	-0.17	73.7
333	475±3	1.16±.12	1.08±.05	6.1±0.3	51.6±5.7	-2.12	20.9
336	524±2	0.99±.10	1.09±.04	5.0±0.3	55.3±5.0	-1.82	50.7
337	524±2	0.98±.10	1.09±.04	6.8±0.4	71.8±3.2	-1.68	56.7
339	525±1	0.95±.10	1.10±.04	4.3±0.2	51.0±5.3	-1.80	47.8
340	525±1	0.94±.10	1.09±.04	7.8±0.4	61.8±6.6	-1.74	61.8
341	525±3	0.96±.10	1.08±.04	9.8±0.5	83.8±6.6	-1.69	70.8
342	525±2	0.96±.10	2.04±.08	5.0±0.3	56.4±5.0	-1.79	53.0
343	525±3	0.96±.10	2.04±.07	6.8±0.4	69.4±3.4	-1.75	53.9
344	525±5	0.94±.10	2.08±.08	8.9±0.5	82.3±2.1	-1.64	62.4
345	525±3	0.99±.10	2.01±.07	4.4±0.2	51.5±5.3	-1.81	46.5
346	524±1	0.99±.10	2.05±.08	5.9±0.3	61.1±5.4	-1.83	51.3
347	524±1	0.98±.10	2.06±.08	7.9±0.4	71.2±3.2	-1.85	57.2
348	524±1	0.73±.08	0.56±.03	5.0±0.3	54.4±5.7	-1.85	56.2
349	524±2	0.73±.08	0.56±.03	6.9±0.4	54.6±5.7	-2.17	71.1

Table 10.6 (Continued)   Experimental Data for Methylene Chloride Oxidation at 246 bar. All intervals shown are to 95% confidence. Carbon balances based only on gaseous products.

Run No.	Temperature °C	$[CH_2Cl_2]_o$ $\times 10^{-6}$ mol/cm³	$[O_2]_o$ $\times 10^{-6}$ mol/cm³	τ seconds	Conversion %	ln k s⁻¹	Carbon Balance Closure %
350	525±1	0.72±.08	0.57±.03	9.1±0.5	69.7±4.1	-2.03	73.5
348A	525±1	1.05±.11	0.57±.03	5.0±0.3	54.8±5.2	-1.84	45.0
349A	525±1	1.05±.11	0.57±.03	6.9±0.4	64.3±4.2	-1.90	50.0
350A	525±1	1.05±.11	0.57±.03	9.2±0.5	78.4±2.9	-1.79	53.5
351	524±1	1.02±.11	0.58±.03	4.4±0.3	49.2±5.8	-1.88	45.8
352	524±1	1.01±.11	0.58±.03	5.9±0.3	58.3±4.8	-1.91	48.0
353	524±2	1.01±.11	0.58±.03	9.9±0.6	80.5±2.3	-1.80	54.2
354	500±1	1.00±.11	1.08±.05	5.0±0.3	44.0±6.5	-2.15	47.9
355	500±2	1.01±.11	1.08±.05	7.8±0.5	44.2±6.5	-2.60	63.2
356	500±2	1.01±.11	1.07±.05	10.8±.6	62.3±4.3	-2.40	55.6
357	500±2	0.86±.10	1.06±.06	4.4±0.3	38.3±8.8	-2.22	54.3
358	501±1	0.85±.10	1.07±.06	6.9±0.5	49.6±10.1	-2.31	54.9
359	502±1	0.87±.10	1.04±.06	9.8±0.,	61.3±5.4	-2.33	58.2
361	525±2	2.01±.21	2.04±.06	7.9±0.4	69.8±3.2	-1.88	54.3
362	525±2	1.98±.20	2.07±.07	8.9±0.5	73.2±2.9	-1.91	58.4
363	525±2	1.99±.20	2.06±.07	9.9±0.5	77.0±3.0	-1.19	59.9

Table 10.7 Experimental Conditions for Methylene Chloride Oxidation Product Species Profiles at 525 °C and 246 bar with Specified Residence Times and Feed Concentrations. All intervals shown are to 95% confidence. Chlorine balances based only on liquid-phase effluent chlorine ion concentrations.

Initial Conditions: 524 ± 2 °C

$$[O_2]_o = (0.58 \pm .01) \times 10^{-6} \text{ mol/cm}^3$$

$$[CH_2Cl_2]_o = (1.03 \pm 0.01) \times 10^{-6} \text{ mol/cm}^3$$

Run #	Residence Time, s	$[CH_2Cl_2]_o$ $\times 10^{-6}$ mol/cm^3	$[O_2]_o$ $\times 10^{-6}$ mol/cm^3	Chlorine Balance Closure, %
348A	5.0 ± 0.3	$1.05 \pm .11$	$0.57 \pm .03$	50.3
349A	6.9 ± 0.4	$1.05 \pm .11$	$0.57 \pm .03$	56.5
350A	9.2 ± 0.5	$1.05 \pm .11$	$0.57 \pm .03$	59.2
351	4.4 ± 0.3	$1.02 \pm .11$	$0.58 \pm .03$	56.2
352	5.9 ± 0.3	$1.01 \pm .11$	$0.58 \pm .03$	56.5
353	9.9 ± 0.6	$1.01 \pm .11$	$0.58 \pm .03$	59.2

Table 10.7 (Continued) **Experimental Conditions for Methylene Chloride Oxidation Product Species Profiles at 525 °C and 246 bar with Specified Residence Times and Feed Concentrations.** All intervals shown are to 95% confidence. Chlorine balances based only on liquid-phase effluent chloride ion concentrations.

Initial Conditions: $525 \pm 3\,°C$

$[O_2]_o = (1.09 \pm .01) \times 10^{-6}\ mol/cm^3$

$[CH_2Cl_2]_o = (0.96 \pm 0.04) \times 10^{-6}\ mol/cm^3$

Run #	Residence Time, s	$[CH_2Cl_2]_o$ $\times 10^{-6}\ mol/cm^3$	$[O_2]_o$ $\times 10^{-6}\ mol/cm^3$	Chlorine Balance Closure, %
336	5.0 ± 0.3	$0.99 \pm .10$	$1.09 \pm .04$	57.2
337	6.8 ± 0.4	$0.98 \pm .10$	$1.09 \pm .04$	61.4
339	4.3 ± 0.2	$0.95 \pm .10$	$1.10 \pm .04$	56.6
340	7.8 ± 0.4	$0.94 \pm .10$	$1.09 \pm .04$	67.5
341	9.8 ± 0.5	$0.96 \pm .10$	$1.08 \pm .04$	71.8

Table 10.7 (Continued)   **Experimental Conditions for Methylene Chloride Oxidation Product Species Profiles at 525 °C and 246 bar with Specified Residence Times and Feed Concentrations.** All intervals shown are to 95 % confidence. Chlorine balances based only on liquid-phase effluent chloride ion concentrations.

Initial Conditions: 525 ± 5 °C

$[O_2]_o = (2.05 \pm .05) \times 10^{-6}$ mol/cm^3

$[CH_2Cl_2]_o = (0.97 \pm 0.04) \times 10^{-6}$ mol/cm^3

Run #	Residence Time, s	$[CH_2Cl_2]_o$ ×10^{-6} mol/cm^3	$[O_2]_o$ ×10^{-6} mol/cm^3	Chlorine Balance Closure, %
342	5.0±0.3	0.96±.10	2.04±.08	54.0
343	6.8±0.4	0.96±.10	2.04±.07	59.0
344	8.9±0.5	0.94±.10	2.08±.08	70.4
345	4.4±0.2	0.99±.10	2.01±.07	51.3
346	5.9±0.3	0.99±.10	2.05±.08	53.8
347	7.9±0.4	0.98±.10	2.06±.08	63.6

Table 10.7 (Continued)   **Experimental Conditions for Methylene Chloride Oxidation Product Species Profiles at 525 °C and 246 bar with Specified Residence Times and Feed Concentrations.** All intervals shown are to 95% confidence. Chlorine balances based only on liquid-phase effluent chloride ion concentrations.

Initial Conditions: 500 ± 3 °C

$[O_2]_o = (1.07 \pm .02) \times 10^{-6}$ mol/cm^3

$[CH_2Cl_2]_o = (0.96 \pm 0.22) \times 10^{-6}$ mol/cm^3

Run #	Residence Time, s	$[CH_2Cl_2]_o$ $\times 10^{-6}$ mol/cm^3	$[O_2]_o$ $\times 10^{-6}$ mol/cm^3	Chlorine Balance Closure, %
354	5.0±0.3	1.00±.11	1.08±.05	61.8
355	7.8±0.5	1.01±.11	1.08±.05	81.4
356	10.8±0.6	1.01±.11	1.07±.05	72.9
357	4.4±0.3	0.86±.10	1.06±.06	70.8
358	6.9±0.5	0.85±.10	1.07±.06	74.7
359	9.8±0.7	0.87±.10	1.04±.06	75.6

Table 10.7 (Continued)   **Experimental Conditions for Methylene Chloride Oxidation Product Species Profiles at 525 °C and 246 bar with Specified Residence Times and Feed Concentrations.** All intervals shown are to 95% confidence. Chlorine balances based only on liquid-phase effluent chloride ion concentrations.

Initial Conditions: $525 \pm 2\ °C$

$$[O_2]_o = (1.99 \pm .03) \times 10^{-6}\ mol/cm^3$$

$$[CH_2Cl_2]_o = (2.06 \pm 0.03) \times 10^{-6}\ mol/cm^3$$

Run #	Residence Time, s	$[CH_2Cl_2]_o$ $\times 10^{-6}\ mol/cm^3$	$[O_2]_o$ $\times 10^{-6}\ mol/cm^3$	Chlorine Balance Closure, %
361	7.9 ± 0.4	$2.01 \pm .21$	$2.04 \pm .06$	63.8
362	8.9 ± 0.5	$1.98 \pm .20$	$2.07 \pm .07$	68.5
363	9.9 ± 0.5	$1.99 \pm .20$	$2.06 \pm .07$	69.6

10.3 Nomenclature

A Arrhenius preexponential factor

C_i concentration of species i

E_a Arrhenius activation energy

F oxygen/organic feed ratio

k reaction rate constant

k' kinetic decay constant

k^* apparent first-order rate constant

R universal gas constant

R_i reaction rate for species i

S oxygen/organic stoichiometric ratio

X conversion

Greek Letters

ϵ dielectric constant

Φ fugacity coefficient

ρ density

τ reactor residence time

τ_{ind} induction time; ignition time

Other

$[A]_o$ initial concentration of A

Aikens, D. A., Bailey, R. A., Moore, J. A., Giachino, G. G., Tomkins, R. P. T. (1984) *Principles and Techniques for an Integrated Chemistry Laboratory*. Prospect Heights, Illinois: Waveland Press, Inc.

Amin, S., Reid, R. C., and Modell, M. (1975) "Reforming and decomposition of glucose in an aqueous phase." ASME Paper #75-ENAs-21, Intersociety Conference on Environmental Systems, San Francisco, CA, July 21-24.

Antal, M. J. Jr. (1982) "Biomass pyrolysis: A review of the literature. Part 1 - Carbohydrate pyrolysis." *Adv. Solar Energy* 1, 61-111.

Antal, M. J. Jr. and Mok, W.S. (1988) "A study of the acid catalyzed dehydration of fructose in near-critical water." In *Research in Thermochemical Biomass Conversion*, A. V. Bridgwater and J.L. Kuester, eds. New York: Elsevier Applied Science, pp. 464-472.

Antal, M. J. Jr., Leesomboon, T., Mok, W. S. L., and Richards, G. N. (1991) "Mechanism of formation of 2-furaldehyde from D-xylose." *Carbohydr. Res.* 217, 71-85.

Antal, M. J. Jr., Manarungson, S., and Mok, W.S. L. (1992) "Hydrogen production by steam reforming glucose in supercritical water." Presented at the Advances in Thermochemical Biomass Conversion Conference, Interlaken, Switzerland, May 11-15.

Antal, M. J. Jr., Mok, W. S. L., and Richards, G. N. (1990a) "Mechanism of formation of 4-(hydroxymethyl)-2-furaldehyde from D-fructose and sucrose." *Carbohydr. Res.* 199, 91-109.

Antal, M. J. Jr.Mok, W. S. L., and Richards, G. N. (1990b) "Four-carbon model compounds for the reactions of sugar in water at high temperatures." *Carbohydr. Research* 199, 111-115.

Anthony, T. (1978) "Chlorocarbons and Chlorohydrocarbons," *Kirk-Othmer Encyclopedia of Chemical Technology*, Vol. 5, 686-693.

Bamford, C. H. and Dewar, J. J. S. (1949) "The thermal decomposition of acetic acid." *J. Chem. Soc.*, 2877-2882.

Barner, H.E., Huang, C.Y., Johnson,T., Jacobs, G., Martch, M.A., Killilea, W.R. (1991) "Supercritical water oxidation: An Emerging Technology." Presented at ACHEMA, June 9, 1991, and accepted for publication in *J. Haz Mat*.

Benson, B. B., Krause, D. Jr., and Peterson, M.A. (1979) "The solubility and isotopic fractionation of gases in dilute aqueous solution. I. Oxygen." *J. Solution Chem.* 8(9), 655-690.

Blake, P.G. and Jackson, G.E. (1968) "Thermal decomposition of acetic acid." *J. Chem. Soc. (B)*, 1153.

Blake, P.G. and Jackson, G.E. (1969) "High-and Low-temperature mechanisms in the thermal decomposition of acetic acid." *J. Chem. Soc. (B)*, 94-96.

Blank, M.R. (1992) "A survey: destruction of chemical agent simulants in supercritical water oxidation." Los Alamos National Laboratory, Los Alamos, NM, Report No. AFIT/CI/CIA-92-063.

Bobleter, O. and Bonn, G. (1983) "The hydrothermolysis of cellobiose and its reaction-product D-glucose." *Carbohydr. Res.* 124, 185-193.

Brelvi, S.W. and O'Connell, J.P. (1972) "Corresponding states correlations for liquid compressibility and partial molal volumes of gases at infinite dilution in liquids." *AIChE J.* 18(6), 1239-1243.

Brett, R.W.J. and Gurnham, C.F. (1973) "Wet air oxidation of glucose with hydrogen peroxide and metal salts." *J. Appl. Chem. Biotechnol.* 23, 239-250.

Buelow, S.T., Dyer, R.B., Atenolo, J.H., Wander, J.D. (1990) "Advanced techniques for soil remediation of propellant components in supercritical water." Los Alamos National Laboratory, Los Alamos, NM, Report No. LA-UR-90-1338.

Buelow, S.T., Dyer, R.B., Harradine, D.M., Robinson, J.M., Funk, K.A., McInroy, R.E., Sanchez, J.A., Sponterelli, T. (1992) "Destruction of explosives and rocket fuels by supercritical water oxidation." Los Alamos National Laboratory, Los Alamos, NM, Report No. LA-CP-92-281.

Dietrich, M. J., Randall, T.L., Canney, P.J. (1985) "Wet Air Oxidation of Hazardous Organics in Wastewater." *Environ. Prog.*, 4(3), 171.

Dudziak, K.H., Franck, E.U., (1966) "Messungen der Viskosität des Wassers bis 560°C und 3500 bar." *Ber. Bunsenges. Phys. Chem. Phys.* 70(9-10), 1120.

Evans, R. J. and Milne, T. A. (1987) "Molecular characterization of the pyrolysis of biomass. 1. Fundamentals." *Energy & Fuels* 1(2), 123-137.

Franck, E.U. (1976) "Properties of water." In *High Temperature, High Pressure Electrochemistry in Aqueous Solutions* D. de G. Jones and R.W. Staehle, eds. Houston, TX : National Association of Corrosion Engineers, pp. 109-116.

Franck, E.U., Rosenqweig, S., Christoforakos, M., (1990) "Calculation of the dielectric constant of water to 1000°C and very high pressures." *Ver. Bunsenges. Phys. Chem.* **94**, 199.

Frisch, M.A. (1992) "Supercritical water oxidation of acetic acid catalyzed by CeO_2/MnO_2." Masters Thesis, The University of Texas, Austin,TX.

Gloyna, E.F. (1989) "Supercritical water oxidation-deep well technology for toxic wastewaters and sludges." The University of Texas, Austin, TX, Tech. Report No. W-89-1

Heger, K., Uematsu, M. Franck, E.U. (1980) "The static dielectric constant of water at high pressures and temperatures to 500 MPa and 550°C." *Ber. Bunsenges. Phys. Chem.* **84**, 758.

Helling, R. K. (1986) "Oxidation kinetics of simple compounds in supercritical water: carbon monoxide, ammonia, and ethanol." Doctoral thesis, Department of Chemical Engineering, Massachusetts Institute of Technology, Cambridge, MA.

Helling, R. K. and Tester, J. W. (1987) "Oxidation kinetics of carbon monoxide in supercritical water." *Energy & Fuels* **1**, 417-423.

Helling, R. K. and Tester, J. W. (1988) "Oxidation of simple compounds and mixtures in supercritical water: carbon monoxide, ammonia and ethanol." *Environ. Sci. Technol.* **22**(11), 1319-1324.

Holgate, H.R. (1993) "Oxidation chemistry and kinetics in supercritical water: hydrogen, carbon monoxide, and glucose." Doctoral Thesis, Department of Chemical Engineering, Massachusetts Institute of Technology, Cambridge, MA.

Holgate, H.R. and Tester, J.W. (1993) "Fundamental kinetics and mechanisms of hydrogen oxidation in supercritical water." *Combust. Sci. and Tech.* **88**, pp.369-397.

Holgate, H. R., Webley, P.A., Tester, J. W., and Helling, R. K. (1992) "Carbon monoxide oxidation in supercritical water: The effects of heat transfer and the water-gas shift reaction on observed kinetics." *Energy & Fuels* **6**(5), 586-597.

Hong, G. T., Fowler, P. K., Killilea, W. R., and Swallow, K.C. (1987) "Supercritical water oxidation: Treatment of human waste and system configuration tradeoff study." SAE Technical Paper Series #87144, 17th Intersociety Conference on Environmental Systems, Seattle, WA, July 13-15.

Hossain, S. U. and Blaney, C. A. (1991) "Method for removing polychlorinated dibenzodioxins and polychlorinated dibenzofurans from paper mill sludge." United States patent # 5,075,017, December 24.

Jolly, G.S., McKenney, D.J., Singleton, D.L., Paraskevopoulos, G., Bossard, A.R. (1986) "Rates of OH radical reactions: Rate-constant and mechanisms for the reaction of hydroxyl radicals with formic acid." *J. Phys. Chem.* 90, 6557-6562.

Killilea, W R., Swallow, K. C., Hong, G. T. (1992) "The fate of nitrogen in supercritical water oxidation." *J. Supercritical Fluids* 5(1), 72-78.

Lamb, W.J., Hoffman, G.A., Jonas, J. (1981) "Self-diffusion in compressed supercritical water." *J. Chem. Phys.* 74(12), 6875.

Lee, D. -S. (1990) "Supercritical water oxidation of acetamide and acetic acid." Doctoral Thesis, University of Texas, Austin, TX.

Lee, D. -S. and Gloyna, E. F. (1990) "Supercritical water oxidation of acetamide and acetic acid." Center for Research in Water Resources, Bureau of Engineering Research, University of Texas at Austin, Technical Report CRWR 209.

Lee, D. -S. and Gloyna, E. F. (1992) "Hydrolysis and oxidation of acetamide in supercritical water." *Environ. Sci. Technol.* 26(8), 1587-1593.

Lee, D. -S., Gloyna, E. F., and Li, L. (1990) "Efficiency of H_2O_2 and O_2 in supercritical water oxidation of 2,4-dichlorophenol and acetic acid." *J. Supercritical Fluids* 3(4), 249-255.

Liepa, M. A. (1988) "A Kinetic Study of the Oxidation of Model Chlorinated Hydrocarbons Catalyzed by Chromia Supported on γ-Alumina." Doctoral Thesis, Department of Chemical Engineering, Massachusetts Institute of Technology, Cambridge, MA.

Marshall, W.L., Franck, E.U. (1981) "Ion product of water substance, 0-1000 °C, 1-10,000 bars. New international formulation and its background." *J. Phys. Chem. Ref. Data* 10(2), 295.

Mednick, M. L. (1962) "The acid-base-catalyzed conversion of aldohexose into 5-(hydroxymethyl)-2-furfural." *J. Org. Chem.* 27, 398-403.

Modell, M. (1982) "Processing methods for the oxidation of organics in supercritical water." United States patent #4,338,199, July 6.

Modell, M. (1985a) "Processing methods for the oxidation of organics in supercritical water." United States patent #4,543,190, September 24.

Modell, M. (1985b) "Gassification and liquefaction of forest products in supercritical water." In *Fundamentals of Thermochemical Biomass Conversion*, R.P. Overend, T. A. Milne, and L.K. Mudge, eds. New York: Elsevier Applied Science Puplishers, pp. 95-119.

Modell, M. (1989) "Supercritical-water oxidation." In *Standard Handbook of Hazardous Waste Treatment and Disposal*, H. M. Freeman, ed. New York, NY: McGraw-Hill, pp. 8.153-8.168.

Modell, M., Larson, J., and Sobczynski, S. F. (1992) "Supercritical water oxidation of pulp mill sludges." *Tappi J.* June, 195-202.

Modell, M., Gaudet, G. G., Simson, M., Hong, G.T., and Biemann, K. (1982) "Supercritical water: testing reveals new process holds promise." *Solid Wastes Management*, August.

Mok, W. S.-L., Antal, M. J. Jr., and Jones, M. Jr. (1989) "Formation of acrylic acid from lactic acid in supercritical water." *J. Org. Chem.* 54, 4596-4602.

Mok, W. S.-L., Antal, M. J. Jr., and Varhegyi, G. (1992) "Productive and parasitic pathways in dilute acid-catalyzed hydrolysis of cellulose." *Ind. Eng. Chem. Res.* 31(1), 94-100.

Moore, J. C., Battino, R., Rettich, T. R., Handa, Y. P, and Wilhelm, E. (1982) "Partial molar volumes of 'gases' at infinite dilution in water at 298.15K." *J. Chem. Eng. Data* 27, 22-24.

Newth, F. H. (1951) "The formation of furan compounds from hexoses." *Adv. Carbohydr. Chem.* 6, 83-106.

Perry, R. H., Green, D., and Maloney, J.O., eds. (1984) *Perry's Chemical Engineers' Handbook, Sixth Edition*. New York: McGraw-Hill.

Ploos van Amstel, J.J.A. and Rietema, K. (1970) "Naßoxidation von Abwasserschlamm. Teil I: Oxidation von Glucose als Modellsubstanz." *Chem.-Ing.-Tech.* 42(15), 981-990.

Press, W.H., Flannery, B.P., Teukolsky, S.A., and Vetterling, W.T. (1986) *Numerical Recipes: The Art of Scientific Computing*. New York: Cambridge University Press.

Ramayya, S. V. and Antal, M.J. Jr. (1989) "Evaluation of systematic error incurred in the plug flow idealization of tubular flow reactor data." *Energy & Fuels* 3, 105-108.

Randall, T. L., and Knopp, P. V. (1980) "Detoxification of Specific Organic Substances by Wet Oxidation." *J. Water Poll. Control Fed.*, 52, 221.

Reid, R.C., Prausnitz, J.M., and Poling, B.E. (1987) *The Properties of Gases and Liquids, Fourth Edition.* New York: McGraw-Hill.

Rettich, T.R., Battino, R., and Wilhelm, E. (1982) "Solubility of gases in liquids. 15. High-precision determination of Henry coefficients for carbon monoxide in liquid water at 278 to 323K." *Ber. Bunsenges. Phys. Chem.* 86, 1128-1132.

Rettich, T.T., Handa, Y.P., Battino, R., and Wilhelm, E. (1981) "Solubility of gases in liquids. 13. High-precision determination of Henry's constants for methane and ethane in liquid water at 275 to 328K." *J. Phys. Chem.* 85, 3230-3237.

Rossberg, M., Lendl, W., Tögel, A., Dreher, E., Kleinschmidt, P., Strack, H., Beck, U. Lipper, K., Torkelson, T.R., Löser, E., Beutel, K. (1987) "Chlorinated Hydrocarbons." *Ullmann's Encyclopedia of Industrial Chemistry*, 5th Edition, Gerhartz, W., Yamamoto, Y.S., Campbell, F.T., Pfefferkorn, R., Rounsaville, J.F., eds. Vol. A6, 233-256.

Rice, S.F. (1993) Telephone conversation and subsequent fascimile, April 27. Sandia National Laboratories, Livermore, CA

Schallenberger, R.S. and Birch, G.G. (1975) *Sugar Chemistry.* Westport, CT: Avi Publishing Co., Inc.

Shanableh, A. and Gloyna, E.F. (1991) "Supercritical water oxidation - wastewaters and sludges." *Water Sci. Technolo.* 23(1-3), 389-398.

Shaw, R.W., Brill, T.R., Clifford, A.A., Eckert, C.A., and Franck, E.U. (1991) "Supercritical water: a medium for chemistry." *Chem. Eng. News* 69(5), 26-39.

Silverstein, R.M., Bassler, G.C., and Morrill, T.C. (1991) *Spectrometric Identification of Organic Compounds, Fifth Edition.* New York: John Wiley and Sons.

Singh, B., Dean, G.R., and Cantor, S.M. (1948) "The role of 5-(hydroxymethyl)-2-furfural in the discoloration of sugar solutions." *J. Am. Chem. Soc.* 70, 517-522.

Singleton, D.L., Paraskevopoulos, G., Irwin, R.S. (1989) "Rates and mechanism of the reactions of hydroxyl radicals with acetic, deuterated acetic, and propionic acids in the gas phase." *J. Am. Chem. Soc.* **111**, 5248-5251.

Skaates, J.M., Briggs, B.A., Lamparter, R.A., and Baillod, C.R. (1981) "Wet oxidation of glucose." *Can. J. Chem. Eng.* **59**, 517-521.

Swallow, K.C., Killilea, W.R., Malinowski, K.C., and Staszak, C. (1989) "The MODAR process for the destruction of hazardous organic wastes-field test of a pilot-scale unit." *Waste Management* **9**, 19-26.

Takahashi, Y., Wydeven, T., and Koo, C. (1989) "Subcritical and supercritical water oxidation of CELSS model wastes." *Adv. Space Res.* **9**(8), (8)99-(8)110.

Tester, J.W., Holgate, H.R., Armellini, F.J., Webley, P.A., Killilea, W.R., Hong, G.T., and Barner, H.E. (1993) "Oxidation of hazardous organic wastes in supercritical water: A review of process developement and fundamental research." *ACS Symposium Series 518: Emerging Technologies in Hazardous Waste Management III*, D.W. Tedder and F.G. Pohland, eds. Washington, D.C.: American Chemical Society, pp. 35-76.

Tester, J.W., Webley, P.A., and Holgate, H.R. (1992) "Revised global kinetic measurements of methanol oxidation in supercritical water." *Ind. Eng. Chem Res.*, **32**(1), 236-239.

Theander, O. and Nelson, D.A. (1978) "Aqueous, high-temperature transformation of carbohydrates relative to utilization of biomass." *Adv. Carbohydr. Chem. Biochem.* **46**, 273-326.

Thomason, T.B. and Modell, M. (1984) "Supercritical water destruction of aqueous wastes." *Haz. Waste* **1**(4), 453-467.

Thomason, T.B., Hong, G.T., Swallow, K.C., and Killilea, W.R. (1990) "The MODAR supercritical water oxidaion process." In *Innovative Hazardous Waste Treatment Technology Series, Volume 1: Thermal Processes*, H.M. Freeman, ed. Lancaster, PA: Technomic Publishing, pp. 31-42.

Thornton, T.D. and Savage, P.E. (1990) "Phenol oxidation in supercritical water." *J. Supercritical Fluids* **3**(4), 240-248.

Timberlake, S.H., Hong, G.T., Simson, M., and Modell, M. (1982) "Supercritical water oxidation for wastewater treatment; preliminary study of urea destruction." SAE Technical Paper Series #820872, 12th Intersociety Conference on Environmental Systems, San Diego, CA, July 19-21.

Tödheide, K. (1972) "Water at high temperatures and pressures." *Water: A Comprehensive Treatise*, F. Franks, ed. New York: Plenum Press, Inc., pp. 463-514.

Tödheide, K. and Franck, E.U. (1963) "Das Zweiphasengebiet und die kritische Kurve im System Kohlendioxid-Wasser vis zu Drucken von 3500 bar." *Z. Phys. Chem. N.F.* 37, 387-401.

Tongdhamachart, C. (1990) "Supercritical water oxidation of anaerobic sludges." Doctoral Thesis, The University of Texas, Austin, TX.

Tsang, W. and Hampson, R.F. (1986) "Chemical kinetic data base for combustion chemistry. Part I. Methane and related compounds." *J. Phys. Chem. Ref. Data* 15(3), 1087-1279.

Uematsu, M. and Franck, E.U. (1980) "Static dielectric constant of water and steam." *J. Phys. Chem. Ref. Data* 9(4), 1291-1306.

Wagner, F. (1983) In *McGraw-Hill Encyclopedia of Chemistry*. New York : McGraw-Hill, Inc., pp. 2

Webley, P.A. (1989) "Fundamental oxidation kinetics of simple compounds in supercritical water." Doctoral Thesis, Department of Chemical Engineering, Massachusetts Institute of Technology, Cambridge, MA.

Webley, P.A. and Tester, J.W. (1988) "Fundamental kinetics and mechanistic pathways for oxidation reactions in supercritical water." SAE Technical Paper Series #881039, 18th Intersociety Conference on Environmental Systems, San Francisco, CA, July 11-13.

Webley, P.A. and Tester, J.W. (1989) ""Fundamental kinetics of methanol oxidation in supercritical water." *ACS Symp. Ser. 406: Supercritical Fluid Science and Technology*, K.P. Johnston and J.M.L. Penninger, eds. Washington, D.C.: American Chemical Society, pp. 259-275.

Webley, P.A. and Tester, J.W. (1991) "Fundamental kinetics of methane oxidation in supercritical water." *Energy & Fuels* 5, 411-419.

Webley, P.A., Holgate, H.R., Stevenson, D.M., and Tester, J.W. (1990) "Oxidation kinetics of model compounds of metabolic waste in supercritical water." SAE Technical Paper Series #901333, 20th Intersociety Conference on Environmental Systems, Williamsburg, VA, July 9-12.

Webley, P.A., Tester, J.W., and Holgate H.R. (1991) "Oxidation kinetics of ammonia and ammonia-methanol mixtures in supercritical water in the temperature range 530-700°C at 246 bar." *Ind. Eng. Chem. Res.* 30(8), 1745-1754.

West, M.B. and Gray, M.R. (1987) "Pyrolysis of 1,3-butanediol as a model reaction for wood liquefaction in supercritical water." *Can J. Chem. Eng.* 65, 645-650.

Wightman, T.J. (1981) "Studies in supercritical wet air oxidation." Masters Thesis, Department of Chemical Engineering, University of California at Berkeley, Berkeley, CA.

Wilhelm, E., Battino, R., and Wilcock, R.J. (1977) "Low-pressure solubility of gases in liquid water." *Chem. Rev.* 77(2), 219-262.

Wilmanns, E.G. and Gloyna, E.F. (1990) "Supercritical water oxidation of volatile acids." Center for Research in Water Resources, Bureau of Engineering Research, University of Texas at Austin, Technical Report CRWR 218.

Woerner, G.A. (1976) "Thermal decomposition and reforming of glucose and wood at the critical conditions of water." Masters Thesis, Department of Chemical Engineering, Massachusetts Institute of Technology, Cambridge, MA.

Wolfrom, M.L., Schuetz, R.D, and Cavalieri, L.F. (1948) "Chemical interactions of amino compounds and sugars. III. The conversion of D-glucose to 5-(hydroxymethyl)-2-furaldehyde." *J. Am. Chem. Soc.* 70, 514-517.

Yetter, R.A., Dryer, F.L., and Rabitz, H. (1985) "Some interpretive aspects of elementary sensitivity gradients in combustion kinetics modeling." *Combust. Flame* 59, 107-133.

Young, P. C. (1982) "A Kinetic Study of the Catalytic Oxidation of Dichloromethane." Masters Thesis, Massachusetts Institute of Technology, Cambridge, MA.